# C1 Domain: Investigation of Diacylglycerol/Phorbol Ester Binding Properties and Development of Ligands

*A dissertation submitted to the*

*Indian Institute of Technology Guwahati as*

*Partial fulfillment for degree of*

*Doctor of Philosophy in Chemistry*


***Submitted by***

***Rituparna Borah***




Department of Chemistry

Indian Institute of Technology Guwahati

Assam-781039, India

Dedicated

To

My Beloved Family

# Contents

**INDIAN INSTITUTE OF TECHNOLOGY GUWAHATI**

**Department of Chemistry**

# STATEMENT

I do hereby declare that the matter embodied in this thesis is the result of investigations carried out by me in the Department of Chemistry, Indian Institute of Technology, India under supervision of associate professor Dr. Debasis Manna.

In keeping with the general practice of reporting scientific observations, due acknowledgements have been made wherever the work described is based on the findings of other investigators.

11th March, 2016 **Rituparna Borah**
IIT Guwahati

**INDIAN INSTITUTE OF TECHNOLOGY GUWAHATI**

**Department of Chemistry**

# CERTIFICATE

This is to certify that Rituparna Borah has been working under my supervision since July, 2011 as a regular registered Ph.D. student. I am forwarding her thesis entitled "**C1 Domain: Investigation of Diacylglycerol/Phorbol Ester Binding Properties and Development of Ligands**" being submitted for the Ph. D. (Science) Degree of this institute. I certify that she has fulfilled all the requirements according to the rules of this institute regarding the investigations embodied in her thesis and this work has not been submitted elsewhere for a degree.

11th March, 2016
IIT Guwahati

**Dr. Debasis Manna**
**Supervisor**
Department of Chemistry
IIT Guwahati

# *Acknowledgements*

I owe my sincere gratitude to all those people who have made this dissertation possible.

Firstly, I would like to express my sincere gratitude to my thesis supervisor Dr. Debasis Manna for his continuous support and motivation during my research work. His patience and friendly nature helped me overcome many crisis situations and finish this dissertation. My everlasting gratitude goes towards him.

Besides my advisor, I would like to thank all my doctoral committee members: Prof. Gopal Das, Prof. Biplab Mondal and Dr. Vishal Trivedi for their insightful comments and encouragement.

I wish to acknowledge my sincere gratitude to Central Instrument Facility (CIF), IIT Guwahati for providing the instrument facility for my research work. Moreover, my sincere thanks goes to Centre for excellence, IIT Guwahati and Centre for environment, IIT Guwahati for allowing me to use different instruments which were very essential to carry out my research work.

I would like to thank all my group members Dr. Narsimha Mamidi, Dr. Sukhamoy Gorai, Saurav Paul, Dipjyoti Talukdar, Subhankar Panda, Ashalata Roy, Abhishek Saha, Sitikantha Biswas, Nirmalya Pradhan and Nandan Haloi for their kind cooperation during my Ph.D. life. I also take this opportunity to thank all my IITG friends for their encouragement.

I'm grateful to my parents, Mr. Khagen Borah and Mrs. Hema Prova Borah for introducing me to this beautiful world as well as for inspiring me to pursue the dream that led me to achieve this position. I deeply appreciate the support and care from my parents in laws, Mr. Suren Neog and Mrs. Smriti Rekha Neog. I would also like to thank my brothers Rupam, Nayan, Paras and Paban; sisters Bornali, Swapnali, Dhanashree and Aparajita for their love and care.

Most importantly, none of this would have been possible without the love and patience of my husband, Dr. Subrat Jyoti Neog. During all the hard times, his support and care helped me stay focused on my work. Words cannot express my feelings, nor my thanks for all his effort that strengthened me enough to reach this position.

*Rituparna Borah*

# List of Abbreviations

| | |
|---|---|
| [3H]PDBu | [3H]phorbol-12,13-dibutyrate |
| 3HF | 3-Hydroxyflavone |
| 6-keto | Cholestane-6-oxo-3β,5α-diol |
| AD | Alzheimer disease |
| ANS | 8-Anilino-1-naphthalenesulfonic acid |
| CAC | Critical aggregation concentration |
| CC domain | Coiled coil domain |
| CD | Circular dichroism |
| Cdc42 | Cell division control protein 42 homolog |
| cDNA | Cromosomal DNA |
| CH domain | Calponin homology domain |
| cPKC | Classical Protein Kinase C |
| DGKs | Diacylglycerol Kinases |
| DMSO | Dimethylsulfoxide |
| dPE | Dansyl-PE |
| DPH | 1,6-Diphenyl-1,3,5-hexatriene |
| DPPC | Dipalmitoylphosphatidylcholine |
| DRM | Detergent resistance membrane |
| DSC | Differential scanning calorimeter |
| ESIPT | Excited state intramolecular proton transfer |
| ESPT | Excited-state proton transfer |
| FRET | Förster resonance energy transfer |
| GTPases | Guanosine Triphosphate |
| HEPES | 4-(2-hydroxyethyl)-1-piperazineethanesulfonic acid |
| HGL | (S)-γ-hydroxymethyl-γ-buiolettyrolactone |
| KSR | Kinase Suppressor of Ras |
| $l_0$ phase | Liquid ordered phase |
| LC | Liquid crystal |
| LE | Liquid-expanded |
| LUV | Large unilamellar vesicles |
| MLC | Myosin light chain |

| | |
|---|---|
| MLV | Multi lameller vesicle |
| MRCK | Myotonic dystrophy-related Cdc42-binding kinases |
| NBD | 2-(4-nitro-2,1,3-benzoxadiazol-7-yl)aminoethyl]trimethylammonium |
| NCBI | National Center for Biotechnology Information |
| NMR | Nuclear Magnetic Rresonance |
| nPKC | Novel Protein Kinase C |
| NpOH | 1-naphthol |
| PBD | Protein binding domain |
| PBS | Phosphate-buffered saline |
| PC | 1-palmitoyl-2-oleoyl-sn-glycero-3-phosphocholine |
| PDB | Protein data bank |
| PDBu | Phorbol-12,13-dibutyrate |
| PE | 1-palmitoyl-2-oleoyl-sn-glycero-3-phosphoethanolamine |
| PG | Phosphatidylglycerol |
| PH domain | Pleckstrin homology domain |
| PI(4, 5)$P_2$ | Phosphatidylinositol 4, 5-bisphosphate |
| PI-3-kinase | Phosphoinositide 3-kinase |
| PI-PLC | Phosphatidylinositol-specific phospholipase C |
| PKC | Protein Kinase C |
| PKD | Protein Kinase D |
| PLCs | Phosphoinositide-specific phospholipase C |
| PS | 1-palmitoyl-2-oleoyl-sn-glycero-3-phosphoserine |
| PSI–Blast | Position specific iterative BLAST |
| RasGRPs | Ras-Guanyl Nucleotide-Releasing Proteins |
| SAPD | 12-N-methylanthraniloylphorbol 13-acetate [sapintoxin D] |
| SG | Solid gel |
| SPR | Surface plasmon resonance |
| SUV | Small unilamellar vesicles |
| TBS | Tris-buffered saline |
| THF | Tetrahydrofuran |
| $T_M$ | Phase transition temperature |
| Triol | Cholestane-3β,5α,6β-triol |
| UV | Ultraviolet |

WT Wild type

| Amino Acid | 3-Letter symbol | 1-Letter symbol | Amino Acid | 3-Letter symbol | 1-Letter symbol |
|---|---|---|---|---|---|
| Alanine | Ala | A | Leucine | Leu | L |
| Arginine | Arg | R | Methionine | Met | M |
| Asparagine | Asn | N | Phenylalanine | Phe | F |
| Aspartic acid | Asp | D | Proline | Pro | P |
| Cysteine | Cys | C | Serine | Ser | S |
| Glutamic acid | Glu | E | Threonine | Thr | T |
| Glutamine | Gln | Q | Tryptophan | Trp | W |
| Glycine | Gly | G | Tyrosine | Tyr | Y |
| Histidine | His | H | Valine | Val | V |
| Isoleucine | Ile | I | | | |

Binding constants

$K_I$ Inhibition constant

$K_D$ Dissociation constant

# Abstract

C1 domain, or Cysteine rich domain has been found in more than 50 mammalian proteins and is well known for its' vital role in cell signaling. Diacylglycerol (DAG) is produced in the cell membrane due to the hydrolysis of $PI(4,5)P_2$. The localization of different kinase proteins to the cellular membrane through the interaction of their C1 domain with DAG regulates different cell signaling processes. It has already been reported that C1 domain mediated cell signaling is widely involved in progression of cancer, Alzheimer's diseases and others. Therefore it has been considered as an attractive therapeutical target. Here we have chosen two C1 domain containing protein- Protein Kinase C (PKC) and Myotonic Dystrophy Kinase related CDC42 binding kinase (MRCK). The introductory chapter (**Chapter 1**) describes the role of C1 domain in different diseases, structure, function and regulation of C1 domain and a brief summary of C1 domain ligands. The C1 domain of PKC is most widely studied till now. Tremendous efforts are underway for the development of PKC activators. The activity of PKC isozymes is also regulated by the biophysical properties of membrane. Therefore a clear understanding of the membrane interaction properties of the PKC activators is also very important. In this regard in **Chapter 2** and **Chapter 3**, we have focused on the development of PKC activators and understanding it's interaction with model membrane. Lipophilic molecules present in the membrane also affect the membrane biophysical properties and thus modulates the PKC activity. In this regard **Chapter 4** deals with the effects of cholesterol and oxysterols on the membrane biophysical properties which is correlated with PKC activity. MRCK is also a C1 domain containing protein which responds to phorbol ester and DAG. Several studies are carried out to understand the involvement of MRCK on different cellular processes and different diseases. But the mechanism through which MRCK interacts with DAG or phorbol ester is still not clear. Therefore **Chapter 5** deals with the mechanistic investigation into the C1 domain binding properties of MRCKα- and MRCKβ-C1 domain.

In effort to develop PKC activators, kojic Acid ester derivatives were designed which contained the required pharmacophores to interact with the C1 domain of PKC. We quantitatively determined the C1 domain binding affinity in monomeric form by fluorescence quenching experiment and in liposomal environment by fluorescence resonance energy transfer (FRET). The localization of the kojic acid esters in the lipid bilayer was qualitatively determined by NBDPE quenching experiment. The effect of these compounds in permeability and phase transition temperature of DPPC lipid bilayer was determined by using 1-Napthol as

the fluorescent probe. Overall, kojic Acid ester derivative was found to strongly bind the C1 domain of PKCδ and PKCθ. These compounds also changed the biophysical properties of the DPPC lipid bilayer which was correlated with the C1 domain binding.

The designing of the γ-hydroxymethyl-γ-butyrolactone derivative was based on the idea of conformationally constrained ligand. The binding affinity is enhanced due to the less entropic loss upon binding. Similar to **Chapter 2**, binding parameters were determined by fluorescence quenching and FRET. Nonradioactive fluorescence peptide based kinase assay was performed to determine PKC dependent phosphorylation capabilities of these compounds. The orientation of these molecules at the air-water interface was determined from Π-A isotherm obtained using Langmuir-Blodgett technique. Again the effect of these molecules on the membrane fluidity and hydration was determined by the use of DPH and Dansyl labeled PE as the fluorescent probe. The localization of the molecules in the lipid bilayer was determined from quenching of NBDPE by sodium dithionite. Molecular docking also suggests that these molecules fit to the binding pocket of PKCδ- and PKCθ-C1b subdomain. All these experimental and theoretical results demonstrate that γ-hydroxymethyl-γ-butyrolactone strongly interacts with the C1 domain of PKCδ and PKCθ where the hydroxymethyl and acyl group of the compounds are very important for binding. Also strong interaction of the HGL-derivatives changes the monolayer/bilayer properties including fluidity and hydration which modulates the PKC activity.

Cholesterol and oxysterols are important constituents of cell membrane. The biophysical properties of membrane e.g. fluidity, hydration, permeability, headgroup spacing etc. are greatly affected by the presence of cholesterol and oxysterols. It has been reported that DAG induced PKC activation is modulated by the membrane biophysical properties. Therefore lipophilic molecules like cholesterol and oxysterols can modulate the PKC activity by interacting with the membrane. Previous studies revealed that cholesterol enhanced the DAG induced PKC activity while oxysterols have the opposite effect. In order to understand this mechanism, we have chosen two oxysterols- cholestane-3β,5α,6β-triol (triol) and cholestane-6-oxo-3β,5α-diol (6-keto). FRET based competitive assay showed that in presence of cholesterol the DAG binding affinity of PKCδ-C1b domain is enhanced while the other two compounds reduced it. Nonradioactive Peptag PKC activity assay clearly showed that DAG induced PKC activation is higher in presence of cholesterol. Temperature dependent DPH anisotropy, hydration studies and turbidity assay confirmed that cholesterol enhances the formation of liquid ordered phase which is less hydrated than the other phases. Also cholesterol has a synergistic effect with DAG for the formation of liquid ordered phase which

may lead to the formation of coexisting DAG-rich and DAG-poor domain. Several studies have already revealed that coexistence of DAG-rich and DAG-poor domain in the membrane greatly enhances the DAG induced PKC activation. On the other hand triol and 6-keto did not exhibit any significant effect on the membrane phase behavior and hydration properties. The shifting of the phase transition temperature ($T_M$) of lipid bilayer in presence of 6-keto signifies tighter headgroup packing of the bilayer. Tighter headgroup packing may resist the penetration of C1 domain into membrane leading to the decrease in the DAG induced PKC activity. Thus cholesterol and oxysterols exert a number of changes in the membrane properties which affect the DAG dependent membrane binding properties of C1 domain of PKC and in turn effects PKC activation also.

MRCK is a serine threonine kinase which is reported to play an important role in cytoskeletal reorganization. It contains C1 domain in its regulatory region. Previous studies have revealed that MRCKα is in inactive form due to the formation of oligomers through intermolecular and intramolecular interactions. Interaction of phorbol ester with the C1 domain releases the kinase domain to activate the enzyme. It has been observed that C1 domain of MRCKα and MRCKβ responds to phorbol ester with 60-90 fold lower affinity than C1b domain of PKCδ. It demonstrates that C1 domain of MRCKα and MRCKβ lack some structural features which is hindering the interaction with PMA. In order to identify these structural requirements we mutated the crucial residues determined through homology alignment with that of PKCδ-C1b and binding parameters were determined by fluorescence polarization and SPR analyses. Monolayer penetration experiments were carried out to determine the extent of membrane penetration by these mutants. Overall these studies showed that a complete recovery of the DAG and phorbol ester dependent membrane binding as well as DAG dependent membrane penetration was observed for both MRCKα-C1-T9M/T10S/M21L/V22W/I25V/R26K and MRCKβ-C1-S9M/M21L/V22W/I25V/R26K. M21L/V22W was found to be crucial mutation for MRCKα/β-C1 while I25V/R26K also plays major role in MRCKβ-C1 domain. However, the regaining of the binding affinity is a cumulative effect of the six mutations in MRCKα-C1 and five mutations in MRCKβ-C1 domain.

Our attempt to design small molecules for C1 domain in order to achieve higher selectivity and specificity, led to the development of kojic acid esters and γ-hydroxymethyl-γ-butyrolactone substituents which showed higher affinity for PKCδ/θ-C1b domain. These lipophilic molecules also interact with membrane to alter a number of biophysical properties that may affect the C1 domain-membrane interaction. Moreover, our studies showed

membrane properties depend upon its lipid constituents e.g. cholesterol, oxysterol and others which also greatly modulates the C1 domain-membrane interaction. DAG/phorbol ester binding mechanism of MRCKα/β-C1 domain was thoroughly investigated that provides the base for designing activator or inhibitor targeting this domain.

# CHAPTER 1

## Introduction

### 1.1. C1 domain

C1 domain is a cysteine rich zinc-finger motif which was first identified as phorbol ester binding module of protein kinase C (PKC) in 1989 by Yasutomi Nishizuka and co-workers.[1] Subsequent studies by Burns and Bells revealed that PKCs contain two diacylglycerol (DAG)/phorbol ester binding sites and C1 domain is principally responsible for the [3H]phorbol-12,13-dibutyrate ([3H]PDBu) binding.[2] Phorbol ester responsive PKCs were found to be different from the phorbol ester unresponsive PKCs in their C1 domain structure, which again signifies that the C1 domain holds the entire requirement for the phorbol ester binding.[3] A number of studies carried out on the interaction of phorbol ester with chimaerins, Unc13/Munc13s, and RasGRPs established that C1 domain is sufficient for phorbol ester responsiveness.[4-10] The DAG responsive character of C1 domain was first identified by Quest and coworkers in 1994. In addition to PKCs, the other proteins with C1 domains that possess the structural requirements for phorbol-ester and DAG binding include protein kinase D (PKD) isoenzymes (which are structurally related to PKCs), Ras-guanyl nucleotide-releasing proteins (RasGRPs), chimaerins, diacylglycerol kinases (DGKs), Munc13 proteins and myotonic dystrophy kinase related CDC42 kinase (MRCK).[11] On the other hand phorbol ester/DAG unresponsive C1 domains include PKC (ζ, λ), DAG kinase (α, δ, η, ε, ζ, ι, θ), VAV (1, 2, 3), RAF1, KSR (1, 2), ROCK (1, 2) and RASSF5.[12] In plasma membrane, the phosphoinositide-specific phospholipase C (PLCs) hydrolyze phosphatidylinositol 4, 5-bisphosphate (PI(4, 5)$P_2$) to generate DAG.[13] C1 domain acts as the binding module of DAGs and as a result its host proteins are recruited to the cell membrane. Membrane localization results in the activation of those proteins which in turn activate different family of signaling proteins. Thus C1 domain-DAG interaction plays important role in different signaling pathways that are involved in the pathology of several diseases like cancer, neurological, immunological, cardiovascular, Alzheimer's diseases and others.[14]

### 1.2. C1 domain in the pathology of diseases

**Cancer-** The role of C1 domain in the pathology of cancer is most widely studied. The recognition of C1 domain as the binding module for tumor-promoting phorbol esters established its potential role in carcinogenesis and as a potentially important target for cancer

therapeutics.[15] The cellular signaling pathways initiated by phorbol ester/DAG binding to the C1 domain are involved in cell proliferation, survival, invasion, migration, apoptosis, angiogenesis, and anticancer drug resistance in cancer cells.[16, 17] The activation of PKC, the major DAG/phorbol ester receptor has been shown to promote human cancer cell growth through down-regulation of p18 (INK4c) oncogene.[18] Altered PKC expression has been observed in many cancers, such as breast, prostate, bladder, colon and brain cancers as well as leukaemia. In addition to PKC, most of the other DAG-effectors also play a significant role in regulating processes associated with cancer development. Protein kinase D (PKD) is involved in the progression of breast, pancreatic, prostate, skin, lung and basal cell carcinoma.[19] RasGRP isozymes-1, 3 and 4 have been recognized as DAG/phorbol ester receptor and reported to stimulate lymphoma in mice, promote tumor in the two-stage skin carcinogenesis model, malignant phenotype of prostate cancer and melanoma cell lines *in vitro* and in mouse xenograft tumours etc.[20] The chimaerins bind phorbol esters in a C1 domain-dependent manner sharing similarity with PKCα regarding ligand binding properties and phospholipid requirement. The target of chimaerin actions, the small GTPase Rac is a central regulator of actin cytoskeleton organization, cell migration, transformation, cell cycle progression and gene expression. Chimaerin is a tumour suppressor, therefore activation or upregulation of β2-chimerin has been found to be beneficial for treatment of cancers. Lower β2-chimaerin expression levels have been reported in high-grade gliomas when compared with normal brain tissue or low-grade brain tumours. β2-Chimaerin mRNA transcript levels are also lower in breast cancer tissue compared with normal breast tissue from the same patients.[21, 22] Moreover, over-expression of β2-chimaerin in cancer cell lines inhibits cell proliferation *in vitro* and *in vivo*, and reduces invasiveness of cancer cells *in vivo*.[22] DAG responsive DGKβ and γ are involved in various processes related to cancer progression. DGKβ was identified as a survival kinase in HeLa cells in a RNA interference (RNAi) screen on human kinases and phosphatases.[23] DGKγ has been reported to positively regulate cell cycle progression in several cell lines.[24] However, it has also been shown to activate β2-chimaerin and thus it may function as a tumor suppressor.[25, 26] Human Munc13 has been reported as DAG-receptor and involved in apoptosis.[27] Munc13-1 was identified as phorbol ester dependent enhancer of spontaneous neuro-transmitter release and thus represents a second messenger pathway alternative to PKC. The MRCKα and β phosphorylate nonmuscle myosin light chain at serine-19, which is known to be decisive for activating actin-myosin contractility and act as a downstream effectors of Cdc42 in cytoskeletal reorganization.[28, 29] The invasion of cancer cells or the metastasis process is regulated by actin-myosin

contractility and thus MRCK is highly involved in cancer progression. Northern blots with MRCKα kinase domain cDNA probe revealed relatively high levels of RNA expression in U937 histiocytic lymphoma, MDA-MB-231 (breast cancer), A549 (lung cancer) and PLB-985 (myelocytic leukemia) cell lines.[30] MRCKα (designated as PK428) was identified in breast cancer cells as being part of a gene expression signature linked to poor prognosis and increased incidence of metastasis.[31] MRCKα was also identified as being part of a seven-gene panel showing considerably elevated expression in pancreatic adenocarcinoma compared to normal pancreas tissue.[32] Upregulation of MRCKα expression was reported to contribute to cutaneous squamous cell carcinoma (SCC) following the repression of the Notch1 tumour suppressor.[33] Similar to this observation, analysis of publicly available gene expression microarray data using oncomine [34] revealed that MRCKα expression is elevated in oral, hypopharyngeal, and head and neck squamous cell carcinoma, oral cavity and tongue carcinoma, and Barrett's esophagus compared to normal tissues.[35-40] These results indicate that there are associations between altered MRCK expression and several cancers, particularly with cancers of squamous epithelia, which may reflect roles in promoting invasion and metastasis.

**Alzheimer disease-** Alzheimer disease (AD), is exclusively interlinked with two pathological hallmarks in the brain: extracellular amyloid plaques and intracellular neurofibrillary tangles.[41] Amyloid plaques have been shown to arise from aggregation of the soluble protein known as β-amyloid (Aβ1–42) and other variants such as Aβ1–40.[42] Amyloid plaques arise after soluble Aβ1–42 monomers begin to oligomerize into progressively larger aggregations that later form fibrils followed by plaques. The amyloidogenic-Aβ fragment generated from β-secretase-mediated hydrolysis of amyloid precursor protein (APP) produces an -NH2 terminus and further cleavage by γ-secretase generates the Aβ-peptide. Cleavage of APP by α-secretase at a different site generates soluble APP (sAPP), which is generally considered to be nontoxic.[43] Most of the available evidences suggest that sAPP production by α-secretase competitively reduces Aβ-production by the β- and γ-secretases. PKCα, ε and possibly other isozymes can activate the α-secretase-mediated cleavage of APP directly/indirectly through phosphorylation of extracellular-signal-regulated kinase (ERK1/2).[41, 44] It has already been demonstrtaed that reduced expression and translocation of PKCβII is involved in neuronal dysfunction observed in the changes in the immunohistochemical staining of AD tissue. PKC activation directly or indirectly enhances the α-processing of APP which results in secretion of sAPPα and reduction of Aβ.[41-48]

More recently, activation of PKC by phorbol-12-myristate-13-Acetate (PMA) has also been shown to prevent Aβ toxicity in rat primary hippocampal neurons. Activation of PKC by PMA and bryostatin 1 has also been shown to prevent Aβ-toxicity in rat primary hippocampal neurons.[42, 49] In addition to PKC, Munc13 also play an imperative role in APP processing: α-secretase mediated processing of APP was impaired in the brains of Munc13-1 knock-out mice, and phorbol-induced sAPPα secretion was less pronounced in brain slices of Munc13-1 knock-out mice than in wild type mice.[50] Consistently, phorbol ester-induced sAPPα secretion was only partially inhibited by the pan-PKC inhibitor Gö6983 in neuroblastoma cells, and overexpression of Munc13-1 augmented phorbol-induced increase of sAPPα secretion. Stimulation of postsynaptic glutamate receptors rescued the defective sAPPα secretion in organotypic brain slice cultures from Munc13 knock-out mice, implying that the defective APP processing results from the lack of postsynaptic glutamatergic stimulation.[51] Treatments that activate Munc13s may thus have potential in directing APP processing to the non-amyloidogenic α-secretase route.

**Other therapeutic conditions-** PKCs and other DAG effectors are also implicated in numerous other pathological conditions, such as cardiovascular diseases, immunological diseases and diabetes. PKC isozymes were also found to regulate cardiac responses, including those associated with the heart failure.[52] PKD1 is known to play an important role in reconciling stress-dependent remodeling and reprogramming of gene expression in the adult heart.[53] PKC-dependent signaling pathways play an important role in many facets of immune responses, from differentiation, activation and others.[54] Activation of DGK plays decisive role in controlling both innate and adaptive immune responses. It is also reported that the DAG levels are abnormally increased in the diabetic environment because of an enhancement of the glycolytic intermediate dihydroxyacetone phosphate. It has been observed that DAG-PKC activation pathway is also connected with diabetic neuropathy.[55] Activation of DAG-sensitive PKC isoforms, for example PKCθ and PKCε, down-regulates insulin receptor signaling. This might be important biochemical machinery linking dysregulated lipid metabolism and insulin resistance in muscle. Atypical PKC isozymes, for example PKCζ and PKCλ have been identified as downstream targets of PI-3-kinase and involved in insulin-stimulated glucose uptake.[56]

### 1.3. C1 domain: structure, function and regulation

The presence of a highly conserved cysteine-rich domain (CRD) with the motif $HX_{11/12}CX_2CX_nCX_2CX_4HX_2CX_{6/7}C$ (n varies between 12 and 14) has been identified in a number of proteins including PKCs, chimerins and diacylglycerol kinase (DGK).[57-60] Also it has been established that this motif may be duplicated in some proteins including DGK and PKCs (α-ε) while single copy is present in chimerin, PKCζ, RAF, VAV and others.[61] Based on the ligand binding properties, C1 domain is divided into two types as follows-(a) typical or phorbol ester/DAG responsive (b) atypical or phorbol ester/DAG unresponsive. Typical or DAG responsive C1 domain is present in conventional PKC (α, βI, βII, γ), novel PKC (δ, θ, ε, η), PKD (1, 2, 3), chimaerin (αI, αII, βI, βII), DAG Kinase (β, γ), Unc-13, Munc13 (1, 2, 3), RasGRPs (1, 2, 3, 4) and MRCK (α, β). Atypical or DAG unresponsive C1 domain are present in PKC (ζ, λ), DAG kinase (α, δ, η, ε, ζ, ι, θ), VAV (1, 2, 3), RAF-1, KSR (1, 2), ROCK (1, 2) and RASSF5.[1] Lim and coworkers showed that coordination of cysteine and histidine residues with $Zn^{2+}$ was indispensable for the structural integrity of C1 domain in chimerin, PKC and DGK.[61] High-resolution crystal structures of PKCα-, PKCγ-, and PKCδ-C1b domains (complexed with phorbol esters) have been published; these C1 domains adopt similar tertiary structures and function as hydrophobic switches to anchor PKCs to membranes.[5, 62-64]

PKCα-C1b was the first C1 domain whose structure was determined in 1994.[5, 62] The crystal structure of the C1b domain of PKCα has revealed a topology of two antiparallel β-sheets formed by three and two strands followed by an alpha-helix at the C-terminus.[65, 66] The residues involved in the coordination of the zinc were Cys14, Cys17, His39 and Cys42 for site I, and His1, Cys31, Cys34 and Cys50 for site II. The structure of the C1b domain of PKCα in complex with phorbol 13-acetate has shown that residues Met9–Thr12 and Leu21–Leu24, which comprise most of the β2 and β3-strands are responsible for the binding. The top-third of the C1 domain consists of hydrophobic residues, while the middle-third contains positively charged side chains. In the absence of phorbol ester, the hydrophilic groove between the strands β2 and β3 are filled by water molecules, which are displaced by C3, C4 and C20 oxygen of the phorbol ring, forming hydrogen bond and connecting the two strands. Phorbol binding to the Gly23, Thr12 and Leu21 form hydrophobic surface which makes it favorable for the interaction with the membrane.[64, 66] Later, it was established that six Cys residues, in addition to the two His-residues involved in $Zn^{2+}$ coordination and loops comprising amino acids Met9 to Phe13 and Leu20 to Gln27 were critical for the interaction of the C1b domain with phorbol esters.[67, 68] It has also been established that

the positively charged residues located at the middle-third of the binding pocket are indispensable for its interaction with negatively charged phospholipids and this facilitates the binding of phorbol esters and related ligands to PKC. A high resolution X-ray crystal structure of the PKCδ-C2 domain complexed with phorbol 13-acetate reveals details of the phorbol-protein interaction.[64] Solution structure analysis of second cysteine rich domain of PKC revealed that it consists of five β-strands and one α-helix. The zinc binding residues include H102, C132, C135, and C151 for site 1, with H140, C115, C118, and C143 for site 2. The residues involved in the phorbol ester binding are S111, T113, F114, L122, Y123, and G124. Also the titration with lipid micelles revealed that only top half of the cys2 domain apparently inserts into the lipid micelle.[69] Based upon a NMR-determined solution structure of the second cysteine rich domain of PKCα, molecular modeling was used to study the structures of the complexes formed between the PKC receptor and a number of PKC ligands, phorbol esters, and DAGs. The binding site for phorbol esters and DAGs is located in a highly conserved, hydrophobic loop region formed by residues 6-12 and 20-27.[70] The crystal structure analysis of C1b domain of PKCβII showed that phorbol ester and DAG binding site on the C1b domain is surrounded on three sides by an extremely hydrophobic rim formed by the exposed side chains of (PKCβII numbering) Pro112, Phe114, Tyr123, and Leu125. The residues responsible for membrane penetration, Tyr123 and Leu125 are buried against the catalytic domain which partially open structure and renders them unavailable for membrane penetration.[71] The presence of Lys22 in PKD-C1b which is replaced by hydrophobic residues like tryptophan, tyrosine and phenylalanine in typical C1 domains, was found to be responsible for its weaker binding affinity towards Dioleoylglycerol (DOG) as compared to its C1a domain.[72] Based on structural differences atypical C1 domains are divided into two types: The first subclass C1 domains are grossly distorted in the binding cleft geometry due to the absence of the key residues in the loop making up the binding cleft e.g. c-Raf or KSR. Members of the second subclass retain the binding cleft geometry but incorporate other factors impeding ligand binding, e.g. atypical PKC.[73] The ligand binding regions identified in the C1 domain are the loops between β1 and β2 strands (β1-β2) and β3 and β4 strands (β3-β4). It has been observed that for typical C1 domains both these loops are flexible enough to accommodate the ligand. But solution structure of the atypical C1 domains of C-Raf and KSR showed that only β1-β2 loop is flexible while β3-β4 loop is immobilized due to the deletion of different residues.[74, 75] We showed that, in the case of the atypical PKCs, a series of three arginine residues lining the rim of the binding pocket were able to rotate into the cleft, making it inaccessible to ligands. Replacement of these arginine residues

with the corresponding residues found in the C1b domain of PKC generated high affinity towards DAG/phorbol ester.[76]

C1 domain mediated activation mechanism initiates through the interaction of the positively charged residues present outside the binding pocket with the anionic lipids of the membrane.[77] This initial interaction anchors the C1 domain to the membrane bilayer and allow to bind specifically with DAG, which is located more deeply within the membrane structure. DAG bind to a narrow polar groove in the otherwise highly conserved hydrophobic surface at the top of the C1 domain (formed by the C1A-Trp58/Phe60 pair and the C1b-Tyr123/Leu125 pairs in PKCα-C1a and C1b domains), and cognate residues in other PKC isoforms. Therefore, capping of this hydrophilic ligand-binding pocket (i.e., generation of a continuous hydrophobic surface), lipid cofactors act as "molecular glue" to increase membrane binding affinity of the C1 domain.[74, 75] Some C1 domains (such as the C1 domain of PKCα) appear to be buried in the resting state and exposed (becoming accessible to DAG/PMA) only following the conformational change that accompanies calcium-dependent membrane binding through the C2 domain of PKC.

The regulatory domains of conventional and novel PKCs have two C1 domains (C1a and C1b) that have been identified as the interaction site for DAG and phorbol ester. The activation mechanism of classical PKC studied by fluorescence imaging revealed that interaction of C1 domain with DAG is indispensable for its activation.[12] Matured PKC in the cytoplasm is in inactive form as the pseudo-substrate region occupies the active site of the kinase domain. When the intracellular calcium level is increased, PKC is recruited to the plasma membrane though C2 domain, which is a calcium dependent lipid binding domain. Then DAG presents in the membrane binds the C1 domain which releases the kinase domain for phosphorylation and autophosphorylation. On the other hand mechanistic study of activation of PKCδ, a novel PKC, revealed that its C2 domain is involved neither in membrane binding nor in its activation. C1a and C1b domains differ in their ligand binding properties. The isolated C1a domain of PKCδ has much higher DAG affinity than the C1b domain, and thus under physiologically relevant conditions only the C1a domain is expected to bind DAG.[78] The C1 domains of nPKCs bind DAG-containing membranes with 2-orders of magnitude higher affinity than those of cPKCs [79]. It has been observed by mutational analysis that the presence of Trp22 in novel PKC which is substituted by Tyr in classical PKC accounts for difference in their binding affinity for DAG. The atypical C1 domain has been implicated in interaction with the second messenger ceramide [73, 76], and with other proteins.[77, 78]

The PKD family is a serine threonine kinase and they have been identified as a subgroup of calcium/calmodulin-dependent protein kinase (CAMK) family based on sequence similarities of the catalytic domains. Similar to PKC, it has an N-terminal kinase domain and C-terminal catalytic domain. The autoinhibitory regulatory domain consists of tandem repeats of C1 domains (C1a and C1b) and a PH domain. C1a and C1b domains differ in their ligand binding affinity e.g. C1b domain of all PKD isoforms have higher affinity towards [3H]PDBu but lower affinity towards synthetic DAG analogues.[80-83] DGK belongs to the lipid kinase that phosphorylates DAG to yield PA and thus modulates their intracellular level. Though it contains five isozymes, only C1 domain of DGKβ and DGKγ are DAG and Phorbol ester responsive. These two isoforms are in inactive form in the absence of $Ca^{2+}$.The conformational change induced by the binding of $Ca^{2+}$ to the EF hand motifs activates the enzyme. The C1 domain of DGK only acts as membrane targeting and protein-protein interaction module.[85, 86] Munc-13s contain a variable N-terminal region that may include C2 domain, and a conserved C-terminal region that includes two C2 domains and in most cases a C1 domain. The large MUN domain between the central and the C-terminal C2 domain takes part in protein-protein interaction. The Munc13-C2 domains play a role in phospholipid recognition in a calcium-independent or calcium-dependent manner, depending on the C2 domain: only the C2b domains are sensitive to $Ca^{2+}$. Immediate to the N-terminal of the C1 domain there is a short sequence of amino acids that serves as a calmodulin binding site and participates in the $Ca^{2+}$-dependent regulation of Munc-13 function. The C1 domains of Unc13 and Munc13-1 bind [3H]PDBu in a phospholipid-dependent manner with low nanomolar affinity. They also bind to DAG and other C1 domain ligands with affinities close to that of PKCδ-C1b domain, and Munc13 isoforms translocate to plasma membrane upon phorbol 12-myristate 13-acetate (PMA) treatment.[86, 87] Chimaerins consist of four isoforms-α1, β1, α2 and β2 and all are Rac GTPase-activating proteins. Isoforms α1 and β1 possess a single C1 domain in the N-terminus and a C-terminal Rac-GAP domain, while the α2 and β2 chimaerins, contain an additional Src homology 2 (SH2)-domain in their N-terminus. The chimaerins bind phorbol esters in a C1 domain-dependent manner sharing similarity with PKCα regarding ligand binding properties and phospholipid requirement. The role of DAG seems to be more in targeting α2- and β2-chimaerins to the membrane than in activating them. The target of chimaerin actions, the small GTPase Rac, is a central regulator of actin cytoskeleton organization, cell migration, transformation, cell cycle progression and gene expression. Chimaerins participate in regulating these phenomena by inhibiting Rac activity in response to GPCR- or RTK-initiated

DAG production.[88, 89] The Ras guanyl releasing protein (RasGRP) modulates the Ras family of small GTPases and thus involved in signal transduction pathways which modulate cell growth and cytoskeletal rearrangements. The C1 domain of RasGRPs is highly homologous to the C1 domain of PKC.[88] In cells, the isolated C1 domains of RasGRP1, RasGRP3 and RasGRP4α co-localize with membranes and relocalize in response to DAG, whereas the C1 domains of RasGRP2 and RasGRP4β do not. RasGRP binds to phorbol 12,13-dibutyrate (PDBu) with nanomolar affinity through its C1 domain. Structure-activity analysis of several phorbol esters revealed that the ligand selectivity of C1-RasGRP is somewhat different from that of C1b-PKC and that the binding of C1-RasGRP to phorbol esters is dependent on the presence of phospholipids. The functions of RasGRPs have been best characterized in the cells of the immune system. RasGRP1 is a central mediator of T cell receptor signaling[90, 91], and indispensable for natural killer (NK) cell cytotoxicity and cytokine production. MRCKs are serine/threonine kinases and consist of three isoforms-α, β and γ. MRCK contains an N-terminal catalytic domain followed by a number of regulatory domains like CC domain, C1 domain, PH domain, CH domain and PBD domain. MRCK is in the inactive form due to the interaction of the kinase domain with the CC domain which is released by C1 domain-Phorbol ester binding leading to the activation of the enzyme.[92-96]

The dependence of PKC activation on the lipid cofactor and $Ca^{2+}$ was first identified by Yasutomi Nishizuka and coworkers.[97] Membrane properties regulated by the phospholipids containing different headgroup conformation also modulate PKC activity. It was observed that PKC affinity to the DAG-containing membrane is increased by two fold in presence of PS and PE while only one fold enhancement is observed in presence of PG.[98] Also it was observed that phosphatidyl-L-serine (L-PS) had greater ability to activate PKC than phosphatidyl-D-serine (D-PS).[99] The *in vitro* binding mechanism of PKCα revealed that the protein initially binds to the membrane surface via the $Ca^{2+}$ dependent PS binding of the C2 domain.[103] It has also been observed that the interaction of PS with C2 domain disrupts the C1-C2 interdomain interaction and release the C1a domain to penetrate into the membrane where it binds DAG.[100]

### 1.4. Role of lipophilic molecules on the modification of membrane properties and C1 domain mediated activation

Formation of the ternary complex C1 domain-ligand-membrane is the key requirement for activation of PKC and other DAG effectors. Cell membrane consists of numerous lipids, ion channels, proteins and other biomolecules which regulates the biophysical properties of the

membrane. C1 domain mediated PKC activation is greatly modulated by membrane biophysical properties. Hence, membrane lipid components other than DAG/PMA that directly don't bind with PKC can significantly modify its activity.

Several studies are carried out on the role of lipophilic molecules on modification of membrane properties and PKC activation. In 1993, a study carried out by Stubb and coworkers first showed that PKC activity is modulated by headgroup spacing and bilayer curvature of the membrane.[101] It was demonstrated that the introduction of unsaturation in the lipids modifies the membrane physical properties which enhances the PKC activation.[102] The importance of hexagonal phase promoting lipid in PKC activation was first observed by Epand et al in 1998. They forwarded the concept that this kind of lipid allows more headgroup separation which makes the acyl chain more accessible to PKC interaction.[103] DAG itself also introduces a number of membrane modification which induce PKC activation e.g.: changes in lipid headgroup conformation, interspacing and hydration, changes in the bilayer propensity to form inverted nonlamellar phases, and lateral phase separations of DAG-rich and -poor domains.[104] It was demonstrated that the presence of polyunsaturated unesterified fatty acids(PUFAs) solubilize a portion of saturated DAG in the liquid crystalline phase which makes it available for the PKC interaction.[105] The synergism between DAG and different fatty acids in enhancing PKC activation was also attributed to the formation of non-bilayer phases.[106] Research carried out on the effect of ceramide on DAG induced PKC activation proved that increased tendency to form nonbilayer lipid phases increases PKC activity while the actual presence of such phases decreases PKC activity.[107] Both theoretical and experimental studies have claimed that cholesterol has a profound effect on PKC activation. Cholesterol, with a small headgroup and large body is structurally similar to DAG and promotes the formation of non-bilayer phases and thus enhances the PKC activity.[108] DAG-lactone, a reported PKC activator showed different translocation of PKC depending upon the substitution at the acyl position with different hydrophobic moieties. It was demonstrated that Synthetic DAG lactones modify the membrane properties like fluidity, lamellar to non-lamellar phase transition etc. which are directly related to PKC activity.[109, 110]

Thus PKC activation is regulated by a number of membrane properties like headgroup spacing, bilayer curvature, interspacing, hydration, and fluidity and lamellar to non-lamellar phase transition temperature etc. Also, PKC activity is enhanced by the increased tendency of the membrane to form hexagonal and non-bilayer phases. As a result, different lipophilic

molecules present in the membrane significantly modulate PKC activity by altering physical properties or inducing the formation of different phases of the membrane.

### 1.5. C1 domain ligands

The involvement of C1 domain mediated signal transduction in different diseases emphasized the development of drugs targeted to this domain. The detailed understanding of the structure and function of C1 domain and its role in DAG-signaling pathways has provided a solid basis for the rational and semi-rational drug designing. The designing of isoenzyme specific drugs for C1 domain is very challenging due to its highly homologous identity (60-80%) among the isozymes.

The major classes of C1 domain ligands are discussed in this section:

**Phorbol ester and its analogs-** Phorbol esters are tetracyclic diterpenoids occur naturally in many plants of the family euphorbiacaeae and thymelaeaceae.[111] Based on the hydroxyl group at the position-4, they are classified into two types-active and inactive and their biological activities are highly structure specific. The extremely potent tumor promoters are β-Phorbol esters which bind to the C1 domains with high affinity while no affinity to the C1 domain is exhibited by inactive α-phorbol esters and are devoid of tumor promoting activity. The actual isomer that mimics the actions of DAG, but with a binding affinity three orders higher than DAG is 4β-Phorbol ester.[34] PMA (also known as 12-O-tetradecanoylphorbol-13-acetate [TPA]) and PDBu have been universally accepted as the best prototypes of PKC activators and used by the researchers in investigating the roles of PKCs and other DAG effectors in physiology. Phorbol esters activate PKC by altering the surface hydrophobicity of the C1 domain, thus promoting the membrane interaction without changing the conformation of the protein. The insertion of the protein into the membrane induced by phorbol ester is irreversible and calcium independent, but dependent on the lipophilicity of the phorbol esters and the PS concentrations. Though they mimic the action of DAG but they are well known as tumor promoters.[111]. Phorbol esters also have antiproliferative, differentiating and proapoptotic effects in various cancer cell lines.[112-114] Prostratin (12-deoxyphorbol-13-acetate) and DPP (12-deoxyphorbol-13-phenylacetate) are non-tumor-promoting phorbol derivatives that also activate PKCs and exhibit potent *in vitro* efficacy in the activation of latent HIV reservoirs and thus represent promising adjuvant for antiretroviral therapy. Phorbol esters also bind to the non-PKC C1 domain, such as Munc13.1, Unc13.1, chimerins,

Ras-GRP3, PKD3 and DGK86 with affinity in the high nanomolar range. Similar to the PKC C1 domains, the binding affinity of DAG is less as compared to the phorbol esters.[115]

**Diacylglycerol (DAG)-** Diacylglycerols are glycerol derivatives, in which two hydroxyl groups are esterified by fatty acids. They are important intermediates in the biosynthesis and degradation of triglycerides, glycerophospholipids and glyceroglycolipids. In plasma membrane, DAG is produced by the hydrolysis of phosphatidylinositol (PIP) or phosphatidylcholine (PC) by phospholipase C. All typical C1 domains respond to DAG through the phorbol ester binding site. Only 1,2-sn-diacylglycerols serves the purpose, other isomers are inactive due to their different conformation in the lipid bilayer. But the activation mechanism of the PKC and the other such enzymes by DAG is complex because DAG exerts multiple effects on the properties of both the protein and lipid bilayer. It has also been demonstrated that both phenomenon may work synergistically in the activation of enzymes. DAG dependent conformational changes induced the enzymes to translocate to the plasma membrane for proper activation. DAG also induces changes on the lipid bilayer properties e.g. propensity to form nonlameller phases, increase negative curvature, dehydration, headgroup spacing, lateral phase separation and others. Also it has been demonstrated that cis-unsaturated DAG and short chain DAG's act as the better activator due to their partition into the fluid domain. DAG is one of the key second messengers mediating immune cell signaling, and several families of DAG effectors, particularly PKC and RasGRPs, have been implicated in regulating immune responses.[13, 116]

**Bryostatins and their synthetic analogues-** Bryostatins are a family of 20-macrocyclic lactones produced by a bacterial symbiont of the bryozoan Bugula neritina.[118] The presence of 11-asymmetric centers adds complexity to the molecule. Only, bryostatin 1 has been found as the ideal C1 domain ligand and its pharmacological effects are extensively studied. Bryostatin 1 competes with the phorbol-ester-binding site of PKCα with very high affinity (1.35 nM), although its selectivity for different C1 domains is very poor. It also binds to C1 domains of PKD, RasGRP, and β-chimaerin with high nanomolar affinities. Bryostain 1 is totally devoid of tumour promoting activity and suppresses the effects of phorbol esters like TPA. Bryostatin 1-induced translocation of PKCδ is dependent on both C1a and C1b domains. It also exhibits biphasic concentration dependent effects in many biological responses such as PKCδ down-regulation and PKD activation.[4, 119-122] Bryostatins are promising candidate in the development of anticancer drugs as it shows inhibition of tumour

growth and invasion. Bryostain 1 also found wide applicability in the research area of Alzheimer disease as it reduces the levels of pathologic Aβ fragments in brains of transgenic AD mice. Being neuroprotective and neurorestorative, it may have potential in the treatment of ischemic stroke, a complication arises when an artery to the brain is blocked.[6, 123, 124] Various bryostatin analogous are synthesized which differs in their selectivity and affinity to different isoforms of PKC and non-PKC enzymes. These are together classified from the natural bryostatin by the name "bryologues" and show promises as anticancer agents and also as activators of latent HIV reservoirs in the eradication of HIV.[125-128]

**Ingenol derivatives-** Macrocyclic diterpene ingenol derivatives share structural similarity with phorbol esters, differing in the presence of seven membered rings and the number and position of hydroxy, carbonyl, and carboxy ester groups. Ingenol-3-angelate, extracted from the sap of the plant euphorbia peplus, has shown promise in the treatment of skin cancer and has been approved by FDA and EMA in 2012 for the treatment of actinic keratosis. It exhibits subnanomolar affinity towards PKC-C1 domain without much selectivity among different isoenzymes. While it acts as an inhibitor for the proliferation of various cancer cell lines and primary acute myeloid leukaemia (AML), it also promotes survival of resting and activated human T cells by activating PKCθ. It has also undergone clinical trial in superficial basal cell carcinoma and its efficacy in other potential indications, such as non-melanoma skin cancers and leukaemia remains to be elucidated. Another compound of this series, ingenol-3-benzoate, has been studied extensively for its binding to different C1 domains, and moderate differences in the binding affinity between the C1a and C1b subdomains of α, δ, and ε were observed.[129, 130]

**Indolactams and benzolactams-** Indolactams were first isolated from Streptomyces mediocidicus. They are indole alkaloids of teleocidin family, containing a core structure of indolactam V. Benzolactams are analogs in which the indole ring is replaced by a benzene ring. These lactam based compounds act as both tumor promoter and inhibitor depending upon the cell lines. They have been shown to strongly bind to the C1 domains of RasGRPs, PKD, phorbol-responsive DGKs, Munc13 and chimaerins. They are also involved in translocation and down-regulation of PKCs. Indolactam and benzolactam derivatives have been reported to inhibit proliferation of several cancer cell lines. Benzolactam derivatives have also shown potential efficacy in both cell-based models of Alzheimer's disease and in a transgenic mouse model of AD. Furthermore, (−)-indolactam V has been identified as an

inducer of human embryonic stem cell differentiation to the pancreatic lineage , partly mediated by PKC activation.[131, 132]

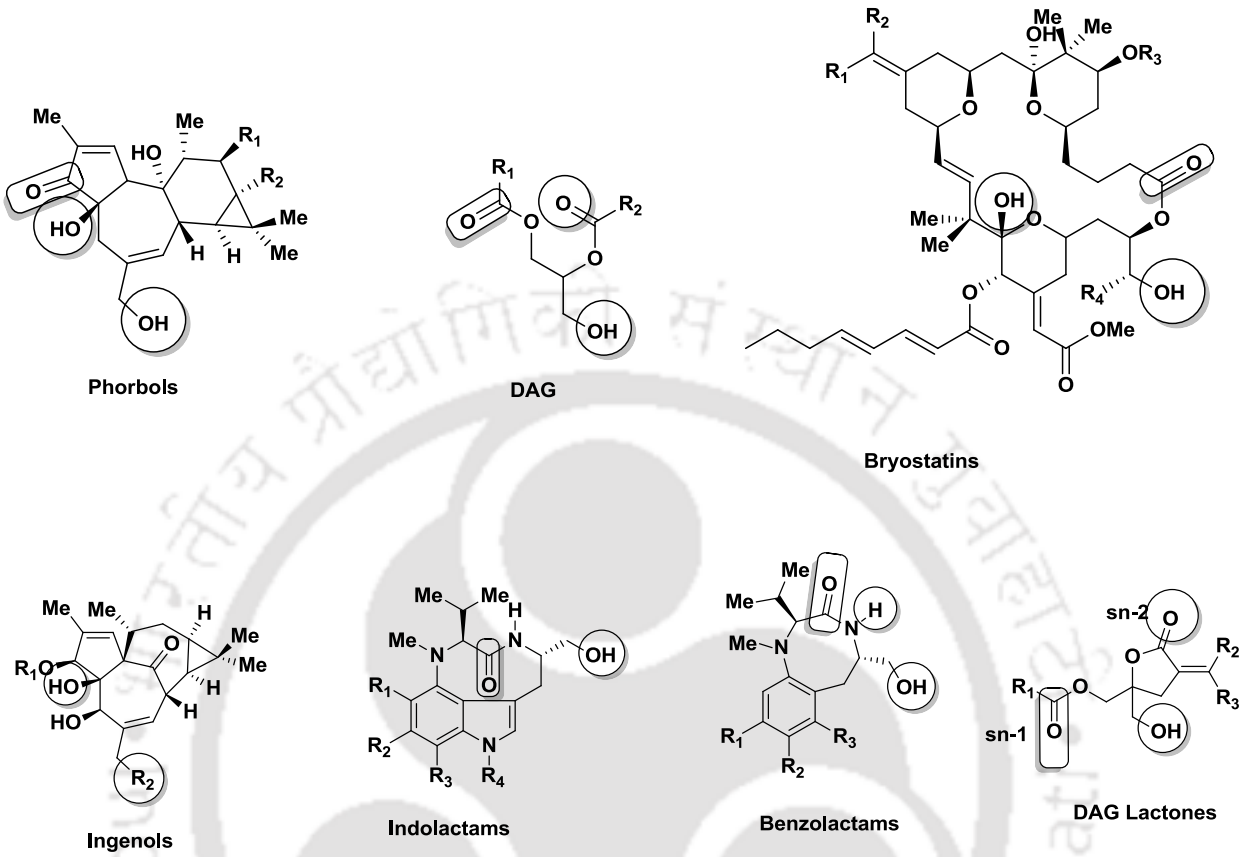


**Figure 1.1.** C1 domain ligands showing the pharmacophores for binding.

**DAG lactones**- The effort in develop conformationally constrained analog DAG led to the development of a new class of C1 domain ligand DAG-lactones. The binding affinities of these DAG-lactones can be easily modulated by altering the lipophilicity and the hydrophilicity of the acyl chain. DAG-lactone binds C1 domain of RasGRP with 100 fold selectivity than PKCα. A DAG-lactone has also been shown to bind to the C1 domains of MRCKα and β, but with lower affinity than PKCs. DAG lactones showed anti-proliferative and pro-apoptotic effects in several cancer cell lines. The DAG-lactone template is considered as a powerful research tool in designing PKC activators. DAG-lactones have extensively been used in studies to explore ligand-C1 domain interactions and interactions of the ligand-C1 domain complex with cellular membranes, thus providing useful information for the design of novel C1 domain ligands.[105, 133.

### 1.7. Concluding remarks

Overall, PKC enzyme dependent phosphorylations of serine and/or threonine residues activate the target protein. In this regard, PKC enzymes play an important role in several physiological and pathophysiological events including, cell proliferation, differentiation, malignant transformation and cancer, diabetes, stroke, heart failure, Alzheimer's disease and others. Recent studies demonstrated that the cellular functions of PKCs can be regulated through its C1 domain. Therefore proper understanding of C1 domain dependent ligand-binding mechanism is essential to properly regulate the functioning of the PKC enzyme. There are many reports where C1-DAG/phorbol ester interaction has been successfully characterized in molecular levels, which immensely help in designing C1 domain ligands and drug developments. A number of *in-vitro* biophysical studies as well as membrane translocation study in cell have been employed. Mutational studies provide the idea of exact role of interacting residues as well as the role of hydrophobic residues in membrane interaction. To date DAG-dependent membrane binding nature of several PKCs, chimerins, Muncs, VAV and other C1 domain containing proteins have been thoroughly characterized. However, mechanistic studies of DAG/phorbol ester binding of the C1 domain of MRCKs have not been described.

Several natural compounds (e.g. bryostatin 1) have been identified, that show potent binding to the C1 domain of PKC enzymes. The C1 domain binding ligands can be obtained from natural sources, but the isolated yields are usually very low with a need to be produced from sensitive ecosystems such as seas and oceans. In addition, the compounds repeatedly have highly complex structures; consequently the total syntheses of the compounds are difficult. Nevertheless, studies with these compounds have resulted valuable pharmacophores, which have been used to develop structurally simplified synthetic analogues of the complex natural compounds. For example, several research groups have achieved in simplifying the chemical structure of the natural bryostatins and those derivatives showed better potency than natural bryostatins. In addition, by using the pharmacophors of phorbol ester, newly designed compounds showed increased binding affinities for the PKC as well as decreased the reaction steps. Furthermore, synthesized compounds like indo- and benzolactams have also shown a strong binding affinity for the C1 domain of PKCs and also considered as potent drug candidates for the treatment of cancer. Conformationally constrained DAG-lactones are the other family of potent C1 domain ligands that depict a good correlation between the synthetic small molecules and PKC activity. Therefore these

studies recommend that synthesis of C1-domain targeted small molecules is very important in developing PKC regulators.

**References**

1. Y. Ono, T. Fujii, K. Igarashi, T. Kuno, C. Tanaka, U. Kikkawa, and Y. Nishizuka, *Proc. Natl. Acad. Sci. U. S. A.*, 1989, **86**, 4868–4871.

2. D. J. Burns and R. M. Belly, *J. Biol. Chem.*, 1991, **266**, 18330-18338.

3. A. C. Newton, *J. Biol. Chem.*, 1995, **270**, 28495–28498.

4. M. J. Caloca, N. Fernandez, N. E. Lewin, D. Ching, R. Modali, P. M. Blumberg and M. G. Kazanietz, *J. Biol. Chem.*, 1997, **272**, 26488-26496.

5. M. J. Caloca, M. L. Garcia-Bermejo, P. M. Blumberg, N. E. Lewin, E. Kremmer, H. Mischak, S. Wang, K. Nacro, B. Bienfait, V. E. Marquez and M. G. Kazanietz, *Proc. Natl. Acad. Sci.*, 1999, **96**, 11854-11859.

6. M. J. Caloca, H. Wang, A. Delemos, S. Wang and M. G. Kazanietz, *J. Biol. Chem.*, 2001 **276**, 18303-18312.

7. M. J. Caloca, H. Wang and M. G. Kazanietz, *Biochem. J.*, 2003, **375**, 313-321.

8. S. Etienne-Manneville and A. Hall, *Nature*, 2002, **420**, 629-635.

9. N. A. Dower, S. L. Stang, D. A. Bottorff, J. O. Ebinu, P. Dickie, H. L. Ostergaard and J. C. Stone, *Nat. Immunol.*, 2000, **1**, 317-321.

10. J. O. Ebinu, S. L. Stang, C. Teixeira, D. A. Bottorff, J. Hooton , P. M. Blumberg , M. Barry, R. C. Bleakley, H. L. Ostergaard and J. C. Stone, *Blood*, 2000, **95**, 3199-3203.

11. E. M. Griner and M. G. Kazanietz, *Nat. Rev. Cancer*, 2007, **7**, 281-294.

12. T. Geczy, M. L. Peach, S. E. Kazzouli, D. M. Sigano, J.-H. Kang,C. J. Valle, J. Selezneva, W. Woo, N.i Kedei, N. E. Lewin, S. H. Garfield,‖ L. Lim,‖ P. Mannan,‖ V. E. Marquez, and P. M. Blumberg, *J. Biol. Chem.*, 2012, **287**, 13137–13158.

13. S. Carrasco and I. Mérida, *Trends Biochem. Sci.*, 2007, **32**, 27–36.

14. M. P. Wymann and R. Schneiter, *Nat. Rev. Mol. Cell Biol.*, 2008, **9**, 162-176.

15. G. Furstenberger, D. L. Berry, B. Sorg and F. Marks, *Proc. Natl Acad. Sci. USA*, 1981, **78**, 7722-7726.

16. P. M. Blumberg, N. Kedei, N. E. Lewin, D. Yang, G. Czifra, Y. Pu, M. L. Peach, and V. E. Marquez, *Curr. Drug Targets*. 2008, **9**, 641–652.

17. J.-H. Kang, *New Journal of Science*, 2014, doi:10.1155/2014/231418.

18. Y. Matsuzaki, Y. Takaoka, T. Hitomi, H. Nishino and T. Sakai, *Oncogene*, 2004, **23**, 5409–5414.

19. C. R. LaValle, K. M. George, E. R. Sharlow, J. S. Lazo, P. Wipf and Q. J. Wanga, *Biochim. Biophys. Acta.* 2010, **1806**, 183–192.

20. O. Ksionda, A. Limnander, and J. P. Roose, *Front. Biol.*, 2013, **8**, 508–532.

21. S. Yuan, D. W. Miller, G. H. Barnett, J. F. Hahn and B. R. Williams, *Cancer Res*., 1995, **55**, 3456-3461.

22. C. Yang, Y. Liu, F. C. Leskow, V. M. Weaver and M. G. Kazanietz, *J. Biol. Chem.*, 2005, **280**, 24363-24370

23. J. P. MacKeigan, L. O. Murphy and J. Blenis, *Nat. Cell. Biol.*, 2005, **7**, 591-600.

24. T. Matsubara, Y. Shirai, K. Miyasaka, T. Murakami, Y. Yamaguchi, T. Ueyama, M. Kai, F. Sakane , H. Kanoh, T. Hashimoto, S. Kamada, U. Kikkawa and N. Saito , *J. Biol. Chem.*, 2006, **281**, 6152-6164.

25. S. Yasuda, M. Kai, S. Imai, H. Kanoh and F. Sakane, *FEBS Lett.*, 2007, **581**, 551-557.

26. F. Sakane, S. Imai, M. Kai, S. Yasuda and H. Kanoh, *Curr. Drug Targets*, 2008, **9**, 626-640.

27. Y. Song, M. Ailenberg, and M. Silverman, *Mol. Biol. Cell*, 1999, **10**, 1609–1619.

28. T. Leung, X.-Q. Chen, I. Tan, E. Manser and L. Lim, *Mol. Cell Biol.*, 1998, **18**, 130–140.

29. I. Tan, C. H. Ng, L. Lim and T. Leung, *J. Biol. Chem.*, 2001, **276**, 21209–21216.

30. Y. Zhao, P. Loyer, H. Li, V. Valentine, V. Kidd and A. S. Kraft, *J. Biol. Chem.*, 1997, **272**, 10013–10020.

31. L. J. van 't Veer, H. Dai, M. J. van de Vijver, Y. D. He, A. A. Hart, M. Mao, H. L. Peterse, K. van der Kooy, M. J. Marton, A. T. Witteveen, G. J. Schreiber, R. M. Kerkhoven, C. Roberts, P. S. Linsley, R. Bernards and S. H. Friend, *Nature*, 2002, **415**, 530-536.

32. S. Balasenthil, N. Chen, S. T. Lott, J. Chen, J. Carter, W. E. Grizzle, M. L. Frazier, S. Sen, A. M. Killary, *Cancer Prev. Res.*, 2011, **4**, 137–149.

33. K. Lefort, A. Mandinova, P. Ostano, V. Kolev, V. Calpini, I. Kolfschoten, V. Devgan, J. Lieb, W. Raffoul and D. Hohl, *Genes Dev.*, 2007, **21**, 562–577.

34. D. R. Rhodes, J. Yu, K. Shanker, N. Deshpande, R. Varambally, D. Ghosh, T. Barrette, A. Pandey, A. M. Chinnaiyan, *Neoplasia*, 2004, **6**, 1–6.

35. D. Pyeon, M. A. Newton, P. F. Lambert, J. A. den Boon, S. Sengupta, C. J. Marsit, C.D. Woodworth, J. P. Connor, T. H. Haugen and E. M. Smith, *Cancer Res*, 2007, **67**, 4605–4619.

36. J. Schlingemann, N. Habtemichael, C. Ittrich, G. Toedt, H. Kramer, M. Hambek, R. Knecht, P. Lichter, R. Stauber and M. Hahn, *Lab. Invest*, 2005, **85**, 1024–1039.

37. M. A. Ginos, G. P. Page, B. S. Michalowicz, K. J. Patel, S. E. Volker, S. E. Pambuccian, F. G. Ondrey, G. L. Adams and P. M. Gaffney, *Cancer Res.*, 2004, **64**, 55–63.

38. S. M. Kim, Y. Y. Park, E. S. Park, J. Y. Cho, J. G. Izzo, D. Zhang, S. B. Kim, J. H. Lee, M. S. Bhutani and S. G. Swisher, *PLoS One*, 2010, **5**, 1-8.

39. S. Wang, M. Zhan, J. Yin, J. M. Abraham, Y. Mori, F. Sato, Y. Xu, A. Olaru, A. T. Berki and H. Li, *Oncogene*, 2006, **25**, 3346–3356.

40. Y. Hao, G. Triadafilopoulos, P. Sahbaie, H. S. Young, M. B. Omary and A. W. Lowe, *Gastroenterology*, 2006, **131**, 925–933.

41. F. Desdouits, J. D. Buxbaum, J. Desdouits-Magnen, A. C. Nairn and P. Greengard, *J. Biol. Chem.*, 1996, **271**, 24670–24674.

42. D. Ibarreta, M. Duchen, D. Ma, L. Qiao, A. P. Kozikowski and R. Etcheberrigaray, *NeuroReport*, 1999, **10**, 1035–1040.

43. C. Jolly-Tormetta and B. A. Wolf, *Biochemistry*, 2000, **39**, 7428–7435.

44. S. W. Yeon, M. W Jung., M. J. Ha, S. U.Kim, K. Huh, M. J.Savage, E. Masliah and I. Mook-Joung, *Biochem. Biophys. Res. Commun*, 2001, **280**, 782–787.

45. S. Rossner, K. Mendl, R. Schlie and l. V. Big, *Eur. J. Neurosci.*, 2001, **13**, 1644–1648.

46. A. P. Kozikowski, I. Nowak, P. A. Petukhov, R. Etcheberrigaray, T. M. Mohamed, N. Lewin, H. Hennings, L. L. Pearce and P. M. Blumberg, *J. Med. Chem.*, 2003, **46**, 364–373.

47. S. Bhagavan, D. Ibarreta, D. Ma, A. P. Kozikowski and R. Etcheberrigaray, *Neurobiol.*, 1998, **5**, 177–187.

48. T. Kinouchi, H. Sorimachi, K. Maruyama, K. Mizuno, S. Ohno, S. Ishiura, and K. Suzuki, *FEBS Lett.*, 1995, **364**, 203–206.

49. J. L. Garrido, J. A. Godoy, A. Alvarez, M. Bronfman and N. C. Inestrosa, *FASEB J.*, 2002, **16**, 1982–1984.

50. S. Rossner, K. Fuchsbrunner, C. Lange-Dohna, M. Hartlage-Rübsamen, I. V. Big, A. Betz, K. Reim and N. Brose, *J. Biol. Chem.*, 2004, **279**, 27841-27844.

51. M. Hartlage-Rübsamen, A. Waniek and S. Rossner, *Int. J. Dev. Neurosci.*, 2013, **31**, 36-45.

52. S. S. Palaniyandi, L. Sun, J. C. B. Ferreira and D. M. Rosen, *Cardiovasc. Res.*, 2009, **82**, 229–239.

53. J. Fielitz, M.-S. Kim, J. M. Shelton, X. Qi, J. A. Hill, J. A. Richardson, R. Bassel-Duby, and E. N. Olson, *PNAS*, 2008, **105**, 3059–3063.

54. S.-L. TAN and P. J. Parker, *Biochem. J.*, 2003, **376**, 545–552.

55. H. Noh and G. L. King, *Kidney International*, 2007, **72**, 49–53.

56. I. Idris, S. Gray and R. Donnelly, *Diabetologia*, 2001, **44**, 659-673.

57. P. J. Parker, L. Coussens, N. Totty, L. Rhee, S. Young, E. Chen, S. Stabel, M. D. Waterfield and A. Ullrich, *Science*, 1986, **233**, 853-859.

58. L. Coussens, P. Parker, L. Rhee, T. L. Yang-Feng., E. Chen, M. D. Waterfield, U. Francke and A. Ullrich, *Science*, 1986, **233**, 859-866.

59. C. Hall, C. Monfries, P. Smith, H. H. Lim, R. Kozma, S. Ahmed, V. Vannaisingham, T. Leung and L. J. Lim, *Mol. Biol.*, 1990, **211**, 11-16.

60. D. Schaap, J. de Widt, J. van der Wal, J. Vandekerckhove, J. van Damme, D. Gussow, H. Pleogh, W. J. van Blittenswijk and R. L. van der Bend, *FEBS Lett.*, 1990, **275**, 151-158.

61. S. Ahmed, R. Kozma, J. Lee, C. Monfries, N. Harden and L. Lim, *Biochem. J.*, 1991, **280**, 233-241.

62. U. Hommel, M. Zurini and M. Luyten, *Nat. Struct. Biol.*, 1994, **1**, 383–387.

63. R. X. Xu, T. Pawelczyk, T. H. Xia and S. C. Brown, *Biochemistry*, 1997, **36**, 10709–10717.

64. G. Zhang, M. G. Kazanietz, P. M. Blumberg and J. H. Hurley, *Cell*, 1995, **81**, 917–924.

65. U. Hommel, M. Zurini and M. Luyten, *Nat. Struct. Biol.*, 1994, **1**, 383-387.

66. S. Ichikawa, H. Hatanaka, Y. Takeuchi, S. Ohno and F. Inagaki, *J. Biochem.*, 1995, **117**, 566-574.

67. A. F. Quest, E. S. Bardes and R. M. Bell, *J. Biol. Chem.*, 1994, **269**, 2953-2960.

68. M. G. Kazanietz, N. E. Lewin, J. D. Bruns and P. M. Blumberg, *J. Biol. Chem.*, 1995, **270**, 10777-10783.

69. R. X. Xu, T. Pawelczyk, T.-H. Xia and S. C. Brown, *Biochemistry*, 1997, **36**, 10709–10717.

70. S. Wang, M. G. Kazanietz, P. M. Blumberg, V. E. Marquez and G. W. A. Milne, *J. Med. Chem.*, 1996, **39**, 2541-2553.

71. T. A. Leonard, B. Różycki, L. F. Saidi, G. Hummer and J. H. Hurley, *Cell*, 2011, **144**, 55–66.

72. J. Chen, F. Deng, J. Li and Q. J. Wang, *Biochem. J.*, 2008, **411**, 333–342.

73. T. Geczy, M. L. Peach, S. E. Kazzouli, D. M. Sigano, J.-H. Kang, C. J. Valle, J. Selezneva, W. Woo, N. Kedei, N. E. Lewin, S. H. Garfield, L. Lim, P. Mannan, V. E. Marquez and P. M. Blumberg, *J. Biol. Chem*, 2012, **287**, 13137–13158.

74. W. Cho, *J. Biol. Chem.*, 2001, **276**, 32407–32410.

75. J. H. Hurley, S. Misra, *Annu. Rev. Biophys. Biomol. Struct.*, 2000, **29**, 49–79.

76. Y. Pu, M. L. Peach, S. H. Garfield, S. Wincovitch, V. E. Marquez and P. M. Blumberg, *J. Biol. Chem*, 2006, **281**, 33773–33788.

77. S. F. Steinberg, *Physiol. Rev.*, 2008, **88**, 1341–1378.

78. M. T. Diaz-Meco, M. M. Municio, P. Sanchez, J. Lozano and J. Moscat, *Mol. Cell. Biol.*, 1996, **16**, 105–114.

79. P. Geraldes, and G. L. King, *Circ. Res*., 2010, **106**, 1319–1331.

80. S. A. Matthews, T. Iglesias, E. Rozengurt and D. Cantrell, *Embo. J*., 2000, **19**, 2935–2945.

81. A. Rykx, L. D. Kimpe, S. Mikhalap, T. Vantusa, T. Seu¡erlein, J. R. Vandenheede and J. V. Lint, *FEBS Letters*, 2003, **546**, 81-86.

82. Q. J. Wang, *Trends Pharmacol. Sci.*, 2006, **27**, 317-323.

83. J. V. Lint, A. Rykx, T. Vantus, J. R. Vandenheede, *Int. J. Biochem. Cell Biol.*, 2002, **34**, 577–581.

84. M. Shindo, K. Irie, A. Masuda, H. Ohigashi, Y. Shirai, K. Miyasaka and N. Saito, *J. Biol. Chem*, 2003, **278**, 18448–18454.

85. R. M. Epand, M. K. Topham, *Lipidomics and Bioactive Lipids: Lipids and Cell Signaling*, 2007, **434**, 293–304.

86. M. G. Kazanietz, *Mol. Pharmacol.*, 2002, **61**, 759–767.

87. I. N. Maruyama and Sydney Brenner, *Proc. Nati. Acad. Sci. USA*, 1991, **88**, 5729-5733.

88. S.-B. Rong, I. J. Enyedy, L. Qiao, L. Zhao, D. Ma, L. L. Pearce, P. S. Lorenzo, J. C. Stone, P. M. Blumberg, S. Wang and A. P. Kozikowski, *J. Med. Chem.*, 2002, **45**, 853-860.

89. J. E. Johnson, R. E. Goulding, Z. Ding, A. Partovi, K. V. Anthony, N. Beaulieu, G. Tazmini, R. B. Cornell and R. J. Kay, *Biochem. J.*, 2007, **406**, 223–236.

90. N. A. Dower, S. L. Stang, D. A. Bottorff, J. O. Ebinu, P. Dickie, H. L. Ostergaard and J. C. Stone, *Nat. Immunol.*, 2000, **1**, 317-21.

91. J. O. Ebinu, S. L. Stang, C. Teixeira, D. A. Bottorff, J. Hooton, P. M. Blumberg, M. Barry, R. C. Bleakley, H. L. Ostergaard and J. C. Stone, *Blood*, 2000, **95**, 3199-3203.

92. T. Leung, X.-Q. Chen, I. Tan, E. Manser and L. Lim, *Mol. Cell. Biol*. 1998, **18**, 130-140.

93. I. Tan, C. H. Ng, L. Lim and T. Leung, *J. Biol. Chem.* , 2001, **276**, 21209–21216.

94. I. Tan, K. T. Seow, L. Lim, and T. Leung, *Mol. Cell. Biol.*, 2001, **21**, 2767–2778.

95. S. Wilkinson, H. F. Paterson, and C. J. Marshall, *Nature Cell. Biol.*, 2005, **7**, 255-261.

96. S. H. Choi, G. Czifra, N. Kedei, N. E. Lewin, J. Lazar, Y. Pu, V. E. Marquez and P. M. Blumberg, 2008, *J. Biol. Chem.*, **283**, 10543-10549.

97. Y. Takai, A. Kishimoto, Y. Iwasa, Y. Kawahara, T. Mori and Y. Nishizuka, *J. Biol. Chem.*, 1979, **254**, 3692-3695.

98. M. Mosior, E. S. Golini and R. M. Epand, *Proc. Natl. Acad. Sci. USA*, 1996, **93**, 1907-1912.

99. M. Medkova and W. Cho, *J. Biol. Chem.*, 1999, **274**, 19852–19861.

100. L. Bittova, R. V. Stahelin, and W. Cho, *J. Biol. Chem.*, 2001, **276**, 4218-4226.

101. S. J. Slater, M. B. Kelly, F. J. Taddeo, C. Ho, E. Rubin, and C. D. Stubbs, *Biochim. Biophys. Acta*, 1994, **269**, 4866-4871.

102. E. J. Bolen and J. J Sando, *Biochemistry*, 1992, **31**, 5945-51.

103. J. R. Giorgione, R. Kraayenhof, and R. M. Epand, *Biochemistry*, 1998, **37**, 10956-10960.

104. F. M. GonÄi, A. Alonso, *Prog. Lipid. Res.*, 1999, **38**, 1-48.

105. E. M. Goldberg and R. Zidovetzki, *Biophys. J.*, 1997, **73**, 2603-2614.

106. E. M. Goldberg and R. Zidovetzki, *Biochemistry*, 1998, **37**, 5623-5632.

107. C. Ho, S. J. Slater, B. Stagliano, and C. D. Stubbs, *Biochemistry*, 2001, **40**, 10334-10341.

108. D. Armstrong and R. Zidovetzki, *Biophys. J.*, 2008, **94**, 4700–4710.

109. N. Gal, S. Kolusheva, N. Kedei, A. Telek, T. A. Naeem, N. E. Lewin, L. Lim, P. Mannan, S. H. Garfield, S. E. Kazzouli, D. M. Sigano, V. E. Marquez, P. M. Blumberg and R. Jelinek, *Chembiochem*, 2011, **12**, 2331–2340.

110. O. Raifman, S. Kolusheva, M. J. Comin, N. Kedei, N. E. Lewin, P. M. Blumberg, V. E. Marquez and R. Jelinek, *FEBS Journal* , 2010, **277**, 233–243.

111. G. Goel, H. P. Makkar, G. Francis and K. Becker, *Int. J. Toxicol.*, 2007, **26**, 279-288.

112. G. Rovera, T. G. O'Brien and L. Diamond, *Science*, 1979, **204**, 868-70.

113. M. L. Day, X. Zhao, S. Wu, P. E. Swanson and P. A. Humphrey, *Cell Growth Differ.*, 1994, **5**, 735-741.

114. U. Troller, R. Zeidman, K. Svensson and C. Larsson *FEBS Lett.*, 2001, **508**, 126-130.

115. E. Afrasiabi, J. Ahlgren, N. Bergelin and K. Törnquist, *Mol. Cell Endocrinol.*, 2008, **292**, 26-35.

116. M. G. Kazanietz, L. B. Areces, A. Bahador, H. Mischak, J. Goodnight, J. F. Mushinski, P. M. Blumberg, *Mol. Pharmacol.*, 1993, **44**, 298-307.

117. G. M. Rahman and Joydip Das, *J. Biomol. Struct. Dyn.*, 2015, **33**, 219-232.

118. R. Mutter and M. Wills, *Bioorg. Med. Chem.*, 2000, **8**, 1841-1860.

119. S. K. Davidson, S. W. Allen, G. E. Lim, C. M. Anderson and M. G. Haygood, *Appl. Environ. Microbiol.*, 2001, **67**, 4531-4537.

120. M. G. Kazanietz, N. E. Lewin, F. Gao, G. R. Pettit and P. M. Blumberg, *Mol. Pharmacol.*, 1994, **46**, 374-379.

121. M. C. Tuthill, C. E. Oki and P. S. Lorenzo, *Mol. Cancer Ther.*, 2006, **5**, 602-610.

122. A. Clamp and G. C. Jayson, *Anticancer Drugs*, 2002, **13**, 673-83.

123. S. H. Choi, T. Hyman and P. M. Blumberg, *Cancer Res.*, 2006, **66**, 7261-7269.

124. M. K. Sun, J. Hongpaisan and D. L. Alkon, *Proc. Natl. Acad. Sci. U S A*, 2009, **106**, 14676-14680.

125. P. A. Wender, B. Lippa, C. M. Park, K. Irie, A. Nakahara and H. Ohigashi, *Bioorg. Med. Chem. Lett.*, 1999. **9**, 1687-90.

126. P. A. Wender, J. L. Baryza, S. E. Brenner, B. A. De Christopher, B. A. Loy, A. J. Schrier and V. A. Verma, *Proc. Natl. Acad. Sci. U S A*, 2011, **108**, 6721-6726.

127. J. C. Stone, S. L. Stang, Y. Zheng, N. A. Dower, S. E. Brenner, J. L. Baryza and P. A. Wender, *J. Med. Chem.*, 2004, **47**, 6638-6644.

128. B. A. DeChristopher, B. A. Loy, M. D. Marsden, A. J. Schrier, J. A. Zack and P. A. Wender, *Nat. Chem.*, 2012, **4**, 705-710.

129. M. Blanco-Molina, G. C. Tron, A. Macho, C. Lucena, M. A. Calzado, E. Muñoz and G. Appendino, *Chem. Biol.*, 2001, **8**, 767-778.

130. M. Fujiwara, K. Ijichi, K. Tokuhisa, K. Katsuura, G.-Y.-S. Wang, D. Uemura, S. Shigeta, S. K. Konno, T. Yokota and M. Baba, *Antivir. Chem. Chemother.*, 1996, **7**, 230-236.

131. P. Yi, L. Schrott, T. P. Castor and J. S. Alexander, *J. Mol. Neurosci.* , 2012, **48**, 234–244.

132. J. J. Mond, A. Balapure, N. Feurstein, C. H. June, M. Brunswick, M.-L. Lindsberg and K. Witherspoon, *J. Immunol.*, 1990, **144**, 451-455.

133. V. E. Marquez and P. M. Blumberg, *Acc. Chem. Res.*, 2003, **36**, 434-443.

# CHAPTER 2

# Bilayer Interaction and Protein Kinase C-C1 Domain Binding Studies of Kojic Acid Esters

This chapter describes the *in-vitro* binding properties of kojic acid esters with C1b domains of PKCδ and PKCθ by using fluorescence techniques. The molecular docking analysis provides the binding orientation of the kojic acid esters within the C1 domain binding site. The bilayer interaction properties and the aggregation properties of kojic acid esters are also determined by using fluorescent probes.

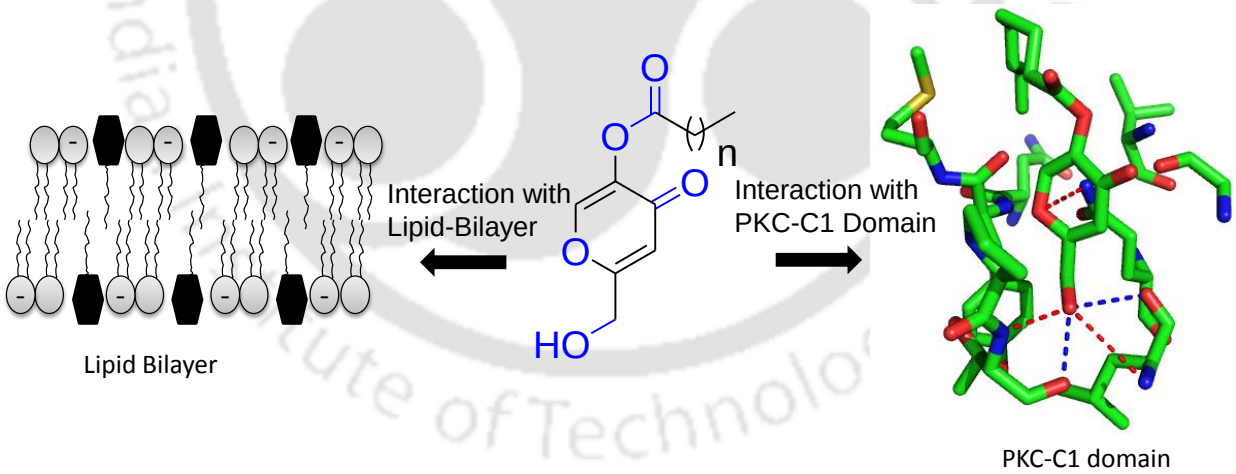

## 2.1. Background and focus of the present work

Protein Kinase C (PKC), a serine threonine kinase, has been considered as a therapeutic target for several diseases including, cancer, neurological, immunological, cardiovascular, and Alzheimer's diseases.[1-6] PKC consists of a C-terminal catalytic domain and an N-terminal regulatory domain. The N-terminal regulatory domain of PKC proteins contains an autoinhibitory sequence and one or two membrane targeting domains (C1 and C2). The activity of the enzyme is controlled by the position of the pseudo substrate sequences of the regulatory domain within/out of the catalytic site. In case of classical PKCs, the conformational change induced by $Ca^{2+}$ binding to the C2 domain followed by DAG binding to the C1 domain translocate the enzyme to the plasma membrane as well as releases the kinase domain for activation. On the other hand, only DAG binding to the C1 domain activates novel PKC isozymes.[7-9] The C-terminal catalytic domain is highly homologous among different kinase proteins.[10] So, development of specific kinase inhibitors has always been a great challenge for the researchers. Therefore, regulation of PKC activity by targeting the C1 domain has been considered as a more rational approach.[10, 11] Comparatively small size and presence of only one ligand binding site of C1 domains also make them ideal therapeutic target for drug designing.

Phorbol ester, Bryostatin, Ingenol etc. are some of the natural compounds which have been identified as ideal C1 domain ligands. However these compounds are structurally very rigid and complex.[3, 12, 13-15] Tremendous efforts are underway for the development of simple surrogates whose structure can be easily modified to achieve higher specificity and selectivity among the C1 domains of the PKC isoenzymes. Among these, DAG-lactones, isophthalic acid derivatives, different bidentate ligands and others have shown to be promising C1 domain ligands.[16] In our continuous effort to develop small C1 domain ligands, we've chosen kojic acid as the template for our present study.

Kojic acid is a secondary metabolite, generated from carbohydrate sources in an aerobic process by various fungi and bacteria, such as Aspergillus and Penicillium.[17] The derivatives of kojic acid are present in a range of natural and synthetic products with intriguing pharmacological activities. Kojic acid is one of the most meticulously studied inhibitor of tyrosinase.[18, 19] This natural pyrone and its derivatives are widely used as a food preservative for preventing enzymatic browning, cosmetic skin-whitening agent for the treatment of melasma, antioxidant, antitumor agent and radioprotective agent. Kojic acid plays a significant role in iron-overloaded diseases like anemia, due to its iron-chelating activity. Kojic acid and its derivatives also show antibiotic, anti-diabetic, anti-inflammatory,

anti-proliferative and other activities.[18-21] Several attempts to improve the anticancer potential of kojic acid by introducing various chemical moieties to the compound have been already attempted by researchers. Kojic acid esters contain both hydrophobic (palmitate, oleate, stearate and others) and hydrophilic (5-hydroxy-2-hydroxymethyl-4-pyrone) groups. In spite of its significant importance, to the best of our knowledge; there is no report available on the interaction of Kojic acid ester molecule with the lipid bilayer and their binding properties with the PKC isoenzymes. Our present study deals with two PKC isozymes- PKCδ and PKCθ. Both of these enzymes belong to the subgroup novel PKC i.e. activation depends on the DAG binding to the C1 domain, $Ca^{2+}$ doesn't have any role. PKCδ was the first novel PKC isozyme identified by screening of mammalian cDNA libraries. PKCδ plays a crucial role in the regulation of cell growth, migration, differentiation, and cell death.[22] PKCθ is involved in signal transduction downstream of the activated T-cell receptor and the CD28 co-stimulatory receptor. PKCθ also plays role in homeostasis through platelet activation and aggregation, regulation of insulin resistance and susceptibility to obesity.[23] The regulatory domain of PKCδ and PKCθ consists of tandem repeats of two C1 domains-C1a and C1b. Our present study includes only C1b domain due to its availability in the soluble form from bacterial cells.

In this context, the present study describes the synthesis, aggregation behavior in aqueous solution, interaction properties with the lipid bilayers, and in vitro binding properties of kojic acid esters to the C1b subdomains of PKCδ and PKCθ. The long chain kojic acid ester analogues increase the fluidity and permeability of the model membranes, which assists their binding capabilities with the PKC-C1b subdomains. The active kojic acid ester analogues can compete with DAG binding to the C1b subdomains of PKCs. The hydroxymethyl group, pyrone ring and a suitable hydrophobic ester group of the compounds play a decisive role in recognizing the C1b subdomains of PKC isoenzymes.

**Design of the Kojic acid esters**

Comprehensive information gained by co-crystallization of the PKCδ-C1B domain with phorbol 13-acetate reveals that hydroxyl and carbonyl functional groups of the phorbol ester form hydrogen bond with the backbone amine and carbonyl groups of the amino acid residues present in the binding cleft of the C1 domain.[24] Several studies also showed that hydrophobicity of the ligands plays an important role in C1 domain binding. The hydrophobic part of the ligands is reported to interact with the hydrophobic amino acids present surrounding the C1 domain binding site and hydrophobic moiety of the lipid

bilayer.[24, 25] We have recently demonstrated that a hydroxymethyl group and ester group with hydrophobic side chain are needed for efficient binding of protocatechualdehyde derivatives with the PKC-C1 domain.

The kojic acid esters contain the required phorbol ester pharmacophores for the C1 domain binding. Kojic acid contains one primary, one secondary hydroxyl groups along with one pyrone ring. The secondary hydroxyl groups provide access to incorporate different fatty acids. The carbonyl of the pyrone ring present at the meta- position of the hydroxymethyl group and oxygen atom of the pyrone ring provides additional hydrogen bonding sites for the C1 domain backbone. The hydrophobic interactions are difficult to model. Thus, we used a series of ester derivatives of kojic acid (of secondary hydroxyl group) with different chain length to study the impact of side chains on the binding affinity. The compound with acyl chain length of C8, C12, C15, and C18 were chosen to study the impact of alkyl chain length on the binding affinity (Figure 2.1). It is reported that DAGs with unsaturated hydrophobic 'tail', generated by PI-PLC are more potent in PKC activation than the saturated DAGs produced by other cellular pathways.[26, 27] We used compound **5** with oleic acid to study the impact of unsaturated hydrophobic 'tail' in protein binding and interaction with lipid bilayers.

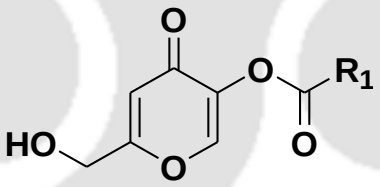


**Figure 2.1.** Kojic acid ester where RCOOH= Octanoic acid (**1**), Lauric acid (**2**), Palmitic acid (**3**), Stearic acid (**4**) and Oleic acid (**5**).

Molecular docking analysis revealed that the kojic acid ester analogues are anchored to the DAG/phorbol ester binding site of the PKCδ-C1b domain (Figure 2.2). The model structure showed that hydroxymethyl group is hydrogen-bonded to the backbone carbonyls of Thr-242 and Leu-251 and amide protons of Thr-242 and Leu-251. The oxygen atom of the pyrone ring was hydrogen-bonded with the Gln-257. The other carbonyl groups might be involved in interaction with the anionic lipid head groups, including phosphatidylserine and others for an activation at the cellular membranes.[12] The model structure showed that there is no interaction between kojic acid ester and backbone amide proton of Gly-253 residue. A similar mode of interactions of kojic acid ester with PKCθ-C1b was observed.

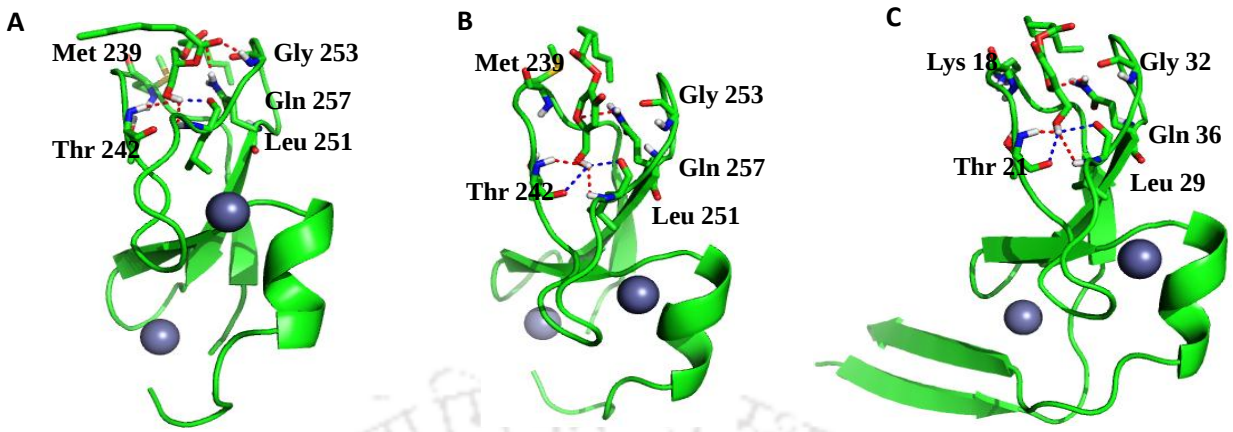


**Figure 2.2.** Structures of ligand bound PKCδ- and PKCθ-C1b subdomains. (A) Modeled structure of $DAG_8$ docked into PKCδ-C1b (1PTR); (B) modeled structure of **1** docked into PKCδ-C1b; (C) modeled structure of **1** docked into PKCθ-C1b (4FKD). The modeled structures were generated using the Molegro Virtual Docker, version 4.3.0. The oxygen atoms and nitrogen atoms are shown in red and blue, respectively. The dotted line indicates possible hydrogen bonds.

## 2.2. Results and Discussion

**Aggregation studies of kojic acid esters—** We first investigated the behavior of kojic acid esters in aqueous solution by measuring the fluorescence properties of 8-anilino-1-naphthalenesulfonic acid (ANS).[28, 29] The ANS have been widely used as a polarity indicator, because of its intramolecular charge transfer property. We measured the critical aggregation concentration (CAC), an analogy to illustrate critical micelle concentrations for surfactants using ANS in the presence of kojic acid esters in aqueous solution. Concentration dependent aggregation of kojic acid esters and simultaneous incorporation of ANS molecules to its hydrophobic core is reflected by the increase in fluorescence intensity and a blue shift of the ANS emission maximum. Increase in compound concentrations from 0-200 μM resulted in a blue shift of ANS emission maxima from 525 to 480 nm, supporting a continuous decrease in polarity of the medium. The plot of fluorescence intensity maximum with compound concentration suggests that around/above 50 μM, kojic acid esters **4** and **5** start aggregating (Figure 2.3). The measured CAC of the compound **4** and **5** were 67 and 51 μM, respectively. These compounds with hydrophobic (palmitate and oleate) and hydrophilic (2-(hydroxymethyl)-4H-pyran-4-one) groups are expected to form aggregation in aqueous solution. However, bilayer, micelles or vesicles of kojic acid esters may not be shaped because of its high hydrophobicity and critical packing parameter (CPP).[30] We presume that, these amphiphilic molecules aggregates with irregular shapes, primarily because of the

hydrophobic interaction. Due to the presence of unsaturated oleic acid, compound **5** has higher hydrophobicity than compound **4**. This allows compound **5** to aggregate at lower concentration in aqueous solution. The CAC values of these amphiphilic molecules are essential in understanding their interaction with lipid bilayer and PKC-C1 domain under monomeric form in aqueous solution.

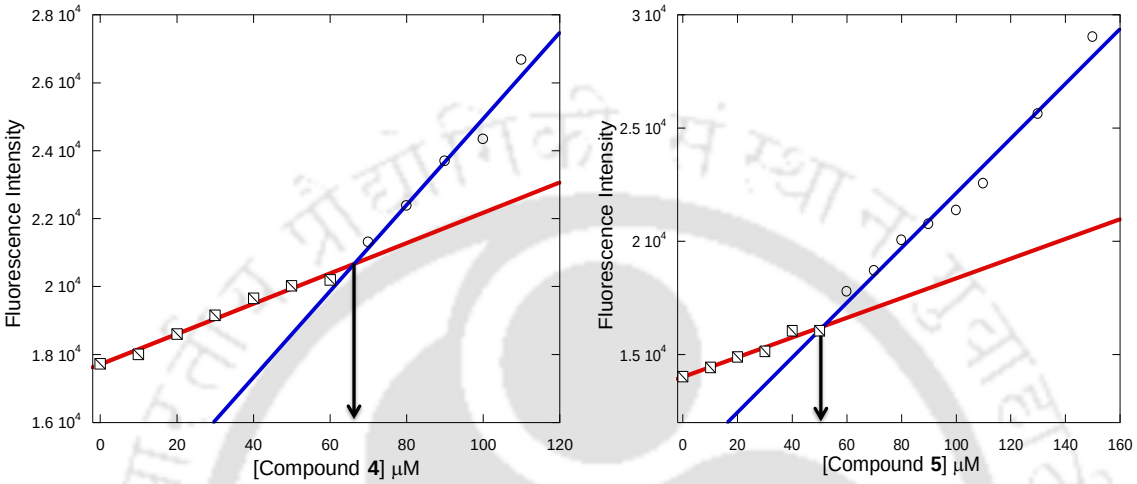


**Figure 2.3.** Measurement of critical aggregation concentration of compound **4** and **5** in aqueous solution. Plot of ANS fluorescence intensity against different concentration of compound **4** (A) and **5** (B)**.** [ANS] = 4 μM, $\lambda_{ex}$ =380 nm.

**Interaction with Lipid Bilayers:**

The effects of drug or drug-like molecules on the structure of the lipid bilayer play an important role in understanding their pathological processes. Cellular membrane properties including fluidity, permeability, surface potential and others get affected by the distribution of drug or drug-like molecules. Fluidity of the lipid bilayer and loose spacing in the polar headgroup region plays a significant role on the PKC kinase activities. Ability of the PKC-active compounds to localize at the membrane-water interface is directly linked with its C1 domain binding properties. The PKC isoenzymes get activated at the membrane interface primarily due to their interaction with the membrane localized lipophilic second messenger DAGs. The C1 domains are peripheral proteins. Therefore, the C1-domain ligands would be expected to interact significantly with the lipid bilayer and alter membrane fluidity, permeability, phase transition and others. In this regard, the effects of kojic acid esters with the liposomes were studied by investigating their effect on permeability and phase transition of lipid bilayer and extent of membrane localization patterns.

**Effect of kojic acid esters on membrane permeability—** Recent studies showed that excited-state proton transfer (ESPT) of 1-naphthol (NpOH) is affected with the change in lipid bilayer organization.[31, 32] The change in microenvironment of the medium was investigated by using the fluorescence properties of NpOH. NpOH exists as neutral form in nonpolar media and anionic form in aqueous media. The ratio of fluorescence intensities of anionic form ($\lambda_{em}$ = 470 nm) to neutral form ($\lambda_{em}$ = 370 nm) is sensitive to the microenvironment of NpOH.[28, 33] Under liposomal environment, the origin of the NpOH* emission is due to the membrane-bound fraction of NpOH while the NpO-* emission is contributed by the presence of NpOH in the semi-polar membrane interface region and unpartitioned NpOH present in water. Dipalmitoylphosphatidylcholine (DPPC) liposomes were used as a model lipid bilayer due to its high abundance in biological membranes. The plasma membrane also contains several other lipids. However, it would be difficult to monitor membrane permeability and other bilayer properties using such complex lipid compositions.

The partition coefficient (Kp) values of NpOH provide information regarding membrane permeability of the DPPC bilayer in the absence/presence of kojic acid esters. Membrane permeability of NpOH which increases with the increase in Kp values is altered by the degree of unsaturation and chain length of the fatty acid present within the membrane active compounds.[28, 32, 33] The changes in Kp values were measured by monitoring the changes in NpOH* fluorescence intensity. We used compound **4** and **5** with the same chain-length for this study as it would reveal the effect of saturation vs. unsaturation on the membrane permeability of the DPPC lipid bilayer. Figure 2.4A shows the double reciprocal plot of NpOH* fluorescence intensity vs. DPPC liposome concentration in the absence of compounds at different temperatures. Figure 2.4B and 2.4C represent the double reciprocal plot in the presence of different concentrations of compounds in the solid gel (SG) and liquid crystal (LC) phases of DPPC SUVs, respectively. The Kp values and mole fraction of NpOH in DPPC liposomes were calculated at different temperatures depending on DPPC lipid phases (Table 2.1). The results clearly showed that partitioning of NpOH is significantly higher at the phase transition temperature, where the permeability of the lipid bilayer membrane is expected to be higher because of the coexistence of solid and liquid domains. The results also showed that the Kp value is lower in SG phase than LC phase. This could be due to the higher fluidity (higher permeability) of the lipid bilayer in the LC phase.

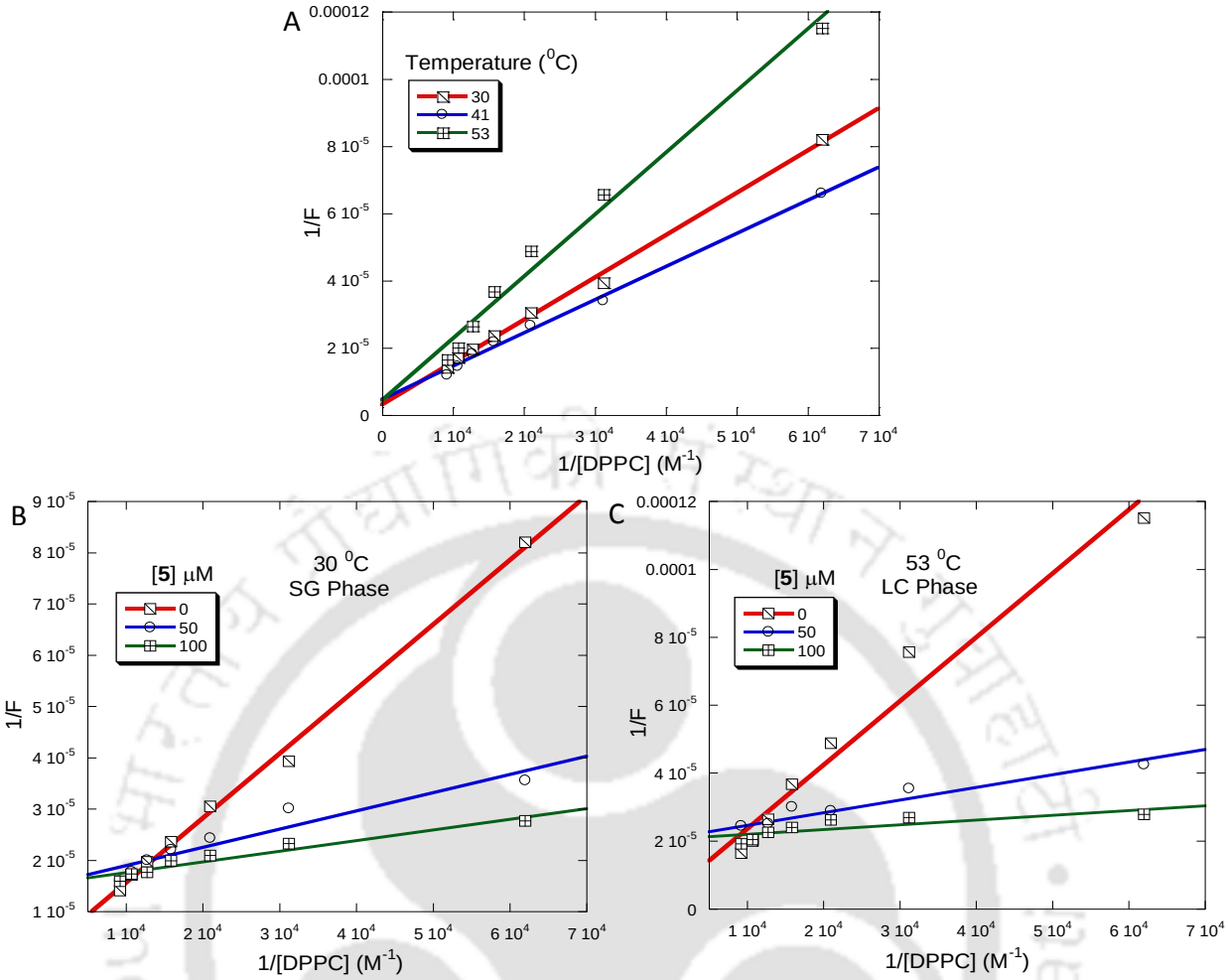


**Figure 2.4.** Double reciprocal plot of NpOH* fluorescence intensity vs. DPPC concentrations in the (A) absence of kojic acid esters, and in the presence of different concentrations of kojic acid esters in (B) SG (30 °C) and (C) LC (53 °C) phases; $\lambda_{ex}$ = 290 nm, $\lambda_{em}$ = 370 nm, [1-naphthol] = 4μM.

The change in Kp values are in good correlation with the change in membrane fluidity. The Kp values of NpOH in the presence of both the compounds **4** and **5** enhanced with the increase in compound concentrations for both phases of the liposomes. Calculated mole fraction of NpOH partitioning into the lipid bilayer also increased in both phases of the liposomes. This clearly indicates that these compounds enhance DPPC membrane permeability and fluidity. However for compound **4**, the increase in Kp value with an increase in concentration is less than that of the compound **5**, which point out that the presence of unsaturation in acyl chain increases the permeability of the lipid bilayer. In absence on DPPC liposomes, there is no NpOH* emission peak with varying concentration of the compounds. This indicates that the compounds have no direct interactions with the NpOH molecules. Presence of kojic acid esters in the lipid bilayer might alter the packing of the polar headgroup of the DPPC molecules. The NpOH* fluorescence intensity decreases with

the increase in compound concentrations (Figure 2.4). This could be either due to the higher membrane permeability of NpOH in the presence of compounds or could be due to the presence of water molecule within the lipid bilayer.[34] The results suggest that the amphiphilic nature of the compounds enhances its interaction with the lipid bilayer membrane with an increase in concentration.

**Table 2.1.** Partition coefficient and mole fractions of 1-naphthol within the DPPC vesicle in the absence/presence of compound **4** and **5**.

| Liposome | Partition coefficient (Kp) and mole fractions of NpOH | | |
|---|---|---|---|
| | 30 °C; SG phase | 41 °C; at $T_M$ | 53 °C; LC phase |
| DPPC only | $0.13 \pm 0.21 \times 10^6$; 20.49 ± 2 % | $3.65 \pm 0.32 \times 10^5$; 40.56 ± 1 % | $0.14 \pm 0.19 \times 10^6$; 21.23 ± 2 % |
| DPPC + **4** (50 µM ) | $1.38 \pm 0.26 \times 10^6$; 72.05 ± 1 % | | $1.99 \pm 0.06 \times 10^6$; 78.79 ± 2 % |
| DPPC + **4** (100 µM ) | $2.10 \pm 0.19 \times 10^6$; 79.71 ± 1% | | $2.11 \pm 0.13 \times 10^6$; 79.82 ± 1% |
| DPPC + **5** (50 µM ) | $2.41 \pm 0.11 \times 10^6$; 81.86 ± 1 % | | $2.67 \pm 0.19 \times 10^6$; 83.34 ± 1% |
| DPPC + **5** (100 µM ) | $4.13 \pm 0.14 \times 10^6$; 88.53 ± 1% | | $8.13 \pm 0.21 \times 10^6$; 93.83 ± 1% |

**Extent of membrane localization—**The partition coefficient values of NpOH clearly showed that the kojic acid esters strongly interact with the lipid bilayer. The change in NpOH* fluorescence intensity with the increase in compound concentration also suggest that the compounds altered the packing of the DPPC headgroups. The hydrophilic part of the amphiphilic kojic acid ester analogues are expected to be positioned near the bilayer/water interfacial region. However, the extent of localization of the pharmacophore containing hydrophilic part at the bilayer/water interface is very important for their C1 domain binding ability under liposomal environment. In this regard, we performed NBD ([2-(4-nitro-2,1,3-benzoxadiazol-7-yl)aminoethyl]trimethylammonium) fluorescence quenching experiments using DPPC/Ligand/NBD-PE liposomes. The NBD probe is embedded close to the bilayer/water interface, providing a useful marker for surface interactions of membrane-active C1 domain ligands.[35-37] Sodium dithionite induced NBD fluorescence quenching provided a measure of membrane localization of the ligands. Figure 2.5 reveals that ligand associated fluorescent liposomes showed significant changes in the rate of dithionite-induced fluorescence quenching of the bilayer-embedded probe. The ligands showed slower quenching rates than the control liposomes (without any ligands). The results indicate that the

NBD probe became more 'shielded' from the soluble dithionite quencher, due to the presence of kojic acid ester analogues in the liposomes. The results also imply that hydrophilic part of these ligands is more localized at the liposome surface compared to $DAG_{16}$. Therefore, the kojic acid ester analogues are accessible for the protein binding, under liposome environment. Figure 2.5 indicates different degrees of localization and perturbation of the bilayer headgroup region by the kojic acid ester analogues. To further investigate the interactions of compounds with lipid bilayers and their effects upon the bilayer properties, we measured the effect of compounds on the phase transition temperature of lipid bilayer.

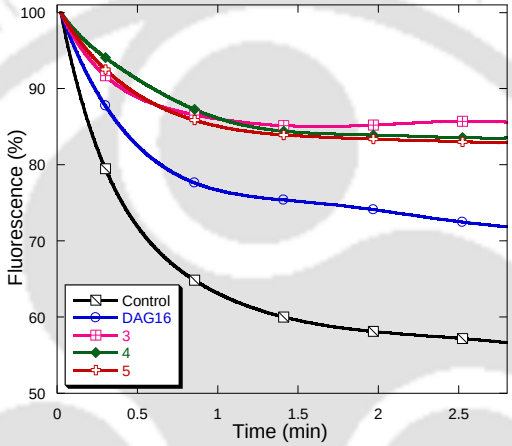


**Figure 2.5.** Fluorescence quenching of NBD-PE embedded in PC/$Ligand_{16}$/NBD-PE (89:10:1) liposomes. Sodium dithionite = 0.6 µM. Control: no ligand.

**Effect of kojic acid esters on the phase transition temperature of lipid bilayer—** It is well documented that the phase transition temperature of the bilayer depends on lipid compositions. The bilayer organization is also affected by nature and chain length of fatty acid, and the headgroup of the lipids.[38-40] To further probe the interaction of membrane active kojic acid esters with lipid bilayers and their effect on the fluidity of the bilayer, we measured $T_M$ values of DPPC bilayers in the absence/ presence of kojic acid esters. We used compound **4** and **5** for this study as it would also reveal the effect of saturation vs. unsaturation on the $T_M$ value of the DPPC lipid bilayer. The DPPC was used as a model lipid for bilayer formation. However, addition of other lipids would complicate the system. NpOH was successfully used to study the thermotropic phase behavior of the lipid bilayer by monitoring the changes in fluorescence intensity of NpOH*. The SG phase of the lipid bilayer is tightly packed and has less capacity to accommodate the probe resulting low fluorescence intensity of NpOH*. Coexistence of SG and LC phase at the transition

temperature makes the bilayer less resistant allowing local maximum in the fluorescence intensity of NpOH*. However, this fluorescence intensity gradually decreases as the region of disorder and the permeability decrease at LC phase. This temperature dependent variation of NpOH* fluorescence intensity is in accordance with the measured partition coefficient of NpOH with temperature. Therefore, we monitored the NpOH* fluorescence intensity change to measure the $T_M$ values. The variation in NpOH* fluorescence intensity with temperature demonstrates that phase transition of only DPPC lipid bilayer occurs at 41 $^{\circ}$C (Figure 2.6). The $T_M$ value of DPPC bilayer is in good correlation with the reported value measured by differential scanning calorimetry (DSC).[41] The results showed that the $T_M$ values of DPPC bilayer decreases from 41 $^{\circ}$C to 40 $^{\circ}$C and 39 $^{\circ}$C in the presence of compound **4** and **5**, respectively. The nature of thermotropic phase behavior also showed that the DPPC bilayer organization remains intact under these experimental conditions (Figure 2.6). The decrease in the $T_M$ value of the DPPC bilayer in the presence of both compounds can be attributed to the decrease in the van der Waal's interactions between hydrophobic 'tails' and alteration of lipid packing by fluidizing the region. Compound **5** with unsaturated acyl chain showed lower $T_M$ value than the compound **4**, which could be due to the increase in the fluidity of the bilayer as observed in partition coefficient measurements. The smaller change in $T_M$ values is in accordance with the NBD fluorescence quenching data, which indicate the prevalent bilayer-surface interactions of compound **4** and **5**. The localization of the headgroup of the kojic acid esters hardly affects thermotropic phase behavior of the lipid bilayers; it primarily depends upon the 'tails' of the compounds.

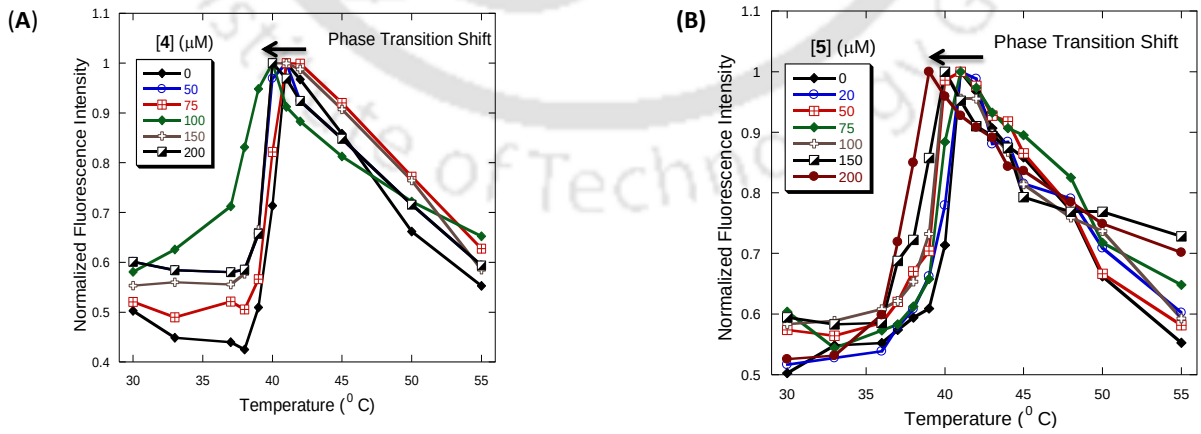


**Figure 2.6.** Effect of compound **4** (A) and compound **5** (B) on the phase transition temperature of DPPC vesicle. Change in NpOH* fluorescence intensity with the increase in compound concentration at different temperatures in DPPC vesicles. $\lambda_{ex}$ = 290 nm, $\lambda_{em}$ = 370 nm, [DPPC] = 0.2 mM, [1-napthol] = 4 μM.

**Protein Binding Studies**

The DAG-responsive C1 domain of classical and novel PKC isoenzymes is duplicated into a tandem C1 domain consisting of C1a and C1b subdomains. We have used the C1b subdomains of PKCδ and PKCθ proteins to measure the in vitro binding properties of the kojic acid ester analogues. These C1b subdomains are reported to have sufficiently strong DAG binding affinities and easy to obtain in soluble form from bacterial cells.[22, 50] The PKCδ- and PKCθ-C1b subdomains contain single tryptophan (Trp-252 in delta, Trp-31 in theta) and tyrosine residues (Tyr-236 and Tyr-238 in delta, Tyr-15 and Tyr-17 in theta), respectively, which account for their intrinsic fluorescence. The protein binding properties of the kojic acid esters were measured by Trp-fluorescence quenching methods, steady-state fluorescence anisotropy and Förster resonance energy transfer (FRET) based competitive binding assay.[21-23]

**Interaction with soluble ligands—** Intrinsic fluorescence is widely used as a tool to detect the change in protein confirmation or microenvironment caused by the ligand binding. It is important to note that these C1b subdomains contain single Trp residue close to the DAG binding pocket. Compounds **1–5** quenched the Trp fluorescence (340 nm) in a concentration dependent manner, and a plateau was reached at around 15–20 μM (Figure 2.7). The ligand concentrations used in monomeric binding measurements were well below their CAC values of the kojic acid esters of long chain fatty acids. This clearly indicates that the compounds were in monomeric form under the experimental conditions.

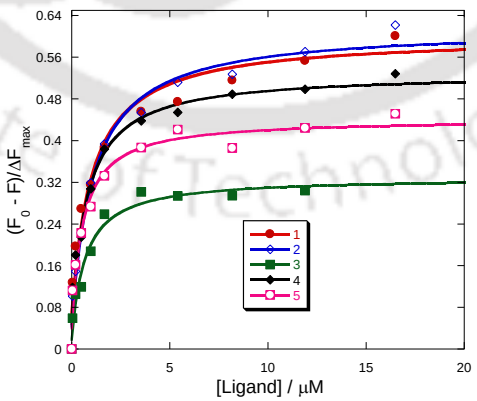


**Figure 2.7.** Binding of ligands with PKCδ-C1b. Representative plot of fluorescence intensity of PKCδ-C1b (1 μM) in buffer (20 mM Tris, 160 mM NaCl, 50 μM $ZnSO_4$, pH 7.4) in the presence of varying concentration of **1-5**, where F and $F_0$ are fluorescence intensity in the presence and absence of the ligands, respectively. The solid lines are nonlinear least squares best fit curves.

The measured binding affinities revealed that kojic acid esters with different chain length strongly interact with the C1b subdomains of PKCδ and PKCθ proteins. The compound **3** showed the highest affinity and other compounds have comparable binding affinities for both the proteins. The ligand **3** shows more than 10 and 13-fold stronger binding affinity than $DAG_{16}$ for PKCδ-C1b and PKCθ-C1b subdomain, respectively (Table 2.2). Whereas ligand **5** with unsaturated fatty acid showed more than 12 and 10-fold stronger binding affinity than $DAG_{16}$ for PKCδ-C1b and PKCθ-C1b subdomain, respectively. However, C1b subdomains binding of the compounds in monomeric form do not show clear PKC-isoform specificity.

**Table 2.2.** $K_D$ (ML) values for the binding of ligands with the PKCδ-C1b and PKCθ-C1b proteins[a] at room temperature.

| Compound | $K_D$ (ML) (μM) | |
|---|---|---|
| | PKCδ-C1b | PKCθ-C1b |
| **$DAG_8$** | 12.41 ± 0.59 | 6.74 ± 0.54 |
| **$DAG_{16}$** | 7.04 ± 0.43 | 6.35 ± 0.37 |
| **1** | 1.04 ± 0.08 | 0.91 ± 0.06 |
| **2** | 1.09 ± 0.12 | 0.79 ± 0.09 |
| **3** | 0.69 ± 0.02 | 0.46 ± 0.01 |
| **4** | 0.77 ± 0.12 | 1.13 ± 0.03 |
| **5** | 0.57 ± 0.04 | 0.61 ± 0.05 |

[a)] Protein, 1 μM in buffer (20 mM Tris, 160 mM NaCl, 50 μM $ZnSO_4$, pH 7.4) Values represent the mean ± S.D. from triplicate measurements.

The molecular model structures of compound-bound protein showed that there were three hydrogen bonds between DAG and PKCδ-C1b; whereas compound **1** showed five hydrogen bonds with PKCδ-C1b. It is important to note that there was no hydrogen bond between ligand and Gly-253 of the molecular models of PKCδ-C1b, an important interaction site for ligand binding to the C1 domain. This however does not exclude the prospect of water mediated hydrogen bond formation between kojic acid ester and Gly-253 (for PKCδ-C1b) or Gly-32 (for PKCθ-C1b), which was not considered during the molecular docking analysis. This clearly indicates that measured binding parameters and docking scores obtained from the models do not always agree. This dissimilarity indicates that both protein and ligand can experience conformational alterations under experimental circumstances to produce strong interactions. Therefore, both hydroxymethyl, carbonyls (of pyrone ring and acyl group) of the kojic acid esters are important for their interaction with the PKC-C1 domains. We hypothesize that the higher binding affinity of the compounds than DAG could

be due to their structural rigidity, which reduce the number of possible rotameric forms of the compounds. We also presume that one of the rigid rotamers would mimic the definite conformation of physiologically active DAG. The stronger binding of compounds to PKC-C1 domain than DAG apparently governed by the structural constrains to reduce the entropic loss due to binding.

The binding parameters also indicate that like other C1 domain ligands, some of the compounds show similar pattern of dependence on the hydrophobicity for C1 domain binding. The hydrophobic residues surrounding the binding site of the C1 domain also interact with the hydrophobic side chains of the ligands. But there is no direct relation between hydrophobicity of these compounds and their C1 domain binding affinities. For compound **1** (XLOGP3 = 2.33) and **2** (XLOGP3 = 4.11) although there is a distinct difference in hydrophobicity, the difference in binding affinity is very small and protein binding affinity for compound **2** is lower than compound **1**. Compound **3** with palmitic acid showed highest binding affinity of 0.46 μM and even higher than the compound **5** with oleic acid (unsaturated fatty acid). For kojic acid esters the difference in binding affinity is very small for both the proteins (Table 2.2). This could be due to the ligand binding orientations within the binding pocket or acyl chain specificity, which was already observed for PKC-C1 domains.[42] The overall high binding affinities of the compounds are probably associated with the presence of the hydroxymethyl and carbonyl groups. Thus, both the binding affinity values of the compounds highlight the importance of ligand hydrophobicity and binding orientation, in a manner similar to those reported for C1-domain ligands.[2, 43-45]

**Interaction with ligand-associated liposomes—** Peripheral proteins like PKCs are reported to interact with the cellular membranes through their lipid-binding C1 and C2 domains.[46-48] The PKC-C1 domains have both a membranes binding surface and a lipid-binding groove. The C1 domains interact with DAGs or ligands localized at the cellular membrane through its lipid-binding groove.[47, 49, 50] Therefore, to understand the C1 domain binding properties of the kojic acid esters under membrane environment, we used protein to membrane Förster resonance energy transfer (FRET)-based assay. The Trp residue of the PKC-C1b subdomains serve as the FRET donor, and a low density of membrane-embedded, dansyl-PE (dPE) lipid serve as the acceptors. For the competitive binding assay active vesicles composed of PC/PE/PS/dPE (60/15/20/5) were used. PE lipid was added to improve the stability of the vesicles. PS is known induce the DAG dependent membrane binding of the C1 domain, hence it was also incorporated into the vesicles. $DAG_8$ was titrated into the

solution containing C1b-subdomain-bound liposomes. The decrease in the protein-to-membrane FRET signal (Figure 2.8) was examined to quantitatively measure the displacement of protein from the bilayer surface to the bulk solution, and apparent inhibitory constant [$K_I(DAG_8)_{app}$] calculation. Figure 2.9A represents $DAG_8$ promoted competitive displacement of PKCδ-C1b subdomain from ligand associated liposomes (PC/PE/dPE/Ligand). The values of $K_I(DAG_8)_{app}$ depend on ligand concentration and the background lipid composition in the liposomes as well as the affinities of the C1b subdomains for ligands.

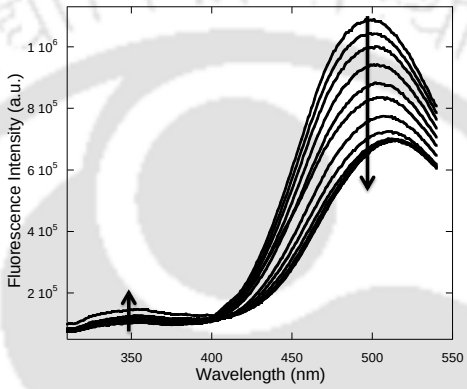


**Figure 2.8.** Representative protein-to-membrane FRET assessment under liposomal environment. Addition of increased concentration of $DAG_8$ (0-80 μM) to PKCδ-C1b sundomain (1 μM) bound to the active liposome (PC/PE/dPE/ligand (75/15/5/5)) of compound **5** decreases the FRET signal at 495 nm. All the measurements were performed in 20 mM Tris, pH 7.4 containing 160 mM NaCl and 50 μM $ZnSO_4$.

These binding parameters showed that the kojic acid esters interact with the C1b subdomains under membrane environment. This competitive binding assay confirmed that the compounds interact with the PKC-C1b subdomains through its DAG/phorbol ester binding site.The results also showed that higher concentration of $DAG_8$ was required for the displacement of PKCθ-C1b protein from the ligand associated liposomes. Finally, the equilibrium dissociation constant ($K_D$(L)) for the PKC-C1b subdomains binding to the liposome-associated targeted ligand was calculated using equation 4.[36, 51] Comparison of the equilibrium dissociation constant also revealed that C1b-subdomains have higher binding affinity for the ligand associated liposomes (Table 2.3). We also measured the interaction of compounds with PKCδ-C1b subdomain using surface plasmon resonance (SPR) analysis. The measured binding parameters also demonstrated that compound **5** strongly interact with the PKCδ-C1b subdomain, under the experimental conditions ($K_D$ = 5.85 ± 0.15 nM). The SPR sensorgrams showed that PKCδ-C1b subdomain binding to these compounds is mostly

directed by a slow dissociation from the membrane interface, a distinctive property of the PKC-C1 domains (Figure 2.9B).[52]

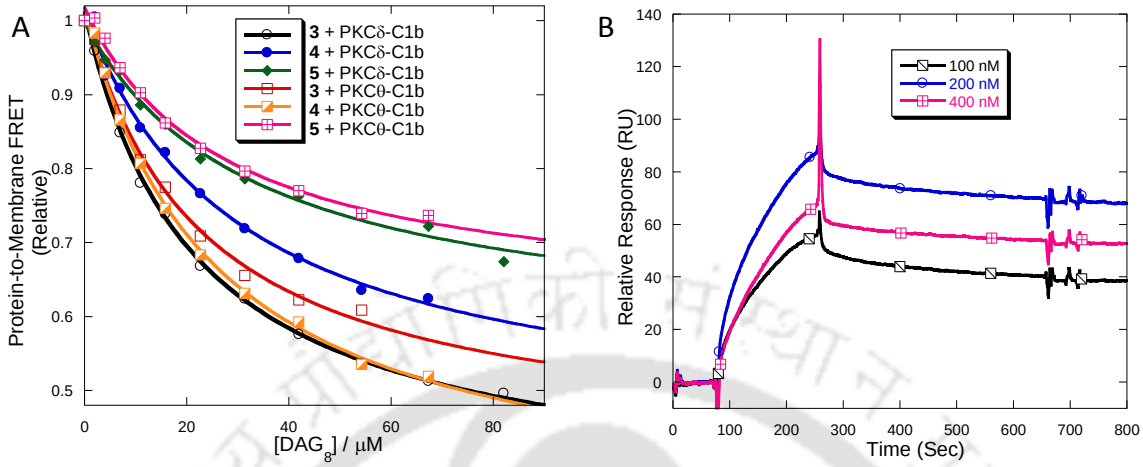


**Figure 2.9.** Binding isotherms under liposomal environment. (A) Competitive displacement assay for the PKCδ- and PKCθ-C1b subdomain (1 μM) bound to liposome containing ligands **3-5**. The bound complex was titrated with the $DAG_8$. (B) Kinetics of membrane binding of PKCδ-C1b subdomain with compound **5** containing liposomes. All sensorgrams were collected using the L1-sensor chip coated with PC/PE/PS and PC/PE/PS/**5** vesicles as reference and active surface, respectively. Flow rate was kept at 30 μl/min.

**Table 2.3.** Equilibrium parameters for PKCδ-C1b and PKCθ-C1b protein[a] binding to the ligand associated liposomes[b] at room temperature.

| Compound | $K_I(DAG_8)_{app}$ (μM) | | $K_D$(L) (nM) | |
|---|---|---|---|---|
| | PKCδ-C1b | PKCθ-C1b | PKCδ-C1b | PKCθ-C1b |
| **3** | 21.73 ± 2.25 | 22.53 ± 2.44 | 86.26 ± 4.56 | 86.26 ± 4.56 |
| **4** | 30.24 ± 2.69 | 25.41 ± 2.44 | 68.72 ± 2.23 | 122.40 ± 5.87 |
| **5** | 33.44 ± 1.19 | 27.26 ± 1.36 | 45.60 ± 1.49 | 45.60 ± 1.49 |

[a] Protein, 1 μM in buffer (20 mM Tris, 150 mM NaCl, 50 μM $ZnSO_4$, pH 7.4)
[b] Active liposome composition, PC/PE/PS/dPE/Ligand (55:15:20:5:5)

It is also important to mention that the protein binding affinities of the compounds in monomeric form are not in complete agreement with that of under liposomal environment. Under liposomal environment compound **5** showed highest binding affinity for the C1 domains, whereas compound **3** strongly interact with the C1 domains in monomeric form. This suggests that the ligand orientation within the binding pocket is different for both in aqueous solution and under liposomal environment. Compound **5** with unsaturated fatty acid showed highest binding affinity for both the proteins. This is in accordance with the reported binding affinity of the unsaturated DAGs to the PKC-C1 domains.[45, 53] The protein binding affinity increases with the increase in compound hydrophobicity. The molecular

docking analysis and protein binding parameters shows that the kojic acid esters interact differentially with the PKC-C1 domains both in monomeric form and under liposomal environment. The binding parameters also highlight the similarity in the importance of hydrophobicity in the ligands as for other C1-domain ligands.

Some of these kojic acid esters were synthesized earlier for several intriguing pharmacological activities including, antioxidant, antitumor and others. Kojic acid esters also have several applications in food and cosmetic industries. In the present investigation, we observe that kojic acid ester interact with the lipid bilayer and influence the bilayer properties including fluidity, permeability, and phase transition temperature. The hydrophilic parts of the compounds are localized at the lipid/bilayer interface and the pharmacophores are accessible for PKC-C1 domain binding under liposomal environment. The hydroxymethyl group and carbonyl groups of pyrone ring and ester group are required for binding activity of the compounds to the C1 domains. The long-chain kojic acid ester analogues can differentially influence the in-vitro membrane interaction properties of PKCδ and PKCθ enzymes.

The higher binding affinity of the compound **5** could be due to either true selectivity of the C1 domains for ligands with unsaturated acyl chain or the effect of these ligands on the lipid bilayer organization. Higher membrane fluidity and PKC-C1 domain binding abilities was observed for the kojic acid ester with unsaturated lipid 'tail'. We hypothesize that, increase in the fluidity makes the structure of the bilayer more loosely packed, allowing the hydrophobic surface of C1 domains to penetrate into the hydrophobic core of the lipid bilayer in a ligand-binding-dependent manner, which is essential for the PKC enzyme activation. The binding affinity differences between PKCδ- and PKCθ-C1b domains could be because of the differences in surface areas and the residues present within the binding site. The PKC activation ability of the kojic acid esters can be lower than that of phorbol ester and other natural products under similar experimental conditions. However, it is important to note that, DAG/phorbol ester binding to the C1 domain is known to activate PKC enzymes by displacing the pseudosubstrate from the catalytic domain of the PKC enzymes. Whereas, ligand binding to the C-terminal catalytic domain generally inhibits the PKC enzyme activities. Therefore, we hypothesize that these kojic acid esters may activate PKC enzymes, due to its strong C1 domain binding capabilities. Undoubtedly further PKC activity studies are needed to fully understand the C1-domain binding mechanism of these compounds and PKC activation/inhibition properties of these ligands.

**Conclusion**

This article illustrated that kojic acid esters interacts with lipid-bilayers and PKC-C1 domains. The results showed that strong interaction between compounds and lipid bilayers increase membrane fluidity, allow partitioning small molecules like 1-naphthol into the lipid bilayer, and decrease phase transition temperatures. The increase in fluidity of lipid bilayer structure allows the PKC-C1 domain to interact strongly with the kojic acid esters through its DAG/phorbol ester binding site. The active compounds can also compete with DAG for binding to the C1 domain under liposomal environment. The results also indicate that both carbonyl and hydroxyl group of kojic acid esters are important for its binding to the protein. These findings suggest that, in addition to their extensive application in food, cosmetic and skin-health industries, the kojic acid esters can also be developed as research tool or lead compound in PKC-based drug development.

## 2.3. EXPERIMENTAL SECTION

**General Information-** 1,2-dipalmitoyl-sn-glycerol ($DAG_{16}$), 1,2-dioctanoyl-sn-glycerol ($DAG_8$), 1,2-dipalmitoyl-sn-glycero-3-phosphocholine (DPPC), 1,2-dipalmitoyl-sn-glycero-3-phospho-L-serine (DPPS), 1,2- dipalmitoyl-sn-glycero-3-phosphoethanolamine (DPPE), 1,2-dioleoyl-sn-glycero-3-phosphoethanolamine-N-(5-dimethylamino-1 naphthalenesulfonyl) (NBD-PE), were purchased from Avanti Polar Lipids (Alabaster, AL). Ultrapure water (Milli-Q system, Millipore, Billerica, MA) was used for the preparation of buffers.

**Critical aggregation concentration (CAC) measurement-** For the CAC calculation, stock solution of compound **4** and **5** were prepared in ultrapure water (with 1% ethanol) and then test solutions of desired concentration were prepared by adding the required volume of the compounds to a fixed concentration of ANS solution (4 μM). All the solutions were equilibrated for 2 hours before analysis. Changes in ANS fluorescence signal at 511 nm ($\lambda_{ex}$ = 380 nm) were measured using a Fluoromax-4.

**Liposome preparation-** Vesicles for the determination of partition coefficient and phase transition temperature were prepared according to the reported procedure. Briefly, lipids were dried out from chloroform solutions to form a thin film. The films were hydrated with phosphate-buffered saline (PBS), pH 7. The preparations were then sonicated at 50 °C for 2 minutes to prepare vesicles (final concentration 1 mM). The small unilamellar vesicles were prepared by extruding through a polycarbonate membrane (100 nm) using a handheld mini-

extruder at room temperature. For labeling experiment, NpOH in PBS buffer at PH 7 was added to the solution containing vesicles. The lipid solution was incubated with NpOH solution at 55 °C for 30 min with lipid/probe ratio at 100.

**Determination of partition coefficient of 1-naphthol in DPPC bilayer-** The partition coefficient of 1-naphthol (NpOH) in aqueous solution of DPPC vesicle was measured by monitoring the NpOH* emission peak as reported earlier. A series of solutions with fixed concentration of NpOH (4 μM) and varying concentrations of DPPC vesicle (0.01-0.1 mM) were prepared for the measurement. The other series of lipid solutions were also prepared accordingly in the presence of compound **4** and **5**. Fluorescence spectra of NpOH were recorded both in SG (30 °C) and LC phase (53 °C) of the DPPC vesicles. The partition coefficient (Kp) of NpOH was calculated from the slope of the double reciprocal plot of 1/F vs. 1/L using the equation 1, where, $F_0$ and F represent the fluorescence intensity of NpOH* ($\lambda_{em}$ = 370 nm) in the absence or presence of DPPC liposomes, respectively.

$$\frac{1}{F} = \frac{55.6}{K_p F_0 L} + \frac{1}{F_0} \quad (1)$$

The membrane bound fraction ($X_L$) of NpOH was calculated using the equation 2. The used molar concentration of lipid (L) was 0.1 mM.

$$X_L = \frac{K_p L}{55.6 + K_p L} \quad (2)$$

**Measurement of phase transition temperature of DPPC liposomes**- For the measurement of phase transition temperature of DPPC liposomes a series of test solutions were prepared with fixed concentration of labeled lipid. The $T_M$ value of DPPC liposome was determined by monitoring the fluorescence intensity of NpOH* ($\lambda_{em}$ = 370 nm) in the temperature range of 30 °C-55 °C. The $T_M$ values of DPPC liposomes were also measured in the presence of varying concentrations (20-200 μM) of compound **4** and **5**.

**Extent of Membrane Localization-** The extent of localization of the ligands at the liposome interface was studied by NBD fluorescence quenching method, using PC/$Ligand_{16}$/NBD-PE liposomes (89/10/1) in 50 mM Tris buffer, pH 8.2, containing 150 mM NaCl, according to the reported procedure. The quenching reaction was initiated by adding sodium dithionite from a stock solution of 0.6 M in 50 mM Tris buffer, pH 11 containing 150 mM NaCl, to

give a final concentration of 1 mM. The change in NBD fluorescence emission intensity at 530 nm ($\lambda_{ex}$ = 469 nm) was recorded for 3 min at room temperature.

**Protein Purification-** The PKCδ- and PKCθ-C1b subdomains were expressed in E. Coli as a GST-tagged protein, purified by glutathione sepharose column and the GST tag were removed by the thrombin treatment using methods similar to those reported earlier.[21-23]

**Fluorescence Measurements-** To calculate the binding parameters under membrane free system, ligand-induced Trp fluorescence quenching measurements were performed on a Fluoromax-4 spectrofluorometer at room temperature. The stock solutions of compounds were freshly prepared by first dissolving complexes in spectroscopic-grade dimethylsulfoxide (DMSO) and then diluted with buffer. The amount of DMSO was kept less than 3% (by volume) for each set of experiment and had no effect on any experimental results. For fluorescence titration, protein (1 μM) and varying concentration of ligands were incubated in a buffer solution (20 mM Tris, 150 mM NaCl, 50 μM $ZnSO_4$, pH 7.4) at room temperature. Protein was excited at 284 nm, and emission spectra were recorded from 300 to 550 nm. Proper background corrections were made to avoid the contribution of buffer and dilution effect. The resulting plot of Trp fluorescence as a function of ligand concentration was subject to nonlinear least-squares best-fit analysis to calculate the apparent dissociation constant for ligands ($K_D$(ML)), using equation 3, which describes binding to a single independent site.

$$(F_0 - F) = \Delta F_{max}\left(\frac{[x]}{[x]+K_D(ML)}\right) + C \qquad (3)$$

Where, F and $F_0$ represented the fluorescence intensity at 339 nm in the presence and the absence of ligand respectively. The $\Delta F_{max}$ represents the calculated maximal fluorescence change; [x] represents the total monomeric ligand concentration.

Analysis of protein-to-membrane Förster resonance energy transfer (FRET) based binding assay was used to measure the binding affinity and specificity of the selected ligands under a liposomal environment. In this assay, membrane-bound C1 domain was displaced from liposomes (PC/PE/dPE/Ligand (75/15/5/5)) by the addition of the $DAG_8$. The vesicles composed of PC/PE/PS/dPE (60/15/20/5) and PC/PE/PS/dPE/Ligand (55/15/20/5/5) was used as control and for ligands, respectively. The stock solution of $DAG_8$ was titrated into the sample containing C1 domain (1 μM) and excess liposome (100 μM total lipid) in a buffer

solution (20 mM Tris, 150 mM NaCl, 50 μM $ZnSO_4$, pH 7.4) at room temperature. The competitive displacement of protein from the membrane was quantitated using protein-to-membrane FRET signal ($\lambda_{ex}$ = 280 nm and λem = 505 nm). Control experiments were performed to measure the dilution effect under similar experimental condition and the increasing background emission arising from direct dPE excitation. Protein-to-membrane FRET signal values as a function of $DAG_8$ concentration were subjected to nonlinear least-squares-fit analysis using eq 5 to calculate apparent equilibrium inhibition constants ($K_I(DAG_8)_{app}$) for $DAG_8$. Where, [x] represents the total $DAG_8$ concentration and $\Delta F_{max}$ represents the calculated maximal fluorescence change.

$$F = \Delta F\left(1 - \frac{[x]}{[x]+K_I(\mathrm{DAG_8})_{app}}\right) + C \qquad (4)$$

The equilibrium dissociation constant ($K_D$(L)) for the binding of the C1 domains to the ligand-associated liposomes was calculated from eq 6, using $K_D$(ML) and $K_I(DAG_8)_{app}$ values. Where, $[L]_{free}$ is the free ligand concentration (2.63 ± 0.04 μM). During calculation, the ligand concentration in the liposome interior was ignored, because of their inaccessibility for the protein. Thus, the protein accesses about half of lipids in the liposomes. The ligand concentration was used excess relative to the protein. The free ligand concentration was calculated by assuming that most of the protein would bind to the liposome and equimolar amount of ligand can be subtracted from the accessible ligand.

$$K_I(\mathrm{DAG_8})_{app} = K_D(\mathrm{ML})(1 + \frac{[L]_{free}}{K_D(\mathrm{L})}) \qquad (5)$$

**Surface Plasmon Resonance Analysis-** All surface plasmon resonance (SPR) measurements were performed (at 25 °C, flow rate of 30 μL/min) using a lipid-coated L1 sensor chip in the Biacore X 100 (GE Healthcare) system as described earlier.[32-34] The vesicles composed of PC/PE/PS (60/20/20) and PC/PE/PS/Ligand (55/20/20/5) was used as control and active surface, respectively.

**References**

1. C. Yang and M. G. Kazanietz, *Trends Pharmacol. Sci*., 2003, **24**, 602-608.

2. P. M. Blumberg, N. Kedei, N. E. Lewin, D. Yang, G. Czifra, Y. Pu, M. L. Peach and V. E. Marquez, *Curr. Drug Targets*, 2008, **9**, 641-652.

3. R. Zeidman, B. Lofgren, S. Pahlman and C. Larsson, *J. Cell Biol.*, 1999, **145**, 713-726.

4. P. J. Parker, L. Coussens, N. Totty, L. Rhee, S. Young, E. Chen, S. Stabel, M. D. Waterfield and A. Ullrich, *Science*, 1986, **233**, 853-859.

5. G. Manning, D. B. Whyte, R. Martinez, T. Hunter and S. Sudarsanam, *Science*, 2002, **298**, 1912-1934.

6. J. B. Smith, L. Smith and G. R. Pettit, *Biochem. Biophys. Res. Commun*., 1985, **132**, 939-945.

7. F. Colon-Gonzalez and M. G. Kazanietz, *Biochim. Biophys. Acta*, 2006, **1761**, 827-837.

8. A. C. Newton, *Chem. Rev*., 2001, **101**, 2353-2364.

9. A. C. Newton and L. M. Keranen, *Biochemistry*, 1994, **33**, 6651-6658.

10. G. Manning, D. B. Whyte, R. Martinez, T. Hunter and S. Sudarsanam, *Science*, 2002, **298**, 1912-1934.

11. P. M. Blumberg, N. Kedei, N. E. Lewin, D. Yang, G. Czifra, Y. Pu, M. L. Peach and V. E. Marquez, *Curr. Drug Targets*, 2008, **9**, 641-652.

12. G. Boije af Gennas, V. Talman, O. Aitio, E. Ekokoski, M. Finel, R. K. Tuominen and J. Yli-Kauhaluoma, *J. Med. Chem*., 2009, **52**, 3969-3981.

13. G. Boije Af Gennas, V. Talman, J. Yli-Kauhaluoma, R. K. Tuominen and E. Ekokoski, *Curr. Top. Med. Chem*., 2011, **11**, 1370-1392.

14. Y. Nishizuka, *Science*, 1992, **258**, 607-614.

15. S. G. Rhee, *Annu. Rev. Biochem*., 2001, **70**, 281-312.

16. J. Das and G. M. Rahman, *Chem. Rev*., 2014, **114**, 12108–12131.

17. T. S. Chang, Int. *J. Mol. Sci*., 2009, **10**, 2440-2475.

18. G. A. Burdock, M. G. Soni and I. G. Carabin, *Regul. Toxicol. Pharmacol*., 2001, **33**, 80-101.

19. C. Z. Blumenthal, *Regul. Toxicol. Pharmacol*., 2004, **39**, 214-228.

20. R. Bentley, *Nat. Prod. Rep*., 2006, **23**, 1046-1062.

21. G. J. Nohynek, D. Kirkland, D. Marzin, H. Toutain, C. Leclerc-Ribaud and H. Jinnai, *Food Chem. Toxicol.*, 2004, **42**, 93-105.

22. D. Breitkreutz, L. Braiman-Wiksman, N. Daum, M. F. Denning, T. Tennenbaum, *J. Cancer Res. Clin. Oncol.*, 2007,**133**, 793-808.

23. P. R. Nath and N. Isakov, *Biochem. Soc. Trans.*, 2014, **42**, 1484-1489.

24. G. G. Zhang, M. G. Kazanietz, P. M. Blumberg and J. H. Hurley, *Cell*, 1995, **81**, 917-924.

25. K. Nacro, B. Bienfait, J. Lee, K. C. Han, J. H. Kang, S. Benzaria, N. E. Lewin, D. K. Bhattacharyya, P. M. Blumberg and V. E. Marquez, *J. Med. Chem*., 2000, **43**, 921-924.

26. N. Brose and C. Rosenmund, *J. Cell Sci*., 2002, **115**, 4399-4411.

27. M. N. Hodgkin, T. R. Pettitt, A. Martin, R. H. Michell, A. J. Pemberton and M. J. Wakelam, *Trends Biochem. Sci*., 1998, **23**, 200-204.

28. J. Swain, M. Mohapatra, S. R. Borkar, I. S. Aidhen and A. K. Mishra, *Phys. Chem. Chem. Phys.*, 2013, **15**, 17962-17970.

29. E. B. Abuin, E. A. Lissi, A. Aspee, F. D. Gonzalez and J. M. Varas, *J. Colloid. Interface Sci*., 1997, **186**, 332-338.

30. A. Manosroi, P. Wongtrakul, J. Manosroi, U. Midorikawa, Y. Hanyu, M. Yuasa, F. Sugawara, H. Sakai and M. Abe, *Int. J. Pharm*., 2005, **298**, 13-25.

31. N. Pappayee and A. K. Mishra, *Photochem. Photobiol*., 2001, **73**, 573-578.

32. M. Mohapatra and A. K. Mishra, *Langmuir*, 2011, **27**, 13461-13467.

33. M. Mohapatra and A. K. Mishra, *J. Phys. Chem. B*, 2010, **114**, 14934-14940.

34. M. B. Lande, J. M. Donovan and M. L. Zeidel, *J. Gen. Physiol*., 1995, **106**, 67-84.

35. O. Raifman, S. Kolusheva, M. J. Comin, N. Kedei, N. E. Lewin, P. M. Blumberg, V. E. Marquez and R. Jelinek, *FEBS J*., 2010, **277**, 233-243.

36. N. Mamidi, S. Gorai, R. Mukherjee and D. Manna, *Mol. Biosys.*, 2012, **8**, 1275-1285.

37. N. Mamidi, S. Gorai, J. Sahoo and D. Manna, *Chem. Phys. Lipids*, 2012, **165**, 320-330.

38. K. E. 46Landgraf, C. Pilling and J. J. Falke, *Biochemistry*, 2008, **47**, 12260-12269.

39. M. Hubert, B. J. Compton, C. M. Hayman, D. S. Larsen, G. F. Painter, T. Rades and S. Hook, *Mol. Pharm.*, 2013, **10**, 1928-1939.

40. C. Huang, Z. Q. Wang, H. N. Lin, E. E. Brumbaugh and S. Li, *Biochim. Biophys. Acta*, 1994, **1189**, 7-12.

41. S. Leekumjorn and A. K. Sum, *Biochim. Biophys. Acta*, 2007, **1768**, 354-365.

42. H. W. Huang, E. M. Goldberg and R. Zidovetzki, *Biophys. J*., 1999, **77**, 1489-1497.

43. G. Boije af Gennas, V. Talman, O. Aitio, E. Ekokoski, M. Finel, R. K. Tuominen and J. Yli-Kauhaluoma, *J. Med. Chem*., 2009, **52**, 3969-3981.

44. N. Mamidi, S. Gorai, R. Mukherjee and D. Manna, *Mol. Biosys*., 2012, **8**, 1275-1285.

45. R. V. Stahelin, *J. Lipid Res*., 2009, **50**, S299-304.

46. M. J. Wakelam, *Biochim. Biophys. Acta*, 1998, **1436**, 117-126.

47. E. M. Griner and M. G. Kazanietz, *Nat. Rev. Cancer*, 2007, **7**, 281-294.

48. F. Colon-Gonzalez and M. G. Kazanietz, *Biochim. Biophys. Acta*, 2006, **1761**, 827-837.

49. M. N. Hodgkin, T. R. Pettitt, A. Martin, R. H. Michell, A. J. Pemberton and M. J. Wakelam, *Trends Biochem. Sci.*, 1998, **23**, 200-204.

50. F. Battaini and D. Mochly-Rosen, *Pharmacol. Res*., 2007, **55**, 461-466.

51. J. A. Corbin, R. A. Dirkx and J. J. Falke, *Biochemistry*, 2004, **43**, 16161-16173.

52. N. Mamidi, S. Gorai, B. Ravi and D. Manna, *Rsc Advances*, 2014, **4**, 21971-21978.

53. H. J. Mackay and C. J. Twelves, *Nat. Rev. Cancer*, 2007, **7**, 554-562.

# CHAPTER 3

# Elucidating the Interaction of γ-Hydroxymethyl-γ-Butyrolactone Substituents with Model Membranes and Protein Kinase C-C1 Domains

The present chapter demonstrates the interaction of γ-Hydroxymethyl-γ-Butyrolactone Substituents with lipid monolayer and bilayer through the use of Langmuir-Blodgett technique, DPH anisotropy and NBD-PE quenching studies. Besides, determining the PKC-C1 domain binding properties by fluorescence techniques, the PKC activation property of γ-Hydroxymethyl-γ-Butyrolactone Substituents is also determined by using nonradioactive fluorescence peptide based kinase assay.

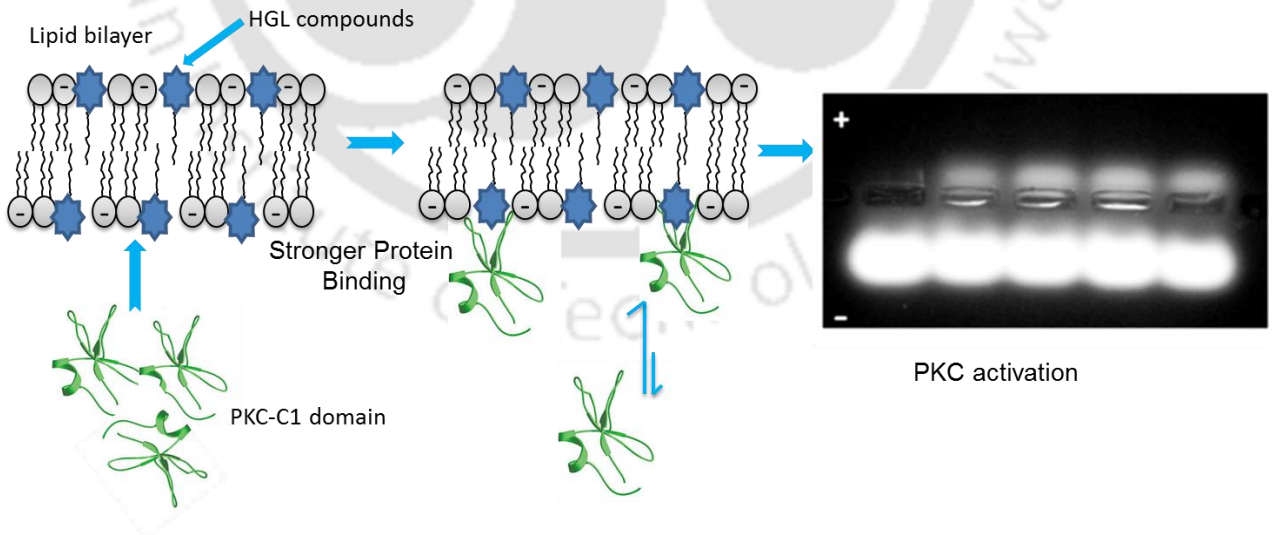

### 3.1. Background and focus of the present work

The lipophilic second messenger sn-1,2-diacylglycerol (DAG) binds to the C1 domains of both the classical (calcium-, DAG-, and phospholipid-dependent), and novel (calcium-independent, but DAG- and phospholipid-dependent) PKCs which leads to its activation. A variety of PKC regulator directed to the C1 domain have been developed as a new class of antitumor agents. [1-3] Phorbol esters, which strongly bind with the C1 domains, have provided pharmacological tools for studying PKC function and activity. However, the phorbol esters are known to promote tumors.[4-6] C1 domain ligands such as bryostatin-1 is in clinical trials and ingenol-3-angelate is in clinical use.[4, 5] Compounds like prostratin, gnidimacrin, and DPP (12-deoxyphorbol-13-phenylacetate) have also shown PKC enzyme dependent antitumor activities in mice and selected human cell lines.[7, 8]

Phorbol esters, bryostatin and other reported high-affinity C1 domain binding ligands are structurally complex, and they bind competitively to the DAG-binding site of the C1 domain with affinities several orders of magnitude higher than only DAGs.[9, 10] Conformationally rigid scaffold of these C1 domain ligands made it difficult to alter their specificity and large-scale production. However, conformationally restricted DAG-lactones are reported to have intermediate potency between DAG and phorbol esters.[6-10] It is also deduced that the structural rigidity of DAG-lactone reduce the number of possible rotameric forms of DAGs, and one of the rigid rotamers mimic the actual conformation of physiologically active DAGs. The stronger binding of DAG-lactone to PKC-C1 domain than only DAG apparently governed by the smaller decrease in entropy. Stronger binding is also governed by the presence of required pharmacophores and proper orientation of the ligands inside the binding pocket and, their localization at the membrane bilayer. Structural and functional studies of the PKC-C1 domains have revealed that Thr-12, Leu-21, and Gly-23 residues play a crucial role in ligand binding. The hydrophobic residues present along the circumference of the binding pocket interact with the hydrophobic moiety of the ligand and facilitate the insertion of the C1 domain into the membrane after ligand binding, thereby stabilizing the formation of the ternary (ligand-receptor-membrane) binding complex. In an attempt to develop C1 domain ligands with simple and readily amenable to the introduction of structural variation template, we used (S)-γ-hydroxymethyl-γ-butyrolactone (HGL). The other aim of designing these simple molecules is to overcome the spread in potency between the complex natural product ligands and DAG.

The present study describes the design, synthesis, aggregation behaviour in aqueous solution, interaction with liposomes, in vitro binding properties of HGL substituents to the

C1b subdomain of PKCδ and PKCθ and their PKC enzyme activity. The results demonstrate that the C1 domain binding potencies of the compounds correlates well with their effect on membrane fluidity and hydration. The potent HGL analogues bind competitively to the DAG-binding site of the C1 domains of PKC. The γ-hydroxymethyl group, carbonyl groups of lactone and ester of the active compounds play a crucial role in PKC-C1 domain binding. At lower micromolar concentrations, these HGL analogs also activate PKC enzyme. Overall, the results expand our understanding on the molecular parameters affecting PKC-C1 domain binding to membranes by synthetic HGL analogues.

**Design of HGL substituents**

Structure-activity relationship (SAR) studies showed that hydroxymethyl and carbonyl functional groups of DAGs, DAG-lactones and phorbol esters play an important role for their interactions with the backbone amide protons and carbonyl of PKC-C1 domains. However, all these ligands have differential C1 domain binding potencies. Conformationally rigid phorbol esters have more than 1000-fold stronger binding affinity for C1 domain than structurally simple and flexible DAGs. Several conformationally-constrained DAG-lactones showed intermediate C1 domain binding potency.[11-13] Inspired by the structural rigidity and higher binding affinity of the DAG-lactones, we selected (S)-γ-hydroxymethyl-γ-butyrolactone (HGL) analogues for the devolvement of PKC-C1 domain modulators. The HGL moiety provides a rigid five-membered ring as in DAG-lactones, but the HGL analogues are structurally different due to its position of ester linkage and number of hydrophobic 'tails' (Figure 3.1). These compounds also retain necessary pharmacophores namely hydroxyl and carbonyl functionalities within the same molecule and hydrophobic tails which are important for membrane interaction (Figure 3.1). Unlike most of the potent C1 domain ligands like phorbol esters, bryostatins and others, HGLs are structurally simpler and contain lesser rigidity. Structural modifications and large scale productions of HGLs are comparatively easier than those potent natural products.[11-13] HGLs with long chain (palmitic acid) and short chain (octanoic acid and propanoic acid) acids were used in order to study the impact of hydrophobicity on the binding affinity. HGL analogous **1a** and **1b** are chosen in order to investigate the role of hydroxymethyl and hydroxyl groups on the binding of C1b subdomains of PKC isoforms. To verify the hydrophobicity effect of the ligands on the biding affinity, we also used HGL ester derivatives by introducing long chain fatty acid (palmitic acid) and short chain acids (octanoic acid, propanoic acid).

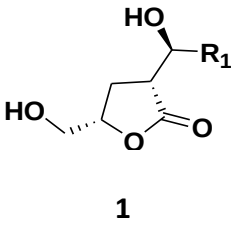


1

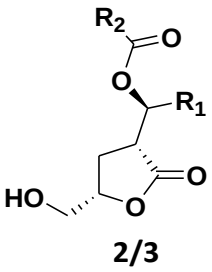


2/3

| Compound | $R_1$ | $R_2$ |
|---|---|---|
| **1a** | $CH_3(CH_2)_{14}$ | — |
| **2a** | $CH_3(CH_2)_{14}$ | $CH_3CH_2$ |
| **3a** | $CH_3(CH_2)_{14}$ | $CH_3(CH_2)_6$ |
| **1b** | $CH_3(CH_2)_6$ | — |
| **2b** | $CH_3(CH_2)_6$ | $CH_3CH_2$ |
| **3b** | $CH_3(CH_2)_6$ | $CH_3(CH_2)_{14}$ |

**Figure 3.1.** Structures of γ-hydroxymethyl-γ-butyrolactone (HGLs).

### 3.2. Results and discussions

**Aggregation Studies of the Compounds —** To check the behaviour of the compounds in aqueous solution; we first investigated their aggregation behaviours by measuring the fluorescence properties of a polarity indicator, pyrene. Concentration-dependent aggregation behaviors of the compounds and simultaneous inclusion of pyrene molecules into its hydrophobic core of the aggregates was reflected by the increase in pyrene fluorescence intensity. The fluorescence intensity ratio, $I_1/I_3$ of pyrene was considered as a measure of the polarity of its microenvironment and was further used to calculate critical aggregation concentration (CAC) values of the compounds (Figure 3.2A).[14] The measured CAC values of the compounds **1a**, **2a**, and **3a** were 60, 22, and 43 μM, respectively (Figure 3.2B). Above the CAC values, the higher and lower ratios of $I_1/I_3$ indicate the polar (loose aggregates) and hydrophobic (compact aggregates) environments. The results show that, above 50−70 μM compound concentrations, the ratio of $I_1/I_3$ reached a plateau region. However, with further increase in concentrations the $I_1/I_3$ ratio gradually reduced, signifying the formation of loosely bound aggregates in aqueous solution with an extensive concentration range. The results also indicate that tested compounds aggregate at lower concentration ranges in aqueous solution, possibly due to the absence of charged headgroups. Investigation of these CAC ranges of aggregate formation is essential in understanding their interaction properties both with the lipid bilayers and PKC-C1 domain under monomeric form in aqueous solution.

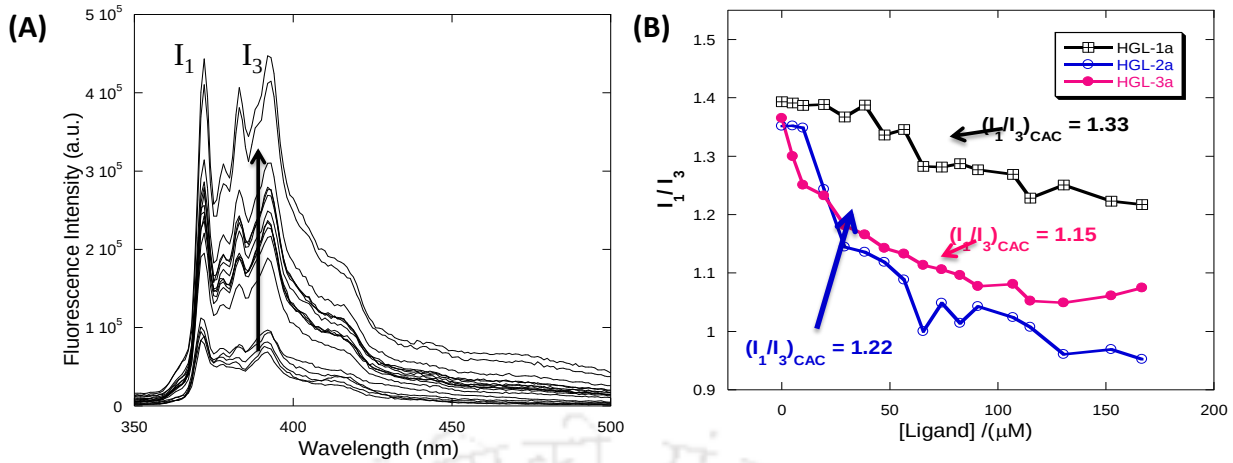


**Figure 3.2.** Measurement of critical aggregation concentration of compounds **1a**, **2a**, and **3a** in aqueous solution. Concentration dependent increase in Pyrene fluorescence intensity upon addition of the compounds(A) and Plot of pyrene fluorescence intensity ratio $I_1/I_3$ against increasing concentration of compounds(B). [pyrene] = 2 μM, $\lambda_{ex}$ = 380 nm.

## Membrane-Ligand Interaction Measurements

**Orientation of Ligands at the Interface —** Surface pressure (π)–area (A) isotherms provide an insight into how chemical structure and physical behaviour including intramolecular and intermolecular interactions modify the assembly of the amphiphilic molecules at the air/water interface.[15, 16] The π–A isotherms of the pure compounds, displayed a slightly different assembly pattern as of compounds in the presence of DPPC lipid (Figure 3.3). However, the assembly properties of the pure compounds **2a** and **3a** are significantly different from pure DPPC lipids under similar experimental conditions. The isotherms also indicate that these compounds become partly soluble with increase in lateral pressure. The π–A isotherms of these pure compounds show a profound liquid-expanded (LE) phase, subsequent LE–liquid condensed (LC) region and a more condensed phase during the compression process. The LE phase of these pure compounds and compounds in the presence of DPPC lipid begin at a much higher molecular area of 250 $Å^2$ indicating a very loose configuration of the molecules within the fluid monolayer. The presence of LE-LC is indicated by the plateau region in the isotherm. The additional ordering in π–A isotherms and significant change in LE-LC region of these compounds in the presence of DPPC lipid may be due to their interaction properties between their headgroups and hydrophobic 'tails' (Figure 3.3). It is also important to note that the presence of acyl groups demonstrate significant effect on the monolayer properties of the compounds, however alternative hydrophobic groups show almost no effect on the monolayer properties of the compounds. Nevertheless, monolayer properties of the

compounds in the presence of DPPC lipid clearly depict their strength of interaction. Therefore, the hydroxyl-lactone moiety of the compounds strongly affects the assembly properties and its interactions with the DPPC molecules, and also lipid interactions play a significant role in the monolayer organization of the molecules.

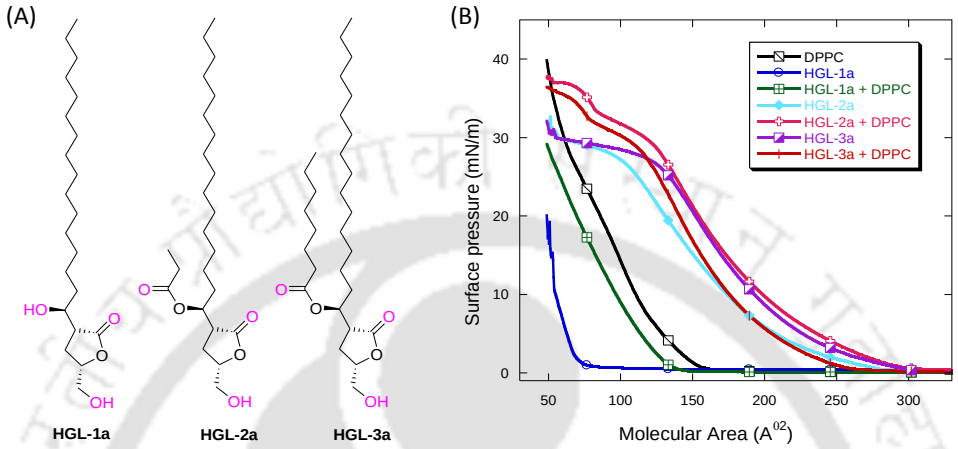


**Figure 3.3.** Structure of the membrane active compounds (A). Surface pressure (π)–molecular area (A) isotherm of the saturated hybrid lipids (B).

**Measurement of Change in Fluidity and hydration of the Lipid Bilayer —** To recognize the consequences of membrane active compounds upon the fluidity of lipid bilayer and dynamics of lipid molecules, we measured the fluorescence anisotropy of the membrane active 1,6-diphenyl-1,3,5-hexatriene (DPH) molecules under liposomal environment. The hydrophobic DPH molecules are known to embed within the hydrophobic core of the lipid bilayers, allow estimating the modulation of lipid-bilayer fluidity induced by membrane-active compounds.[14] Figure 3.4A represents the anisotropy values of DPH molecules in the presence/absence of the compounds under liposomal environment. The anisotropy value of DPH in the presence of compound **2a** is slightly smaller than the other compounds, indicating increase in bilayer fluidity. Changes in membrane surface were monitored by dansyl-PE probe. Fluorescence signal of dansyl is an environment sensitive and efficiently gets quenched by water.[17, 18] The increase in %mole of membrane active HGL compounds induces an increase in dansyl fluorescence quenching (Figure 3.4B). The increase in quenching can be correlated with the increase in dansyl-PE head group hydrations at the membrane surface, which correlates well with the increase in membrane fluidity in the presence of compounds.

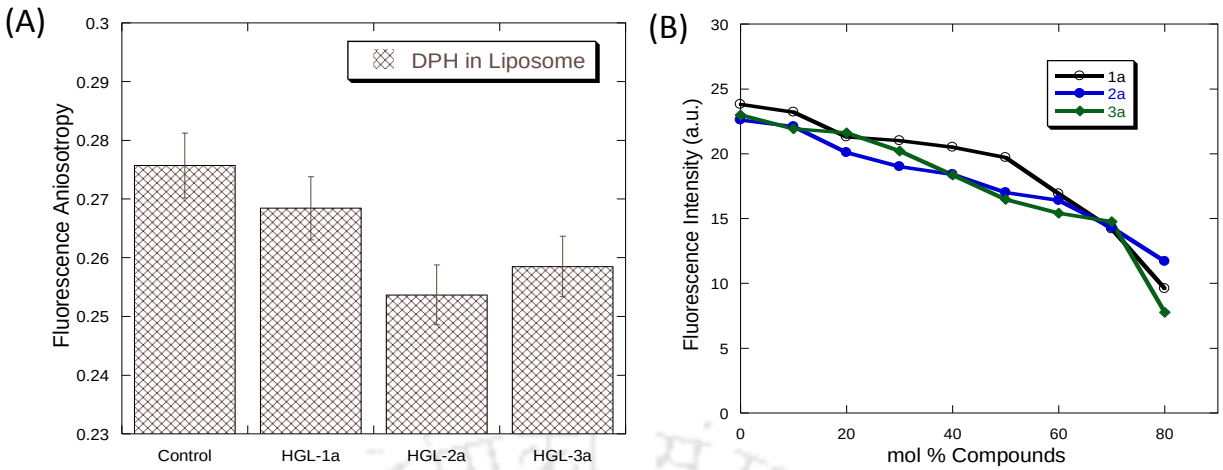


**Figure 3.4.** Membrane fluidity and hydration change measurements. Fluorescence anisotropy of DPH embedded in PC/Cholesterol/Ligand (60/20/20) liposomes. Control: no ligand was added to the liposomes (A). Effect of compounds on the fluoresce intensity of dansyl-PE embedded in PC/Cholesterol/dansyl-PE (79/20/1) liposomes (B). Values represent the mean ± SD from triplicate measurements.

**Extent of Membrane Localization —** The structural analysis reveals that the headgroups of DAG and HGLs are anticipated to be placed near the bilayer/water interfacial region. However, the extent of localization of these pharmacophores containing headgroups at the bilayer/water interface is crucial for their capability to interact with the C1 domains. For this reason we determined sodium dithionite-induced fluorescence quenching rates of NBD moiety using DPPC/Ligand/NBD-PE liposomes. The NBD moiety of NBD-PE lipid is reported to be embedded close to the bilayer interface, providing a useful marker for surface interactions of membrane-active C1 domain ligands.[19-21]

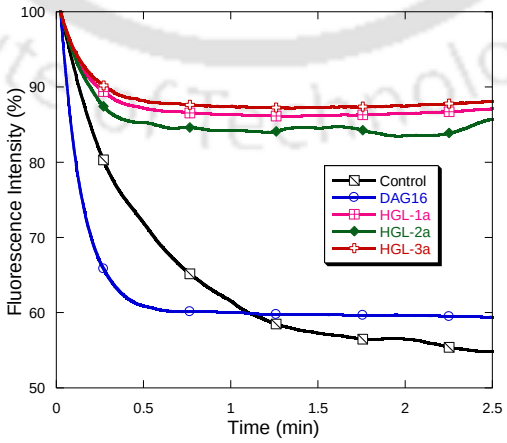


**Figure 3.5.** Fluorescence quenching of NBD-PE embedded in PC/Ligand$_{16}$/NBD-PE (89:10:1) liposomes. Sodium dithionite = 0.6 µM. Control: no ligand.

The measured NBD fluorescence quenching rates propose that, the NBD moiety became more "shielded" from the soluble dithionite quencher, because of the presence of ligands within the liposomes (Figure 3.5). Therefore membrane environment modification by these compounds may enhance the ability of C1 domain to insert into the membrane. The results also suggest that these compounds are more localized at the bilayer/water interface and more accessible for protein binding than $DAG_{16}$.

**Protein-Ligand Interaction Measurements**

In the present study, the C1b subdomains of PKCδ and PKCθ isoenzymes were used to measure the binding parameters of HGLs. These C1b subdomains have sufficiently strong DAG binding affinities and easy to purify from bacterial cells. The binding-potencies of the compounds were measured by Trp-fluorescence quenching method, steady-state fluorescence anisotropy and Förster resonance energy transfer (FRET)-based competitive binding assay.

**Interaction with Soluble Ligands —**Tryptophan fluorescence quenching method (as described in chapter 2) was used to measure the binding affinity of the ligands to C1b subdomains of PKCδ and PKCθ isoenzymes in soluble form. The calculated binding parameters revealed that compounds **2** and **3** with different chain length strongly interact with the C1b subdomains. In particular, monomeric ligand **2b** and **3b** shows more that 9- and 15-fold stronger binding affinity than $DAG_8$ for PKCδ-C1b subdomain (Table 3.1). To understand the importance of hydrophobicity of the compounds in protein binding, a similar analysis was performed with the long-chain HGL derivatives. Although, there is a distinct difference in hydrophobicity between the compounds like **3a** and **3b**, they show only a subtle difference in their protein binding affinities. This could be due to their binding orientations with the C1b subdomains. The binding of these compounds with the C1b subdomains is mostly governed by the hydrogen bonding with amino acid backbone through their γ–hydroxymethyl and carbonyl functionalities. In addition hydrophobic interaction among the compounds and amino acid residues at the circumference of the binding pocket may play an important role in ligand binding affinities of the protein. The long alkyl chains facilitate the compounds to interact with the membrane bilayer, where PKC proteins interact with the membrane through the C1 domain for activation and regulation of various cellular pathways. A similar trend in binding affinities was also observed with the reported C1 domain ligands. However, these binding parameters of the compounds in monomeric form do not show a clear specificity for either PKCθ or PKCδ-C1 domains.

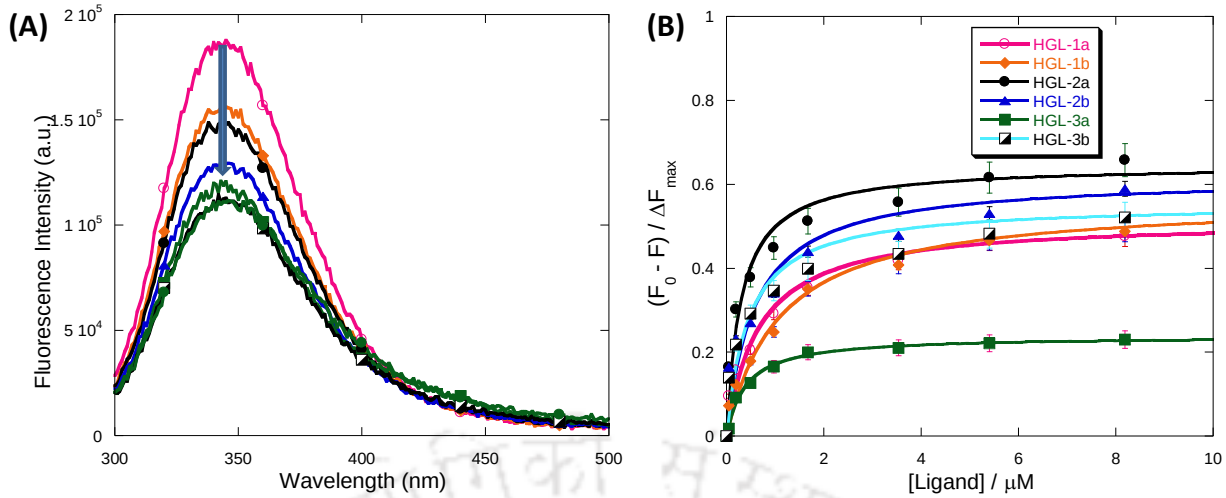


**Figure 3.6.** Binding of compounds with the PKCδ-C1b subdomain. Quenching of Trp Fluorescence intensity upon addition of compounds (A) and Representative plot of Trp-fluorescence intensity of PKCδ-C1b (1 μM) in buffer (20 mM Tris, 160 mM NaCl, 50 μM $ZnSO_4$, pH 7.4) in the presence of varying concentration of **1-3**, where F and $F_0$ are fluorescence intensity in the presence and absence of the ligands, respectively (B). The solid lines are nonlinear least-squares best-fit curves. Values represent the mean ± SD from triplicate measurements.

**Table 3.1.** Ligand binding parameters of PKCδ-C1b and PKCθ-C1b proteins[a] at room temperature.

| Compound | $K_D$ (ML)/(μM) | | Compound | $K_D$ (ML)/(μM) | |
|---|---|---|---|---|---|
| | PKCδ-C1b | PKCθ-C1b | | PKCδ-C1b | PKCθ-C1b |
| **$DAG_{16}$** | 6.57 ± 0.23 | 7.14 ± 0.39 | **$DAG_8$** | 11.37 ± 0.69 | 6.92 ± 0.39 |
| **1a** | 0.89 ± 0.11 | 0.81 ± 0.12 | **1b** | 1.33 ± 0.12 | 0.68 ± 0.11 |
| **2a** | 0.40 ± 0.14 | 0.33 ± 0.08 | **2b** | 1.02 ± 0.15 | 0.30 ± 0.09 |
| **3a** | 0.38 ± 0.09 | 0.98 ± 0.09 | **3b** | 0.73 ± 0.19 | 1.19 ± 0.19 |

[a] Protein, 0.25 μM in buffer (20 mM Tris, 160 mM NaCl, 50 μM $ZnSO_4$, pH 7.4,
Values represent the mean ± SD from triplicate measurements.

**Molecular Docking Analysis —** For better understanding of the possible binding mode of the compounds and the interacting residues of the proteins, we performed molecular docking analysis using the crystal coordinates of the PKCδ-C1b in complex with phorbol-13-O-acetate (1PTR).[22] The molecular models revealed that the HGLs were anchored to the binding site in a similar fashion, as phorbol esters and DAG-lactones.[12] The most effective compound **2b** showed three possible hydrogen bonds with the amino acid backbone. The hydroxymethyl group was hydrogen bonded to the carbonyls of L251. The carbonyl group of the lactone moiety formed a hydrogen bond with the backbone amide proton of G253. An additional hydrogen bonding was also observed between side chain amine of Q257 with the

carbonyl group of ester moiety. A similar hydrogen bonding network was also observed between compound **3b** and PKCδ-C1b protein. Whereas, the hydroxyl group of compound **1b** showed five hydrogen bonding with the backbone amide proton and carbonyls of T242 and L251 and side chain amide proton of Q257 (Figure 3.7). However, the binding affinity measurements and molecular docking analysis do not corroborate. This could be due to the strength of interaction and the conformational adjustments of the protein and compounds under experimental conditions and the contribution of bridging water molecules between HGLs and C1 domains could generate stronger interactions.

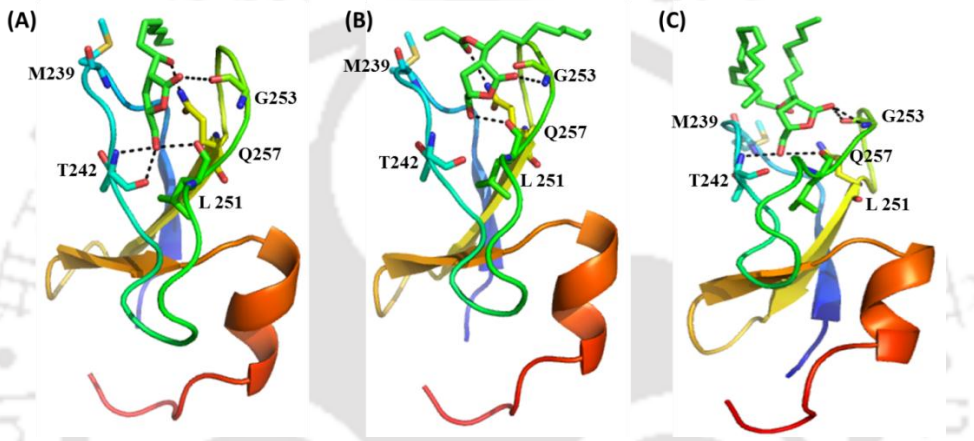


**Figure 3.7.** Structures of ligand-bound PKCδ-C1b subdomains. Modelled structure of **1b** (A), **2b** (B) and **3b** (C) docked into PKCδ-C1b (1PTR) subdomain. The modelled structures were generated using the Molegro Virtual Docker, version 4.3.0. The oxygen atoms and nitrogen atoms are shown in red and blue, respectively. The dotted line (black) indicates possible hydrogen bonds.

**Interaction with ligand Associated Liposomes —** C1 domain binding properties of the compounds were measured under membrane environment using protein to membrane FRET-based competitive binding assay (as described in chapter 2). The measurements were performed for membrane active compounds **1a**, **2a** and **3a**. The binding parameters demonstrated that compound **2a** has stronger binding affinity for the PKCθ-C1b subdomain than the other compounds under the liposomal environment. This competitive displacement assay also verifies that the potent compounds preferably interact with the C1b subdomains through its DAG/phorbol ester binding site. We have also calculated the equilibrium dissociation constant ($K_D$(L)) for the C1b subdomains binding to the liposome-associated targeted ligand using equation 4. Comparison of the equilibrium dissociation constant also revealed that C1b subdomains have higher binding affinity for the compound **2a** associated

liposomes (Table 3.2). Therefore, the in vitro C1 domain binding measurements pointed out that higher concentration of $DAG_8$ was required for the displacement of C1b subdomains from the compound **2a** associated liposomes.

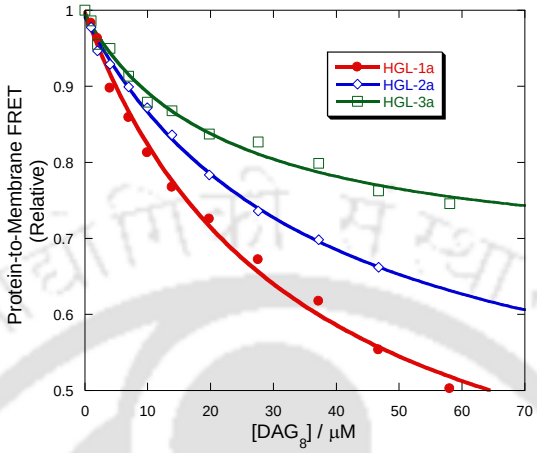


**Figure 3.8.** Competitive displacement assay for the PKCδ-C1b. Representative plot of FRET signal against $DAG_8$ concentration.

**Table 3.2.** Equilibrium binding parameters for PKCδ-C1b and PKCθ-C1b protein[a] with the ligand associated liposomes[b] at room temperature.

| Compound | $K_I(DAG_8)$app/(μM) | | $K_D(L_{16})$/(nM) | |
|---|---|---|---|---|
| | PKCδ-C1b | PKCθ-C1b | PKCδ-C1b | PKCθ-C1b |
| **1a** | 33.39 ± 1.95 | 34.12 ± 1.19 | 72.02 ± 5.91 | 63.95 ± 5.12 |
| **2a** | 36.95 ± 2.01 | 51.75 ± 3.74 | 28.78 ± 7.89 | 16.88 ± 1.95 |
| **3a** | 22.19 ± 1.68 | 25.90 ± 2.57 | 45.82 ± 7.01 | 103.43 ± 6.98 |

[a] Protein, 1 μM in buffer (20 mM Tris, 150 mM NaCl, 50 μM $ZnSO_4$, pH 7.4).
[b] Active liposome composition, PC/PE/PS/dPE/Ligand (55/15/20/5/5)
Values represent the mean ± SD from triplicate measurements.

**PKC Activity Assay —** To verify the feasibility of the synthesized HGL compounds in activating PKC enzymes, PepTag-nonradioactive kinase activity assay was performed in the presence of PS.[25, 26] In this assay, PKC enzyme specific florescent peptide was used as substrate. PKC dependent phosphorylation of the fluorescent peptide changes the net charge from +1 to -1, allowing the phosphorylated and nonphosphorylated fluorescent peptide to be separated by agarose gel electrophoresis method. The phosphorylated fluorescent peptide migrated toward the positive electrode and relative amount of phosphorylated fluorescent peptide was further quantified by fluorescence spectral analysis according to the manufacturer's protocols. The results showed that under the similar experimental condition

the potent compounds have similar or better PKC activating capabilities than DAG (Figure 3.9). In contrast to our C1 domain binding affinities for both monomeric form and under liposomal environment, PKC activity assay did not show any significant difference in their phosphorylation capabilities among the potent compounds. Therefore further studies are required to resolve their potency differences. However, the activity assay confirms that the synthesized potent HGL compounds activate PKC enzyme under the experimental conditions. These studies describe that the membrane active HGL derivatives interact with phospholipids and influence its monolayer/bilayer properties. The pharmacophores containing moiety, γ-hydroxymethyl-γ-butyrolactone of the compounds are preferably localized at the water/bilayer interface and accessible for PKC-C1 domain binding. The binding parameters and molecular docking analysis of the compounds highlight the importance of pharmacophores, hydrophobicity, binding orientations of the ligands. The binding properties also suggest that membrane active compounds can differentially influence the in-vitro membrane interaction properties of the C1 domains of PKCδ and PKCθ enzymes. The compound **2a** has a little stronger binding affinity for both the C1 domains, than other compounds. We hypothesize that the stronger binding affinities of compounds **2a** could be because of the presence of propionate group along with membrane active hydrophobic 'tail', which allow the compound to interact strongly with the hydrophobic residues surrounding the ligand binding site of the C1 domains or the effect of compound **2a** on the lipid bilayer organization. We also presume that, the presence of compounds makes the bilayer structure more loosely packed, allowing the C1 domains to bind with the HGLs and penetrate into the lipid bilayer, which is critical for the PKC enzyme activation at the inner-plasma membrane surface. However, the negligible binding potency difference between PKCδ- and PKCθ-C1b domains could be because of the dissimilarities in surface areas and the residues present within the binding site. Our nonradioactive kinase activity assay clearly showed that HGLs activate the PKC enzymes in similar manner as of DAG. PKC activating capabilities of these compounds could be lower than phorbol ester or other structurally complex molecules under the similar experimental condition; however we successfully developed structurally restricted γ-butyrolactone-based simple C1 domain ligands.

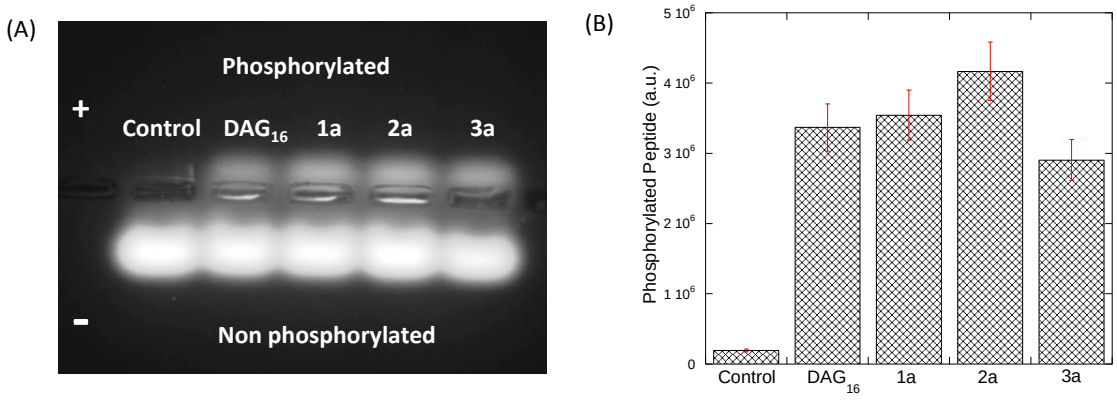


**Figure 3.9.** The PKC activity in the absence and presence of $DAG_{16}$ and potent compounds (8 μM). Representative UV-illuminated agarose gel image of the product of reactions run with PKC full-length enzyme. Control with no PS containing PKC activator solution and activator (lane a). Activity assay in the presence of $DAG_{16}$ (lane b) and potent compounds **1a** (lane c), **2a** (lane d) and **3a** (lane e). Relative amount of phosphorylated PepTag C1 peptide were calculated from fluorescence spectral analysis (B).

## Conclusion

In this study we have demonstrated that γ-hydroxymethyl-γ-butyrolactone substituents strongly interact with the model membrane and C1 domain of novel PKC isoenzymes. Strong interaction between compounds and model membrane alter its monolayer/bilayer properties including fluidity and hydration. The protein binding properties suggest that hydroxymethyl and acyl-groups of the compounds are important for C1 domain binding through its DAG/phorbol ester binding site. The enhancement in fluidity of the lipid bilayer structures could allow the PKC-C1 domains to interact strongly with the HGL derivatives in the presence of anionic phospholipids. Protein kinase activity assay also confirm that theses potent compounds can activate PKC enzymes. Therefore, our findings suggest that these γ-hydroxymethyl γ-butyrolactone substituents are potential regulator of PKC isoforms and can be used in PKC-based drug development process.

## 3.3. Experimental Section

**General Information-** 1,2-dipalmitoyl-sn-glycerol ($DAG_{16}$), 1,2-dioctanoyl-sn-glycerol ($DAG_8$), 1,2-dipalmitoyl-sn-glycero-3-phosphocholine (DPPC), 1,2-dipalmitoyl-sn-glycero-3-phospho-L-serine (DPPS), 1,2- dipalmitoyl-sn-glycero-3-phosphoethanolamine (DPPE), 1,2-dioleoyl-sn-glycero-3-phosphoethanolamine-N-(5-dimethylamino-1-naphthalenesulfonyl) (NBD-PE) and N-[5-(dimethylamino)naphthalene-1-sulfonyl]-1,2-dihexadecanoyl-sn-glycero-phosphoethanol -amine (Dansyl-PE) were purchased from Avanti Polar Lipids (Alabaster, AL). The PepTag-nonradioactive kinase activity assay kit was obtained from

Promega (Madison, WI). Ultrapure water (Milli-Q system, Millipore, Billerica, MA) was used for the preparation of buffers.

**Aggregation Studies-**The aggregation behaviours of the compounds in aqueous solution were examined by fluorescence measurements at room temperature, using Fluoromax-4 spectrofluorometer. The fluorescence properties of pyrene were monitored to measure the critical aggregation concentrations (CAC) of the compounds.[20, 27] The stock solutions of compounds were freshly prepared by first dissolving compounds in spectroscopic-grade dimethylsulfoxide (DMSO) and then diluted with water. The amount of DMSO was kept less than 1% (by volume) for each set of experiment and had no effect on any experimental results. For fluorescence measurements, saturated ethanolic solution of pyrene (2 μM) and varying concentration of ligands were incubated in water at room temperature. Pyrene was excited at 335 nm, and emission spectra were recorded from 345 to 550 nm. Pyrene produces five intense fluorescence peaks, but only $I_1$ (373 nm) and $I_3$ (383 nm) were considered for the measurement of CAC values.

**Interfacial Behavior Measurement by Langmuir Trough Techniques**- The air-water interfacial behaviors of the amphiphilic compounds were investigated by using Langmuir trough technique (NIMA technology Ltd.) according to the Wilhelmy plate method.[15, 21] Stock solutions of the compounds were prepared in a chloroform/methanol mixture [4:1 (v/v)]. The sub-phase consisted of Milli-Q water (Millipore, Bedford, MA) had a resistance of 18.4 MΩ-cm. Before each experiment, the cleanliness of the sub-phase was verified by repeated compression without lipids. If the surface pressure changed by less than 0.2 mN/m the surface was considered to be clean. Lipid solutions (5 μL of 0.5 mg/mL stock solution) were deposited onto the surface of the sub-phase. After the solvent had been allowed to evaporate for 10 min, the monolayer was compressed at a constant rate of 10 mm/min, and the surface pressure (π)–area (A) isotherm was continuously recorded. All experiments were conducted at room temperature (25 °C). The π–A isotherm was analyzed by inbuilt software.

**Measurement of the Change in Bilayer Fluidity and Hydration**- To measure the change in membrane fluidity anisotropy of DPH under liposomal environment was measured according to the reported procedure.[28] The fluorescence probe DPH was incorporated into the liposomes by adding the dye dissolved in THF(1 mM) to liposomes (PC/Cholesterol/Ligand (60/20/20)) up to a final concentration of 1.25 μM. After 30 min of incubation at room

temperature DPH fluorescence anisotropy was measured at 430 nm (excitation 355 nm). The concentration of compounds was 2.9 μM. To measure the change of membrane hydration, dansyl-PE doped liposomes (PC/Cholesterol/ dansyl-PE (79/20/1)) were prepared separately with and without doping of membrane active HGL compounds at different concentrations (0-80 mol %) and the change in dansyl fluorescence signal was recorded.[17, 18]

**Extent of Membrane Localization**- As described in chapter 2, section 2.3.

**Protein Purification**- As described in chapter 2, section 2.3.

**Fluorescence-Based Protein Binding Analysis**- As described in chapter 2, section 2.3.

**Molecular modeling**- As described in chapter 2, section 2.3.

**PKC activity analysis**-The PKC enzyme activity was measured using PepTag non-radioactive protein kinase assay kit in the presence of $DAG_{16}$ and potent compounds with modified assay protocol. The assay was stopped after 30 min by incubating the sample vials at 95 °C for 10 min and 2 μl of 80% glycerol was added to the samples. Agarose gel (0.8%) electrophoresis was run at 110 V for 20 min and the gel image was captured under UV light. The phosphorylated fluorescent peptide bands were excised from agarose gel, and PKC activity was quantitatively estimated by fluorescence spectral analysis ($\lambda_{ex}$ = 540 nm).

| | Reagents for the assay | Control | Reactions |
|---|---|---|---|
| 1 | PepTag PKC reaction 5X buffer | 5 μl | 5 μl |
| 2 | PepTag C1 peptide (0.4μg/μl) | 5 μl | 5 μl |
| 3 | PKC activator 5X solution | 0 μl | 5 μl |
| 4 | Compounds (DAG/**1a**/**2a**/**3a**; 80 μM) | 0 μl | 2.5 μl |
| 5 | Peptide protection solution | 1 μl | 1 μl |
| 6. | Protein kinase C (2.5μg/ml in PKC dilution buffer) | 4 μl | 4 μl |
| 7 | Deionized water for final reaction volume of 25μl | 5 μl | 2.5 μl |

**References**

1. E. M. Griner and M. G. Kazanietz, *Nat. Rev. Cancer*, 2007, **7**, 281-294.

2. D. L. Alkon, M. K. Sun and T. J. Nelson, *Trends Pharmacol. Sci*., 2007, **28**, 51-60.

3. J. P. Arcoleo and I. B. Weinstein, *Carcinogenesis*, 1985, **6**, 213-217.

4. N. Kedei, D. J. Lundberg, A. Toth, P. Welburn, S. H. Garfield and P. M. Blumberg, *Cancer Res.*, 2004, **64**, 3243-3255.

5. J. Kortmansky and G. K. Schwartz, *Cancer Invest.*, 2003, **21**, 924-936.

6. J. Koivunen, V. Aaltonen and J. Peltonen, *Cancer Lett*., 2006, **235**, 1-10.

7. G. Boije Af Gennas, V. Talman, J. Yli-Kauhaluoma, R. K. Tuominen and E. Ekokoski, *Curr. Top. Med. Chem.*, 2011, **11**, 1370-1392.

8. J. H. Kang, Y. Kim, S. H. Won, S. K. Park, C. W. Lee, H. M. Kim, N. E. Lewin, N. A. Perry, L. V. Pearce, D. J. Lundberg, R. J. Surawski, P. M. Blumberg and J. Lee, *Bioorg. Med. Chem. Lett.*, 2010, **20**, 1008-1012.

9. V. E. Marquez and P. M. Blumberg, *Acc. Chem. Res*., 2003, **36**, 434-443.

10. V. Talman, R. K. Tuominen, G. B. af Gennas, J. Yli-Kauhaluoma and E. Ekokoski, *Plos One*, 2011, **6**, e20053.

11. O. Raifman, S. Kolusheva, M. J. Comin, N. Kedei, N. E. Lewin, P. M. Blumberg, V. E. Marquez and R. Jelinek, *Febs J*., 2010, **277**, 233-243.

12. P. M. Blumberg, N. Kedei, N. E. Lewin, D. Yang, G. Czifra, Y. Pu, M. L. Peach and V. E. Marquez, *Curr. Drug Targets*, 2008, **9**, 641-652.

13. S. Benzaria, B. Bienfait, K. Nacro, S. M. Wang, N. E. Lewin, M. Beheshti, P. M. Blumberg and V. E. Marquez, *Bioorg. Med. Chem. Lett*., 1998, **8**, 3403-3408.

14. R. Borah, D. Talukdar, S. Gorai, D. Bain and D. Manna, *RSC. Adv*., 2014, **4**, 25520-25531.

15. M. Hubert, B. J. Compton, C. M. Hayman, D. S. Larsen, G. F. Painter, T. Rades and S. Hook, *Mol. Pharm.*, 2013, **10**, 1928-1939.

16. M. A. Bos, B. Vennat, M. T. Meunier, M. P. Pouget, A. Pourrat and J. Fialip, *Biol. Pharm. Bull.*, 1996, **19**, 146-148.

17. L. W. Runnels, J. Jenco, A. Morris and S. Scarlata, *Biochemistry*, 1996, **35**, 16824-16832.

18. C. Ho, S. J. Slater and C. D. Stubbs, *Biochemistry*, 1995, **34**, 6188-6195.

19. N. Mamidi, R. Borah, N. Sinha, C. Jana and D. Manna, *J. Phys. Chem. B*, 2012, **116**, 10684-10692.

20. D. Talukdar, S. Panda, R. Borah and D. Manna, *J. Phys. Chem. B*, 2014, **118**, 7541-7553.

21. N. Mamidi, S. Gorai, B. Ravi and D. Manna, *RSC. Adv*., 2014, **4**, 21971-21978.

22. G. G. Zhang, M. G. Kazanietz, P. M. Blumberg and J. H. Hurley, *Cell*, 1995, **81**, 917-924.

23. D. Duan, D. M. Sigano, J. A. Kelley, C. C. Lai, N. E. Lewin, N. Kedei, M. L. Peach, J. Lee, T. P. Abeyweera, S. A. Rotenberg, H. Kim, Y. H. Kim, S. El Kazzouli, J. U. Chung, H. A. Young, M. R. Young, A. Baker, N. H. Colburn, A. Haimovitz-Friedman, J. P. Truman, D. A. Parrish, J. R. Deschamps, N. A. Perry, R. J. Surawski, P. M. Blumberg and V. E. Marquez, *J. Med. Chem*., 2008, **51**, 5198-5220.

24. G. Boije af Gennas, V. Talman, O. Aitio, E. Ekokoski, M. Finel, R. K. Tuominen and J. Yli-Kauhaluoma, *J. Med. Chem*., 2009, **52**, 3969-3981.

25. S. K. Sukumaran and N. V. Prasadarao, *J. Biol. Chem*., 2002, **277**, 12253-12262.

26. V. A. Verriere, D. Hynes, S. Faherty, J. Devaney, J. Bousquet, B. J. Harvey and V. Urbach, *J. Biol. Chem*., 2005, **280**, 35807-35814.

27. Q. Zhang, Z. Gao, F. Xu, S. Tai, X. Liu, S. Mo and F. Niu, *Langmuir*, 2012, **28**, 11979-11987.

28. N. Mamidi, S. Panda, R. Borah and D. Manna, *Mol. Biosyst*., 2014, **10**, 3002-3013.

# CHAPTER 4

# Effect of Cholesterol and Oxysterols on Diacylglycerol Activation of Protein Kinase C and Membrane Biophysical Properties

The present chapter describes the effect cholesterol and two oxysterols- cholestane-3β,5α,6β-triol (triol) and cholestane-6-oxo-3β,5α-diol (6-keto) on diacylglycerol (DAG) binding properties of PKCδ-C1b domain as well as PKC activation. This study also illustrates the effect of cholesterol and oxyaterols on membrane properties including phase behavior, headgroup packing and hydration.

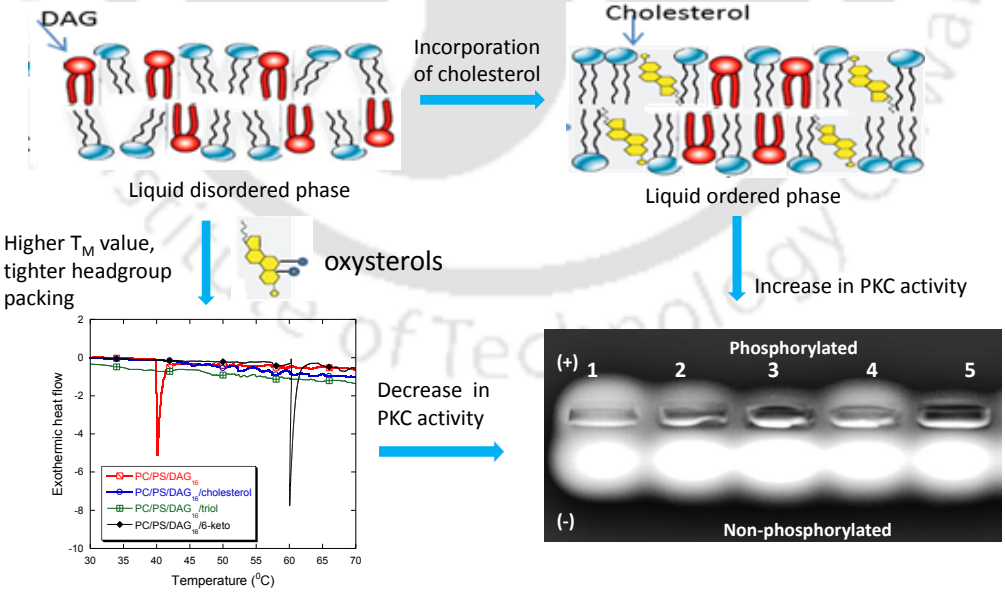

### 4.1. Background and Focus of the Present work

Protein kinase C (PKC) is a family of phospholipid-dependent serine threonine kinases that regulates several cellular functions such as proliferation, differentiation, apoptosis, metastasis, malignant transformation, and cancer progression.[1-4] The C-terminal kinase domain is conserved among all PKC isozymes, while N-terminal regulatory domain is divergent among them. An auto-inhibitory pseudo-substrate region residing in the regulatory region blocks the substrate binding pocket of the functional kinase domain, which leads to the inactivation of the enzyme. Interaction of diacylglycerols (DAGs) or some other allosteric effectors to the regulatory domain at the plasma membrane displaces the bound pseudo-substrate region from the active site and activates PKC enzyme.[1] It is well documented that the presence of different lipophilic compounds along with DAG in the plasma membrane greatly affects PKC activity.[5-7] Several studies have been performed on the perturbation of membrane structure by fatty acids, cholesterol, sphingosine and lysophosphatidic acid and its role with PKC activity.[8-12] It has been proposed that these lipophilic compounds may change the orientation of the lipid-headgroups in the membrane bilayer and also induce non-bilayer phases in the membrane, which highly modulates PKC activity.[8-12]

Lipophilic cholesterol is the primary sterol present in cell membranes that maintain structural integrity and fluidity.[13] Cholesterol constitutes upto 30-40% of the total lipid in erythrocyte and myelin membrane.[14] Cholesterol exerts a number of changes in bilayer properties which include reducing molecular surface area[15-17] and membrane permeability[18, 19], broadening gel to liquid-crystalline phase transition[20], altering lateral diffusion rates for both proteins and lipids[21, 22], moderating acyl chain order in both the gel and liquid-crystalline phases and so on. However cholesterol is highly susceptible to oxidation by reactive oxygen species generated through different pathways e.g. metabolism[23], exposure to ozone[24] and others. Oxysterols are the oxidized product of cholesterol and both have high structural similarity. Oxysterols contain additional functional groups such as hydroxyl, ketone, epoxide in the sterol nucleus or at the side chain of the molecule. It has been reported that depending on the nature and position of the oxygen containing functionalities, different oxysterols interact with the membrane in different ways.[25] Cholestane-6-oxo-3β,5α-diol (6-keto) is an oxysterol produced abundantly in lung epithelial cells through the oxidation of cholesterol (Figure 4.1). Cholesterol is the major constituent of the pulmonary surfactant, a lipid-rich material that lines the epithelial cells in the airways. Exposure of lung to the ozone molecule in the ambient air yield a complex series of products including 3β-hydroxy-5-oxo-5,6-secocholestan-6-al, 5-hydroperoxy-homo-6-oxa-

cholestan-3β,7α-diol and 5β,6β-epoxycholesterol. Cholestane-6-oxo-3β,5α-diol (6-keto) is the major metabolite generated from 5β,6β-epoxycholesterol and found to be cytotoxic in nature.[24, 25] On the other hand, cholestane-3β,5α,6β-triol (triol) is the most abundant oxysterol generated in the metabolic pathways of cholesterol and has been found to be involved in endogenous neuroprotection (Figure 4.1).[26] Recent studies have revealed that triol exhibits anti-cancer activity against human prostate cancer cells.[27]

There are several reports on the modification of membrane properties by cholesterol and oxysterols. Also studies have been carried out on the effect of these compounds on PKC activation. Zidovetzki and coworkers have shown that cholesterol itself does not activate PKC but it enhances the DAG induced activation of PKC by destabilizing the membrane structure.[12] Through MD simulation, Huang and coworkers have reported that DAG and cholesterol share the similarity in having small polar headgroup and large hydrophobic bodies. As a result both exert similar effects on the properties of POPC bilayers e.g. increasing the distance between the phospholipid headgroups, promoting the formation of cubic phase and others.[28] Luu and coworkers have reported that modification of membrane properties by 7β, 25-dihydroxy cholesterol leads to the inhibition of phorbol ester induced PKC activation in the membrane.[29] Thus oxysterols can also play a major role in the modulation of PKC activity by modifying the membrane biophysical properties. From those reported studies, it has been established that both cholesterol and oxysterols have a profound effect on the DAG or phorbol ester induced PKC activation. It is also well documented that PKC activation mechanism involves the formation of the C1 domain-ligand-membrane ternary complex i.e. C1 domain plays a crucial role in targeting PKCs from the cytosol to membrane both in response to phorbol ester or DAG.[30] This strongly recommends the investigation of the effect of cholesterol and oxysterols on DAG or phorbol ester binding properties of the C1 domain in membrane environment.

In this chapter, we examined the effects of cholesterol and two oxysterols; cholestane-3β,5α,6β-triol (triol) and cholestane-6-oxo-3β,5α-diol (6-keto) on the DAG induced activation of PKC and its C1 domain binding with DAG in liposomal environment as well as biophysical properties of DAG containing lipid bilayer. We found that the presence or absence of the oxygen functionalities on the cholesterol ring has a profound effect on DAG containing lipid bilayer perturbation which directly correlates with PKC activity.

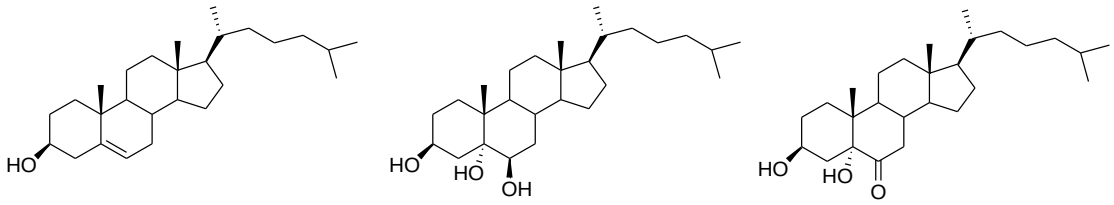


**Figure 4.1.** Structures of the cholesterol and oxysterols used in our present study.

## 4.2. Results and discussions

**Role of cholesterol, triol and 6-keto on PKC activation-** PKC activation process show that the cellular translocation of classical PKC isoenzymes to the plasma membrane is initially mediated by $Ca^{2+}$ binding through the C2 domain, followed by C1 domain-DAG interactions in the presence of anionic phospholipids. In contrast, only DAG binding to the C1 domain in the presence of anionic phospholipids activates novel PKC isoenzymes. It has already been reported that cholesterol amplifies the diacyl glycerol activation of PKC.[12] it is also reported that oxysterols decrease membrane associated PKC activity in immune cells.[29] Therefore it is important to understand the effect of these cholesterol and oxysterols on the PKC activity under liposomal environment and DAG-dependent bilayer interaction of the PKC-C1 domain.

To understand the role of cholesterol, triol and 6-keto on PKC activation, PepTag-nonradioactive kinase activity assay was performed under liposomal environment.[31] The assay is based on the phosphorylation of a PKC enzyme specific fluorescence peptide, which transforms to -1 charge from +1 charge upon phosphorylation. The phosphorylated part moves towards the positive electrode and the non-phosphorylated part moves towards its opposite in agarose gel electrophoresis. Our present study was carried out by incubating the full length PKC enzyme with the fluorescence peptide and liposome containing PC/PS/$DAG_{16}$/Compound (50/20/5/25) where compounds are cholesterol, triol and 6-keto. The highest cholesterol concentration in cell membrane is reported as 25-30% of the total lipid content in the cell and $l_o$ phase is often present at concentrations of 20–25% (mol%).[12] Though DAG concentration can reach upto 10% in some transformed cells, PKC activation can be induced by a few mole % of DAG.[11, 12] On the other hand phosphatidylserine (PS) acts as a membrane cofactor in the activation of PKC.[1] The agarose gel electrophoresis image (Figure 4.2) demonstrates maximum phosphorylation in presence of PC/PS/$DAG_{16}$/cholesterol liposome. However, PC/PS/$DAG_{16}$/triol showed very little

phosphorylation while almost no phosphorylation is observed for PC/PS/$DAG_{16}$/6-keto. Overall, the results show that the presence of cholesterol increases the DAG-induced PKC activation, while triol and 6-keto showed the reverse effect.

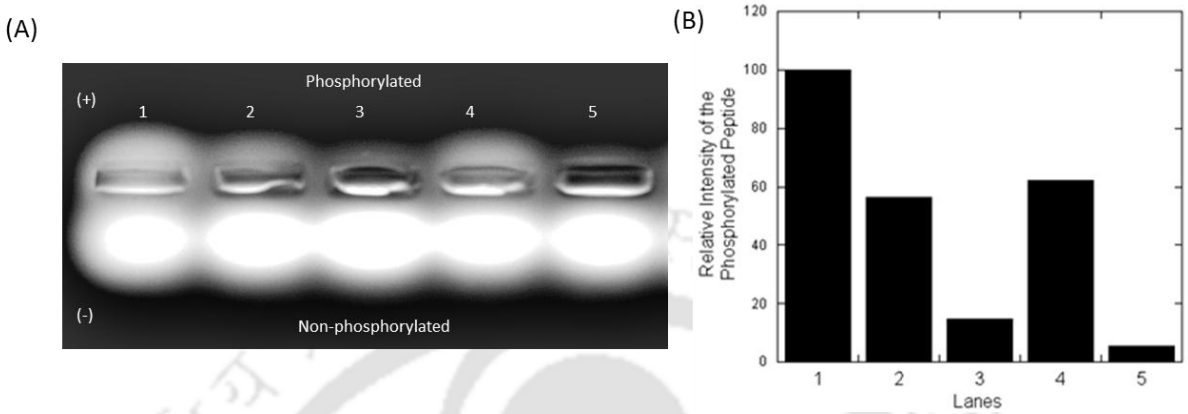


**Figure 4.2.** Representative UV-illuminated agarose gel image of the product of reactions run with PKC full-length enzyme (A) and Relative amounts of phosphorylated Pep-Tag C1 peptide (B). Activity assay in the presence of PC/PS/$DAG_{16}$ liposome containing cholesterol (lane 1), triol (lane 2) and 6-keto (lane 3) are shown in both the figures. Activity assay containing PC/PS/$DAG_{16}$ liposome (lane 4) and no liposome (lane 5) are used as control.

**Role of cholesterol, triol and 6-keto on DAG binding to PKCδ-C1b domain**- The cysteine rich domain or C1 domain of PKC plays major role in its activation through its interaction with DAG or phorbol ester which leads to membrane translocation.[30] Several studies have demonstrated that presence of cholesterol and oxysterols modulate the DAG or phorbol ester induced PKC activation.[12, 29] Already from our PKC activity assay, we showed that cholesterol, triol and 6-keto have a pronounced effect on DAG induced PKC activation. In this regard, the binding properties of the isolated C1b domain of PKCδ with DAG in presence of cholesterol, triol and 6-keto were quantitatively measured by protein-to-membrane FRET-based binding assay.[32, 33] The Trp residue of the PKCδ-C1b subdomains serve as the donor, and a low density of membrane-embedded, dansyl-PE (dPE) lipids serve as the acceptor for these FRET measurements. Water soluble $DAG_8$ was titrated into the solution containing C1b-subdomain-bound liposomes containing PC/PS/$DAG_{16}$/dPE (65/25/5/5), PC/PS/$DAG_{16}$/Compound/dPE (45/20/5/25/5) and PC/PS/Compound/dPE (50/20/25/5) where compounds are cholesterol, triol and 6- keto. The decrease in the protein-to-membrane FRET signal was monitored to measure the displacement of the protein from the liposome surface to the bulk solution, and to calculate apparent inhibitory constant [$K_I(DAG_8)_{app}$](Equation 1).

Figure 4.3 represents $DAG_8$ promoted displacement of the PKCδ-C1b subdomain from ligand associated liposomes.

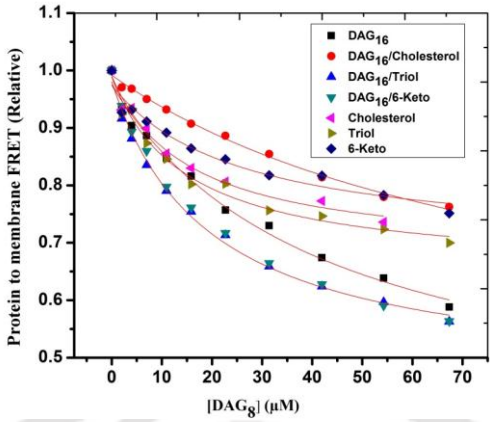


**Figure 4.3.** Competitive displacement assay for the PKCδ-C1b subdomains (1 μM) bound to liposome PC/PS/$DAG_{16}$/dPE (65/25/5/5), PC/PS/$DAG_{16}$/Compound/dPE (45/20/5/25/5) and PC/PS/Compound/dPE (50/20/25/5) where compounds are cholesterol, triol and 6- keto. The bound complex was titrated with the $DAG_8$.

The values of $K_I(DAG_8)_{app}$ depend on ligand concentration and the lipid compositions as well as the affinities of the C1b subdomains for ligands/$DAG_8$. The binding parameters obtained from the FRET based binding assay (Table 4.1) show that the binding affinity of the $DAG_{16}$ containing liposome to the PKCδ-C1b domain is increased by two fold in the presence of cholesterol whereas, triol and 6-keto decreased it by four fold. Also binding studies carried out in the absence of $DAG_{16}$ rules out the presence of any direct interaction of cholesterol, triol and 6-keto with C1b domain of PKCδ.

**Table 4.1.** Equilibrium binding parameters for PKCδ-C1b protein[a] with the ligand associated liposomes[b] at room temperature

| Liposome | $K_I(DAG_8)$(μM) |
|---|---|
| 1. PC/PS/$DAG_{16}$/dPE | 42.77±9.7 |
| 2. PC/PS/Triol/dPE | 14.83±3.4 |
| 3. PC/PS/6-Keto/dPE | 25.39±9.4 |
| 4. PC/PS/Cholesterol/dPE | 15.51±3.7 |
| 5. PC/PS/$DAG_{16}$/Triol/dPE | 19.54±2.6 |
| 6. PC/PS/$DAG_{16}$/6-Keto/dPE | 22.41±1.9 |
| 7. PC/PS/$DAG_{16}$/Cholesterol/dPE | 87.15±17.5 |

[a] Protein, 1 μM in buffer (20 mM Tris, 150 mM NaCl, 50 μM $ZnSO_4$, pH 7.4).
[b] Active liposome composition: PC/PS/$DAG_{16}$/dPE (65/25/5/5), PC/PS/$DAG_{16}$/Compound/dPE (45/20/5/25/5) and PC/PS/Compound/dPE (50/20/25/5) where compounds are cholesterol, triol and 6- keto.

**Lipid bilayer interaction properties of cholesterol, triol and 6-keto**

Several studies have already revealed that PKC activation is largely modulated by the membrane properties e.g. headgroup spacing, lamellar to non-lamellar phase transition, hydrocarbon volume, bilayer curvature and others.[8-12] Cholesterol and oxysterols alter a number of membrane properties including, changing in liquid ordered phase or formation of membrane microdomains, changing hydration properties, condensing the membrane and others.[34-37] It has already been observed that our compounds have a profound effect on the DAG induced PKC activation. Therefore, investigation of the interaction of our compounds with lipid bilayer is very important to understand their role in PKC activation.

**Effect of the compounds in membrane microdomain formation in DAG containing membrane—** Membrane microdomain, also known as liquid ordered phase ($l_0$) is an intermediate phase between lameller and non-lameller phase. Cholesterol is reported to form this phase with sphingolipid or saturated phospholipid like DPPC.[38] Oxysterols, depending upon type and position of the oxygen functionalities either promotes or inhibits the formation of $l_0$ phase.[37] In this regard, temperature dependent fluorescence anisotropy measurements and detergent resistance membrane (DRM) formation experiments were carried out to determine the effect of our compounds on $l_0$ phase.or microdomain formation.

**Temperature dependent DPH anisotropy study**- 1,6-Diphenyl-1,3,5-hexatriene (DPH), which locates itself in the hydrophobic chain area of the lipid bilayer, either perpendicular or parallel, was used as probe to monitor the change in membrane microenvironment.[38] DPH loaded PC/PS/$DAG_{16}$ (55/20/5) vesicle containing 10%, 20% and 25% cholesterol, triol and 6-keto were excited by polarized light varying the temperature from 20 $^{\circ}$C-80 $^{\circ}$C and the anisotropy values were recorded. Figure 4.4 illustrates the change in anisotropy values of DPH with temperature. From the plot, it is observed that there is a sharp decrease in the anisotropy value in the control liposome(PC/PS/$DAG_{16}$) at around 41 $^{\circ}$C which can be attributed to the transition from the lameller to non-lamellar phase. The phase between the lamellar and the non-lamellar phase is called the ripple phase and it is well known that the presence sterols convert this phase to the liquid ordered ($l_0$) phase.[39] This kind of phase generally appears in biological membrane, is termed as the lipid raft and possesses some unique characteristics than the other phases of the membrane.[40]

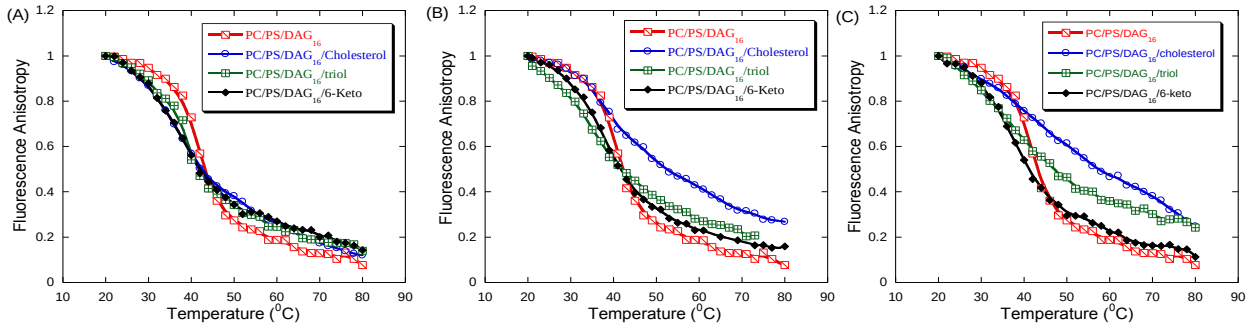


**Figure 4.4.** Representative plot of change in fluorescence anisotropy with temperature. DPH (1µM) containing PC/PS/DAG$_{16}$ (55/20/5) liposome containing 10% (A), 20% (B) and 25% (C) cholesterol, triol and 6-keto are excited by polarized light at 355nm and the anisotropy values are collected at 430 nm.

The temperature dependent change of DPH anisotropy in PC/PS/DAG$_{16}$ liposome containing different mole% of the cholesterol, triol and 6-keto showed the propensity of the DAG containing lipid bilayer to form $l_0$ phase with increasing concentrations of the compounds. The tendency to form phase follows the order cholesterol > triol > 6-keto.

**Effect of the compounds on membrane phase transition temperature-** The solid gel to liquid crystalline phase transition is the major energetic event of the lipid bilayer which involves rotameric disordering of hydrocarbon chains, increased head-group hydration and increased intermolecular entropy.[41] Therefore it can be considered as a very important parameter for understanding the stability of a lipid bilayer. Several reports are there on the correlation of PKC activity with the thermotropic phase behaviour of the membrane.[42, 43] It is well documented that the side chains of the DAG lactone moiety have a profound effect on the solid gel phase to liquid crystalline phase of the membrane which is involved in the translocation of PKC.[42] Also from the analysis of thermotropic phase behavior of membrane it is established that the coexistence of the DAG rich and the DAG poor phases greatly enhances the PKC activity.[43]

The analysis of the DSC spectra reveals that the liposome containing PC/PS/DAG$_{16}$ (75/20/5) has a gel to liquid phase transition temperature around 40.13 $^{\circ}$C (Figure 4.5). The DSC peak disappears with the addition of 25% cholesterol and triol due to the formation of the $l_0$ phase which broadens the phase transition. On the other hand in presence of 25% 6-keto, the phase transition temperature increases very significantly showing a sharp peak at 60.13 $^{\circ}$C. This data correlates well with the fluorescence anisotropy data where it has already been shown that 6-keto does- not have significant contribution towards the formation of $l_0$

phase. The shifting of the phase transition to higher temperature in presence of 6-keto signifies that the headgroup packing is becoming tighter in presence of this compound.

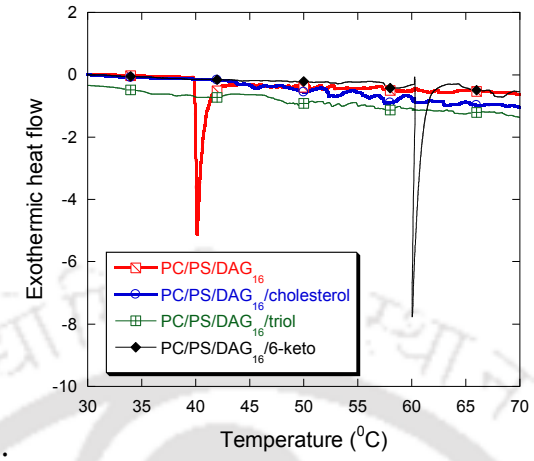


**Figure 4.5.** DSC thermograms illustrating the effect of cholesterol and oxysterols on the gel/liquid-crystalline phase transition of PC/PS/$DAG_{16}$ liposome. The thermograms shown were acquired at a scan rate of 1°C/min.

**Detergent resistance membrane (DRM) Solubilization Experiment -** From the DPH anisotropy it is already observed that cholesterol, triol and 6-keto induce the $l_0$ phase in PC/PS/$DAG_{16}$ bilayer. The formation of the $l_0$ phase greatly diminishes the detergent solubility of the lipid bilayer.[37] Therefore the determination of percentage detergent resistance of a lipid bilayer provides the propensity of the lipid bilayer to form $l_0$ phase. In our present study, multilamellar vesicles (MLVs) of PC/PS and PC/PS/$DAG_{16}$ comprised of 25% cholesterol, triol and 6-keto were prepared and incubated with triton-x-100 for 12 hours. The percentage detergent resistance was calculated from the change in turbidity of the liposomes at 400 nm. Figure 4.6 illustrates the detergent solubility of our prepared bilayers. It is observed that the in presence of cholesterol, PC/PS liposome showed only 28% detergent resistance while the addition $DAG_{16}$ has raised it to 68%. This sharp increase in the % detergent resistance value demonstrates a strong synergism between $DAG_{16}$ and cholesterol for the formation of $l_0$ phase. However very little change in the % detergent value was observed for triol and 6-keto with the addition of $DAG_{16}$. This indicates the absence of any synergism of these two compounds with $DAG_{16}$ in the formation of $l_0$ phase.

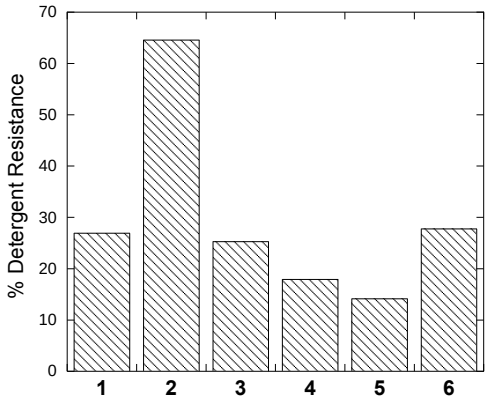


**Figure 4.6.** Representative plot of % detergent resistance of the membrane. It was determined from turbidity measurement after incubation of the PC/PS liposome containing cholesterol (1), triol (3) and 6-keto (5) and PC/PS/$DAG_{16}$ liposome containing cholesterol (2), triol (4) and 6-keto (6) with triton-x-100.

**Effect of the compounds on membrane hydration properties-** Hydration of the lipid bilayer interface is an important parameter for understanding its physical state.[46] Water molecules may form hydration layer at the lipid-bilayer interface through hydrogen bonds with the phospholipid headgroups or penetrate the lipid bilayer to form inter-chain hydration. Bilayer hydration is modulated by the presence of different lipophilic compounds.[44-46] Gratton and coworkers demonstrated that in presence of cholesterol, the phospholipid molecules become more tightly packed which lead to decrease in water concentration in the hydrophilic-hydrophobic surface of the lipid bilayer.[46] Similarly, glycerophospholipids, e.g. sphingolipids also regulate the interfacial hydration of the lipid bilayer by forming H-bonds with the the 3-OH group of cholesterol through its phosphate oxygen and intramolecular hydrogen bonding through their N-H groups.[47, 48] Several studies also showed that this hydration properties of the membrane is highly related to the PKC enzyme activity.[5, 8, 11, 45] It has been reported that DAG, the major PKC activator itself induces dehydration in the membrane interface.[49, 50] DAG carbonyl groups are less hydrated than the corresponding phospholipid carbonyl groups which results in a net decrease in the bilayer hydration sphere facilitating penetration of PKC to the membrane for its activation.[11] In this regard, a study on the effect of cholesterol, triol and 6-keto in the hydration property of PC/PS/$DAG_{16}$ bilayer can explain their effect on PKC activation obtained from PKC activity assay and FRET based binding assay. A highly sensitive fluorescent molecule, 3-Hydroxyflavone (3HF) is used to probe the hydration properties of PC/PS/$DAG_{16}$ in the presence of varying concentrations of cholesterol, triol and 6-keto. 3HF is considered as one of the best model to study the excited state intramolecular proton transfer (ESIPT) and widely

applied as a probe to study micelles, reverse micelles, liposomes and proteins.[51] In water at pH 7.4, 3HF exhibits two emission peaks at 410 nm and 510 nm which corresponds to the neutral form (N*) and anionic form (NH*) respectively. In nonpolar, noninteracting solvents such as hydrocarbons, 3HF mainly shows emission from the excited state intramolecular proton-transferred species known as the phototautomer (T*). Previous studies revealed that in lipid vesicles, dual emission of 3HF is composed of three overlapping bands: the emission of the normal (N*) and tautomer (T*) forms, resulting from the ESIPT reaction, and the emission of the H-bonded (hydrated) form (H-N*) that does not participate in ESIPT (Figure 4.7). The emission band resulting from the H-N* form, which is located between the N* and T* emission bands, can be obtained by deconvoluting the emission spectra (Figure 4.8A). The relative contribution of the H-bonded and H-bond free form of the dye obtained by deconvolution of the fluorescence spectra, provides a quantitative description of the bilayer hydration (equation 1).[44] Figure 4.8B represents the change in hydration values (determined by equation1) of the PC/PS/$DAG_{16}$ membrane with increasing concentrations of the studied compounds.

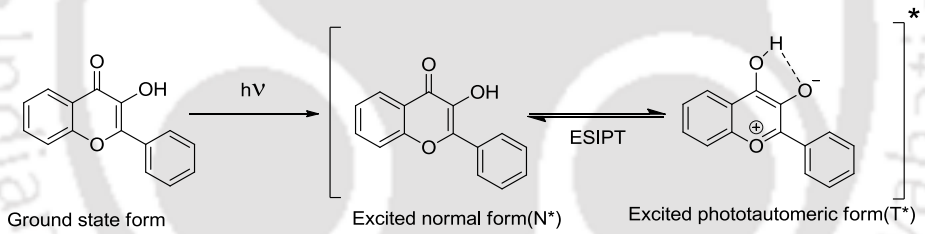


**Figure 4.7.** Representative diagram of excited state intramolecular proton transfer (ESIPT) of 3-Hydroxyflavone.

It has been observed that the in presence cholesterol the hydration values of the membrane decreases very significantly. Addition of triol also induced dehydration of the membrane which is less prominent than cholesterol. On the other hand addition of 6-Keto has almost no effect on membrane hydration properties. These results correlate with the results obtained from temperature dependent DPH anisotropy study. The $l_0$ phase is less hydrated than the other phases of the membrane. Cholesterol, which shows more significant contribution for the formation of the $l_0$ phase, dehydrates the membrane to more extent than the other two compounds.

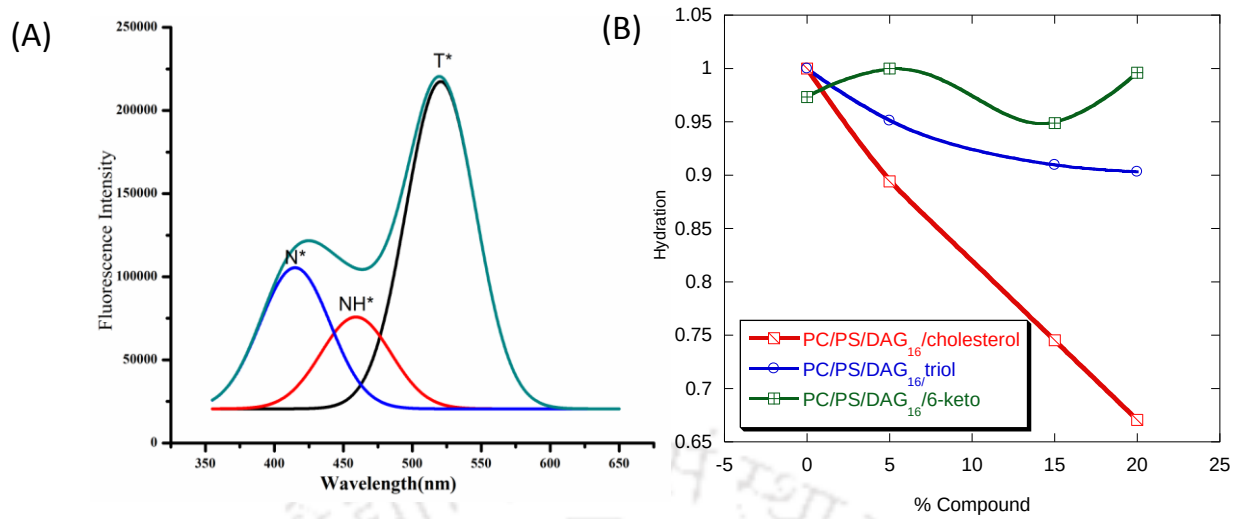


**Figure 4.8.** Representative deconvulated-spectra of 3-hydroxy flavone loaded in liposome (A) and Change in %hydration of PC/PS/$DAG_{16}$ liposome with different concentrations of cholesterol, triol and 6-keto (B).

## Discussion

It is well documented that the activation of PKC isoenzymes is modulated by different lipophilic molecules present in the membrane. Cholesterol is one of the major constituents of cell membrane which regulates the physical properties of the membrane. Oxysterols, the oxygenated products of cholesterol also modulates the membrane properties. But due to their difference in headgroup/body ratio, cholesterol and oxysterols have different orientation in membrane and thus modulate the PKC activity to different extent. Cholesterol is already reported to enhance the DAG induced PKC activity.[12] On the other hand 7β, 25-dihydroxy cholesterol, which is an oxysterol are reported to inhibit the PKC activity.[29]

In our present study, we synthesized two oxyterols-cholestane-3β, 5α, 6β-triol (triol) and cholestane-6-oxo-3β,5α-diol (6-keto) and performed various biophysical analyses to understand their role in PKC activation and its correlation with DAG/phorbol ester-dependent membrane binding. PepTag non-radioactive kinase assay showed enhancement of DAG induced PKC activity in the presence of cholesterol and reduction of PKC activity in the presence of both the oxysterols. Since C1 domain of PKC is mainly responsible for DAG binding, it can be proposed that these compounds may have a profound effect on DAG binding to the C1 domain. FRET-based competitive assay demonstrates that DAG binding to the PKCδ-C1b subdomain is enhanced by two-fold in presence of cholesterol, whereas it got reduced by two-fold in presence of triol and 6-keto. PKC activity is greatly regulated by the membrane phase behavior. It has been reported that the coexistence of DAG-enrich and DAG-poor domain greatly contributes to PKC activity.[43] Temperature dependent

fluorescence anisotropy study showed broadening of the phase transition region of the PC/PS/$DAG_{16}$ liposome in the presence of cholesterol, triol and 6-keto in a concentration dependent manner. This phenomenon may be attributed to the formation of $l_0$ phase of the bilayer in the presence of these compounds. It has been observed that when the compounds are present at 10% there is very little broadening which signifies that the formation of the $l_0$ phase is less pronounced at this concentration.[52-54] As the concentration is varied from 10% to 25%, it has been observed that the $l_0$ phase has become more pronounced in presence of cholesterol and triol. On the other hand, concentration dependent changes of the phase transition is not observed in the presence of 6-keto. Cholesterol has already been reported to form $l_0$ phase with dipalmitoylphosphatidylcholine.[55, 56] Cholesterol orients in biological membranes roughly perpendicular to the bilayer plane so that the 3β-hydroxyl group is located at the membrane–water interface together with phospholipid head groups, and the iso-octyl side chain points at the hydrophobic interior of the bilayer. The cholesterol ring structure tends to package tightly with the tail region of the phospholipid bilayer and thus facilitates the formation of the $l_0$ phase.[36] In case of triol, the addition of hydroxyl groups to the 5α and 6β position effects the headgroup/body ratio and greatly disturbs the packing order. The insertion of oxygen moieties to the hydrophobic tail region is thermodynamically unfavorable. Location of the 5α and 6β hydroxyl group at the membrane-water interface is thermodynamically favorable, which tilt the sterol nucleus with respect to the bilayer plane greatly disturbing the packing order.[37] On the other hand, addition of 6-Keto is more inhibiting the formation of $l_0$ phase which established that the presence of keto group at the 6β position greatly enhances the tilting of the sterol nucleus compared to hydroxyl group at that position. It has also been reported that at cholesterol concentrations above 20–25 mol%, only the $l_0$ phase exists at all temperature.[52] Our recent study also showed that the phase transition region of the lipid bilayer containing PC/PS/$DAG_{16}$ totally disappears in the presence of 25% cholesterol. Similarly disappearance of the solid gel to liquid cryastalline phase transition peak in the differential scanning calorimetry (DSC) thermogram in the presence of 25% cholesterol and triol signifies the formation of the $l_0$ phase of the PC/PS/$DAG_{16}$ bilayer.[52, 57] But shifting of the SG to LC phase transition of PC/PS/$DAG_{16}$ to higher temperature (40.13 $^{\circ}$C to 60.13 $^{\circ}$C) in presence of 6-keto established its role in tighter headgroup packing which restricts the C1 domain to penetrate into the membrane. Also the sharpness of the DSC peak in presence of 6-keto signifies that it does not induce the formation of $l_0$ phase in PC/PS/$DAG_{16}$ bilayer.[57] Our detergent resistance membrane experiment clearly showed that among all three sterols, only cholesterol exerts a synergistic

effect towards the formation of detergent resistance membrane. The resistance of a membrane to the solubilization by detergent has a great significance in the formation of lipid raft or liquid ordered phase.[58, 59] The synergism between cholesterol and DAG for the formation of the raft domain can be attributed to their structural similarity in having smaller headgroup and larger hydrocarbon volume that assists in tighter packing which is absent in other two compounds. It can be assumed that this type of synergism may lead to the formation of coexisting DAG rich and DAG poor domains in the membrane which greatly enhances PKC activity.[43] Our lipid bilayer hydration studies showed that there is a gradual decrease in the membrane hydration with increase in the mole % of cholesterol which may be related with the amplification of DAG induced PKC activation.

**Conclusion**

Over all our present study showed that DAG activation of PKC is greatly modulated by the presence of cholesterol, triol and 6-keto, which can be related to the membrane biophysical properties. Cholesterol, triol and 6-keto also have profound effect in C1 domain interaction with DAG, which is important for PKC activation. DPH anisotropy data showed that Cholesterol, triol and 6-keto have the tendency towards formation of $l_0$ phase in the order of cholesterol>triol>6-keto. But DRM study showed that only cholesterol has a synergism with DAG for the formation of $l_0$ phase or raft domain and thus induces the formation of DAG rich and DAG poor domains. This type of phase is highly responsible for enhancement of PKC activation. On the other hand, triol and 6-keto do not exhibit any synergism for the formation of $l_0$ phase with DAG which indicates the absence of the coexisting DAG rich and DAG poor phases in the lipid bilayer in presence of these two compounds. The much higher solid gel to liquid crystalline phase transition in presence of 6-keto signifies tighter headgroup packing in presence of this compound which leads to decrease in PKC activity in presence of 6-keto. Also membrane dehydration induced by cholesterol may enhance DAG activation of PKC. The overall lowering of PKC activation in presence of triol and 6-keto can also be attributed to the increase in the width of the bilayer hydrophilic head group region or increase in the width of the potential energy barrier which restricts the insertion of the hydrophobic region of the C1 domain of PKC into the core of the lipid bilayer. Thus cholesterol, triol and 6-keto have a profound effect on DAG activation of PKC which can be highly related to the effects of these compound on membrane biophysical properties.

### 4.3. Experimental Section:

**General Information-** All chemicals were purchased from Sigma (St. Louis MO), SRL (Mumbai, India). 1-palmitoyl-2-oleoyl-sn-glycero-3-phosphocholine (PC), 1-palmitoyl-2-oleoyl-sn-glycero-3-phospho ethanolamine (PE) and 1-palmitoyl-2-oleoyl-sn-glycero-3-phosphoserine (PS) and cholesterol were purchased from Avanti Polar Lipids.

**Preparation of phospholipid vesicles-** Phospholipids were dissolved in chloroform/methanol/water (1.0:1.2:0.4) at the desired molar ratio, dried under vacuum, and resuspended with vortexing in lipid storage buffer (140 mM KCl, 0.5 mM $MgCl_2$, 15 mM NaCl, 0.02% $NaN_3$, 25 mM HEPES, pH 7.5) yielding a concentration of 1.0 mM multilameller vesicles used in the turbidity assay.(39) Small unilamellar vesicles(SUV) used in the FRET, anisotropy and PKC activity assay were prepared by sonication. For hydration studies, large unilamellar vesicles (LUV) were obtained by the classical extrusion method as described previously.[45]

**PKC activity assay-** Kinase assays were performed at 22 ± 0.5 $^{\circ}$C using the PepTag Non-Radioactive Protein Kinase C system (Promega Corp., Madison, WI). The manufacturer's protocol was followed, except the PKC lipid activator was replaced with liposomes containing PS. Here the total lipid concentration was 200 μg/mL in kinase assay buffer [10 mM $MgCl_2$, 26 μM $CaCl_2$, 20 μM EGTA, 1 mM DTT, 1 mM ATP, and 20 mM HEPES (pH 7.4)].[32]

**FRET based Competitive binding assay-** As described in chapter 2, section 2.3.

**DPH anisotropy-** To determine the effect of the compounds on the membrane microdomain formation, the temperature induced change in the DPH anisotropy values was recorded. The fluorescence probe DPH was incorporated into the liposomes by adding the dye dissolved in THF (1 mM) to PC/PS/$DAG_{16}$ (55/20/5) vesicles containing 10%, 20% and 25% cholesterol, triol and 6-keto. The anisotropy values were recorded at 430 nm (excitation wavelength=355nm) varying the temperature from 20 $^{\circ}$C to 80 $^{\circ}$C.[38]

**DRM Solubilization Experiment-** The resistance to the membrane solubilization by Triton-x was determined by measuring the optical absorbance at 400 nm. MLV was prepared by the above mentioned procedure and the turbidity of the liposomal solution was measured at 400

nm. To each of the samples, 50 µL of 10% (w/v) triton X-100/TBS was added. The samples were then mixed, incubated at room temperature (23 °C) overnight, and then the optical density was measured again. The change in optical density was calculated as the ratio of the optical density after the Triton X-100 incubation (not corrected for dilution with Triton X-100 solution) to the optical density before the addition of Triton X-100.[38]

**Differential scanning calorimetry (DSC)-** The samples used for the DSC experiments were prepared by dispersing appropriate amounts of the dried PC/PS/$DAG_{16}$/Sterol mixture in 1 ml of deionized water. DSC heating and cooling thermograms were obtained at a scan rate of 1 °C /h using a Q20-DSC (TA Instruments) calorimeter.[64]

**Hydration studies-** Large unilamellar vesicles (LUV) were obtained by the classical extrusion method as described previously. LUVs were labeled by adding aliquots (generally 2 ml) of probe stock solutions (2 mM, in dimethyl sulfoxide) to 2-ml solutions of vesicles.[45] Because the binding kinetics is very rapid for both probes, the fluorescence experiments were processed a few minutes after addition of the aliquot. A 15-mM phosphate-citrate, pH 7.0 buffer was used in all experiments. Concentrations of the probes and lipids were 2 and 200 µM, respectively. Fluorescence emission spectra were recorded by Fluoromax-4. The excited wavelength was 435 nm and deconvultion of the emission spectra into three bands (N*, H-N* and T*) were carried out by Origin 9.0. The hydration can be estimated as

$$\text{Hydration}=I_{HN^*}/ (I_{N^*}+0.4\times I_{T^*}). \quad (1)$$

Where $I_{HN^*}$, $I_{N^*}$ and $I_{T^*}$ are the intensities of the three bands originated from deconvultion.

**References**

1. A. C. Newton, *J. Biol. Chem*., 1995, **270**, 28495–28498.

2. D. Breitkreutz, L. Braiman-Wiksman, N. Daum, M. F. Denning and T. Tennenbaum, *J. Cancer Res. Clin. Oncol.*, 2007, **133**, 793-808.

3. J. Koivunena, V. Aaltonena, J. Peltonena, *Cancer Lett.*, 2006, **235**, 1–10.

4. G. C. Blobe, L. M. Obeid and Y. A. Hannun, *Cancer Metastasis Rev*., 1994, **13**, 411-431.

5. E.M. Goldberg and R. Zidovetzki, *Biophys. J.*, 1997, **73**, 2603-2614.

6. E. M. Goldberg and R. Zidovetzki, *Biochemistry*, 1998, **37**, 5623-5632.

7. C. Ho, S. J. Slater, B. Stagliano and C. D. Stubbs, *Biochemistry*, 2001, **40**, 10334-10341.

8. S. J. Slater, M. B. Kelly, F. J. Taddeo, C. Ho, E. Rubin, and C. D. Stubbs, *J. Biol. Chem*., 1994, **269**, 4866-4871.

9. E. J. Bolen and J. J. Sando, *Biochemistry*, 1992, **31**, 5945-5951.

10. J. R. Giorgione, R. Kraayenhof, and R. M. Epand, *Biochemistry*, 1998, **37**, 10956-10960.

11. F. M. Goñi and A. Alonso, *Prog. Lipid Res.*, 1999, **38**, 1-48.

12. D. Armstrong and R. Zidovetzki, *Biophys. J*., 2008, **94**, 4700–4710.

13. F. Meyera and B. Smit, *Proc. Natl. Acad. Sci. USA*, 2009, **106**, 103654–3658.

14. S. Bhattacharya, S. Haldar, *Biochim Biophys Acta*, 2000, **1467**, 39-53.

15. R. A. Demel, L. L. van Deenen and B. A. Pethica, *Biochim. Biophys. Acta*, 1967, **135**, 11-19.

16. P. Joose and R. A. Demel, *Biochim. Biophys. Acta*, 1969, **183**, 447-457.

17. S. F. Bush and I. W. Levin, *Chem. Phys. Lipids*, 1980, **27**, 101–111.

18. S. Clejan, R. Bittman, P. W. Deroo, Y. A. Isaacson and A. F. Rosenthal, *Biochemistry*, 1979, **18**, 2118-2125.

19. R. A. Demel, *Biochim. Biophys. Acta*, 1976, **457**, 109-132.

20. R. Semer and E. Gelerinter, *Chem. Phys. Lipids*, 1973, **23**, 201-211.

21. J. L. R. Rubenstein, B. A. Smith and H. M. McConnell, *Proc. Natl. Acad. Sci. USA*, 1979, **76**, 15-18.

22. A.-L. Kuo and C. G. Wade, *Biochemistry*, 1979, **18**, 2300-2308.

23. J. C. D. Verhagen, P. Braake, J. Teunissen, G. van Ginkel, and A. Sevanian, *J. of Lipid Research*, 1996, **37**, 1488-1502.

24. M. K. Pulfer and R. C. Murphy, *J. Biol. Chem*, 2004, **279**, 26331–26338.

25. M. K. Pulfer, C. Taube, E. Gelfand, and R. C. Murphy, *J. Pharm. Exp. Ther*., 2004, **312**, 256-264.

26. H. Hu, Y. Zhou, T. Leng, A. Liu, Y. Wang, X. You, J. Chen, L. Tang, W. Chen, P. Qiu, W. Yin, Y. Huang, J. Zhang, L. Wang, H. Sang and G. Yan, *J. Neurosci*., 2014, **34**, 11426 – 11438.

27. C.-L. Lin, C. Huo, L.-K. Kuo, R. A. Hiipakka, R. B. Jones, H.-P. Lin, Y. Hung, L.-C. Su, J.-C. Tseng, Y.-Y. Kuo, Y.-L. Wang, Y. Fukui, Y.-H. Kao, J. M. Kokontis, C.-C. Yeh, L. Chen, S.-D. Yang, H.-H. Fu, Y.-W. Chen, K. K. C. Tsai, J.-Y. Chang, C.-P. Chuu, *PLoS One*, 2013, **8**, 1-18.

12. D. Armstrong and R. Zidovetzki, *Biophys. J*., 2008, **94**, 4700–4710.

28. M. Alwarawrah, J. Dai, and J. Huang, *J. Chem. Theory Comput*., 2012, **8**, 749–758.

29. C. Moog , J. C. Deloulme , J. Baudier , M. O. Revel, P. Bischoff , H. Hietter and B. Luu, *Biochimie*, 1991, **73**, 1321-1326.

30. F. Colón-González and M. G. Kazanietz, *Biochim. Biophys. Acta*, 2006, **1761**, 827–837.

31. B. P. Ziemba, J. Li, K. E. Landgraf, J. D. Knight, G. A. Voth, and J. J. Falke, *Biochemistry* 2014, **53**, 1697−1713.

32. N. Mamidi, S. Gorai, R. Mukherjee and D. Manna, *Mol. Biosys*., 2012, **8**, 1275-1285.

33. J. A. Corbin, R. A. Dirkx and J. J. Falke, *Biochemistry*, 2004, **43**, 16161-16173.

34. V. M. Olkkonen and R. Hynynen, *Mol. Aspects Med.*, 2009, **30**, 123–133.

35. B. N. Olsen, P. H. Schlesinger, D. S. Ory and N. A. Baker, *Biophys. J*., 2011, **100**, 948–956.

36. B. N. Olsen, P. H. Schlesinger, and N. A. Baker, *J. Am. Chem. Soc*., 2009, **131**, 4854–4865.

37. J. B. Massey and H. J. Pownall, *Biochemistry*, 2006, **45**, 10747-10758.

38. D. Lingwood and K. Simons, *Nat. Protoc*., 2007, **2**, 2159–2165.

39. H. M. Seeger, G. Marino, A. Alessandrini and P. Facci, *Biophys. J*., 2009, **97**, 1067–1076.

40. K. Simons and D. Toomre, *Mol. Cell Biol*., 2000, **1**, 31-39.

41. R. Koynova and B. Tenchov, *O. A. Biochemistry*, 2013, **1**, 1-9.

42. O. Raifman, S. Kolusheva, M. J. Comin, N. Kedei, N. E. Lewin, P. M. Blumberg, V. E. Marquez and R. Jelinek, *FEBS J*., 2010, **277**, 233–243.

43. A. R. G. Dibble, A. K. Hinderliter, J. J. Sando and R. L. Biltonen, *Biophys. J*, 1996, **71**, 1877-1890.

44. G. M'Baye, Y. Mély, G. Duportail, and A. S. Klymchenko, *Biophys. J*., 2008, **95**, 1217–1225.

45. V. Micol, P. Sánchez-Piñera, J. Villalaín, A. D. Godos, and J. C. Gómez-Fernández, *Biophys. J*., 1999, **76**, 916–927.

46. T. Parasassi, M. D. Stefano, M. Loiero, G. Ravagnan, and E. Gratton, *Biophys. J.*, 1994, **66**, 763-768.

47. P. Niemela, M. T. Hyvonen, and I. Vattulainen, *Biophys. J.*, 2004, **87**, 2976–2989.

48. B. Térová, R. Heczko, and J. P. Slotte., *Biophys. J.*, 2005, **88**, 2661–2669.

49. F. LoÂpez-GarcõÂa, V. Micol, J. Villalain, J. C. GoÂ mez-FernaÂ ndez., *Biochim. Biophys. Acta*, 1993, **1169**, 264-272.

50. F. LoÂpez-GarcõÂa, J. Villalain, J. C. GoÂmez-FernaÂndez, *Biochim. Biophys. Acta*, 1994, **1190**, 264-272.

51. M. Mohapatra, U. Subuddhi and A. K. Mishra, *Photochem. Photobiol. Sci*., 2008, **8**, 1373–1378.

52. T. P. W. McMullen, R. N. A. H. Lewis and R. N. McElhaney, *Curr. Opin. Colloid Interface Sci*., 2004, **8**, 459–468.

53. C. Sergelius and J. P. Slotte, *Biochim. Biophys. Acta*, 2011, **1808**, 2841–2848.

54. A. Gidwani, D. Holowka, and B. Baird, *Biochemistry*, 2001, **40**, 12422-12429.

55. L. Chen, Z. Yu and P. J. Quinn, *Biochim. Biophys. Acta*, 2007, **1768**, 2873–2881.

56. D. Marsh, *Biochim. Biophys. Acta*, 2010, **1798**, 688–699.

57. M. G. K. Benesch, R. N. McElhaney, *Chem. Phys. Lipids*, 2016, 195, 21–33.

58. D. A. Brown, *Physiology*, 2006, **21**, 430–439.

59. L. Rajendran and K. Simons, *J. Cell Sci*., 2005, **118**, 1009-1102.

60. C. Faure, J.-F. Tranchant, and E. J. Dufourc, *Biophys. J.*, 1996, **70**, 1380-1390.

61. D. Allende, A. Vidal, S. A. Simon and T. J. McIntosh, *Chem. Phys. Lipids*, 2003, **122**, 65-76.

# CHAPTER 5

# Mechanistic Insight into the Diacylglycerol/Phorbol Ester Binding Properties of C1 Domains of Myotonic Dystrophy Kinase Related CDC42 Binding Kinase (MRCK)

This chapter demonstrates the diacyl glycerol/phorbol ester binding properties of C1 domain of MRCKα and MRCKβ using homology modeling, fluorescence and SPR based binding assays, monolayer penetration study and molecular docking analyses.

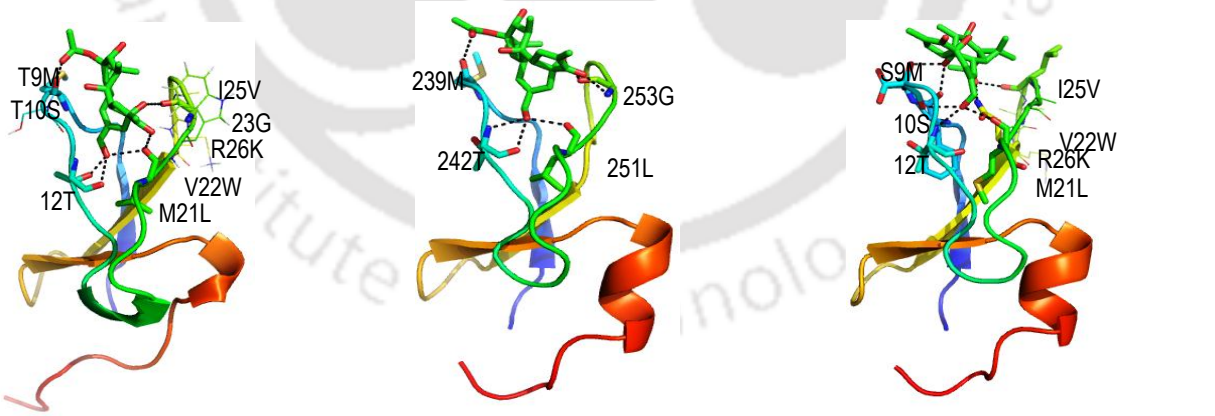


MRCKα-C1-T9M/T10S/M21L/V22W/I25V/R26K PKCδ-C1b MRCKβ-C1-S9M/M21L/V22W/I25V/R26K

### 5.1. Background and Focus of the present work

The Myotonic dystrophy-related Cdc42-binding kinases (MRCKs) are members of serine/threonine kinase enzymes.[1] MRCK isoforms are downstream effectors of Cdc42, structurally related to the dystrophia myotonica protein kinase (DMPK) family and contribute to myosin light chain (MLC) phosphorylation and thus involved in actin-myosin dynamics.[2, 3] Elevated MRCK expression is found to be involved in invasive and metastatic cancer e.g. histiocytic lymphoma, breast cancer, lung cancer, pancreatic adenocarcinoma, cutaneous squamous cell carcinoma and myelocytic leukemia and others.[2-7] MRCK isoforms consist of a highly conserved kinase domain followed by regulatory domain arranged in the order of C1-PH-CH-CRIB domains in the carboxyl-termini. MRCKα and MRCKβ share 61% homology identity, while MRCKγ has only 44% with the latter. The PH- domain is indispensable targeting proteins to appropriate subcellular localizations through binding to lipid and/or protein partners. Also the PH-CH domain together can take parts in protein-protein interaction that specify protein localization or substrate docking. The CRIB domain binds CDC42-GTP which assists membrane recruitment of MRCK isoforms. MRCK isoforms are in the inactive form when cells are in resting phase. The mechanism for the activation of MRCK was first forwarded by Tan and coworkers.[5] According to their findings, MRCKα is oligomerized through the homotrophic interactions between the respective individual coiled coil (CC) domains. There exist three CC domains in between N-terminal kinase domain and regulatory domain in MRCK isoforms. These CC domains also interact with their kinase domain to retain MRCK in a closed conformation. Thus both intermolecular and intramolecular interactions contribute to MRCKα inactivation. It was observed that the treatment of MRCKα with phorbol 12-myristate 13-acetate (PMA) activated the enzyme in HeLa cells.[5] PMA is a well-known C1 domain ligand. Therefore, these findings suggest that PMA binding to the C1 domain of MRCK may disrupt the CC domain-kinase domain interactions and subsequent release of kinase domains may lead to the dimerization, autophosphorylation and activation. The dependence of MRCK on the phorbol ester for activation includes this kinase to the growing list of characterized intracellular phorbol ester receptors, such as PKC, DAG kinase, n-chimaerin, Vav, RasGRPs and others. To further investigate the phorbol ester binding properties of MRCK, Blumberg and coworkers recently carried out a comparative study of the isolated C1 domain of MRCKα and MRCKβ with that of PKCδ. They found out that 50-100 fold higher concentration of phorbol ester is required for the induction of membrane translocation of MRCK compared to PKCδ.[8] This study encourages us to investigate the structural requirements in MRCK-C1 domain to respond to the DAG/ phorbol ester at concentrations comparable with those that modulate PKC.

In this study we wished to characterize the phorbol ester as well as DAG binding properties of the C1 domain of MRCKα and MRCKβ. We confirmed the lack of phorbol ester and DAG binding affinity of C1 domain of MRCKα and MRCKβ by using fluorescence polarization and surface plasmon resonance (SPR) analysis. Through homology modeling and docking studies we first identified the probable amino acid residues present within the binding cleft of C1 domain of MRCKα and MRCKβ that might be responsible for its low binding affinity towards phorbol ester or DAG compared to PKCδ. The presence of S9, M21, V22, I25 and R26 residues surrounding the binding pocket muddles the ligand dependent membrane binding surface of the C1 domains which is crucial for stabilizing the ternary binding complex of ligand-receptor-membrane. Then we carried out site directed mutagenesis and quantitative binding analyses to understand the role of those predicted residues in DAG/ phorbol ester dependent membrane binding. Mutating these residues in the MRCKα- and MRCKβ-C1 domain to correspond to the ones in the potent phorbol ester receptor PKCδ-C1b, we found out almost complete recovery of the in vitro binding affinity. These results propose that suitable DAG/ phorbol ester derivatives or other amphiphilic compounds might have the potential to selectively bind to the C1 domain and regulate MRCK activity.

## 5.2. Results

### Identification of the Amino Acid Residues for Mutational Analyses

It is already reported that the C1 domains of MRCKα and MRCKβ have 50-100 fold less binding affinity for phorbol ester in comparison with PKCδ-C1b domain. A plausible reason for these high affinity-differences may be the presence of unique amino acid residues in and around the binding pocket of the C1 domains. We presume that these residues might inhibit the interaction between C1 domain and the membrane lipids, thereby preventing the formation of C1-ligand-membrane ternary complex or blocking the binding pocket. In general the C1 domain is composed of 50 or 51-amino acid residues and contain a signature motif of $HX_{12}CX_2CX_nCX_2CX_4HX_2CX_7C$, where H is histidine, C is cysteine, X is any other amino acid, and n is 13 or 14. Several studies have been carried out to understand the DAG/Phorbol ester dependent membrane binding properties of different C1 domain.[9, 10, 11] To determine the probable residues present within the C1 domain of MRCKα and MRCKβ that obstruct their binding with phorbol ester or DAG molecules, we first performed multiple sequence alignment studies. The alignment studies of MRCKα- and MRCKβ-C1 domains with several PKC-C1 domains (selected through PSI–Blast analysis (http://blast.ncbi.nlm.nih.gov/Blast.cgi)) were performed by using Praline multiple sequence alignment programs. This amino acid based multiple sequence alignment studies identified several unique residues within the C1 domain of MRCKα and MRCKβ (Figure 5.1A). The results showed

that diverse amino acid residues present in PKCδ-C1b responsible for phorbol ester binding are not conserved in MRCKα- and MRCKβ-C1 domain. We also prepared model structures of MRCKα- and MRCKβ-C1 domains by EasyModeller 4.0 software based on those templates identified by PSI-BLAST analyses.[12] To identify the residues which are involved in binding with phorbol ester, we then performed molecular docking analyses using Molegro virtual docker 6.0.[13] It has been demonstrated that C1 domain sequences of phorbol ester receptors possess several conserved amino acid residues like histidine, cysteine, glycine (positions 23 and 28 in the consensus), glutamine (position 27) and proline (position 11) in their binding pocket.[14] In our present study, homology sequencing of MRCKα/β-C1 domain with the other C1 domains showed conservation of these residues in their structures. Through mutational analysis, it was first established that the two loops at positions 7–12 and 20–27, which comprise most of the β2 and β3 segments, constitute the phorbol ester binding site. The exposed hydrophobic residues Tyr-8, Met-9, Phe-13, Leu-20, Tyr-22 (in PKCα) or Trp-22 (in PKCδ, ε, η, θ), Leu-24, and Ile-25 are found to facilitate the membrane insertion of the protein.[15] Our homology modeling results showed that Tyr-8, Met-9, Ser-10, Phe-13, Leu-21, Trp-22, Val-25 and Lys-26 of PKCδ-C1b are replaced by Phe, Thr, Thr, Lys, Met, Val, Ile and Arg respectively in MRCKα-C1 domain. Similarly, in MRCKβ-C1 domain Tyr-8, Met-9, Phe-13, Leu-21, Trp-22, Val-25 and Lys-26 of PKCδ-C1b were replaced by Phe, Ser, Glu, Met, Val, Ile and Arg respectively. Previous studies have confirmed that replacement of Tyr-8 by hydrophobic residues does not alter the membrane affinity of C1 domain.[9] Therefore, it can be predicted that the presence of Phe in place of Tyr-8 may not have any significant change in the binding affinity as well as membrane penetration of MRCKα-C1 domain. Both molecular modeling and experimental studies have already showed that Phe-13 does not have any significant hydrophobic interaction with PDBu.[10, 16] Therefore, mutations at positions 8 and 13 were not considered for our present study. Studies have shown that that Leu-20, Leu-24, and Trp-22 contributed to the hydrophobic interactions between PDBu and PKCδ-C1b.[10, 16] Medkova and Cho showed that Trp-58 and Phe-60 (equivalent to the Trp-22 and Leu-24 in PKCδ-C1b) in the C1a domain of PKCα played significant role in membrane penetration and PKC activation.[17] Also it has been shown that mutations at Trp-22 exerts a large reduction in the binding affinity to DAG but not to PDBu which could be attributed to the flexibility of its side chain allowing it to adopt different conformation when interacting with different ligands.[10] Therefore, alternation of Trp-22 by other residues may have a significant effect in both the binding affinity as well as membrane penetration properties. Similarly Leu-21 has been found to be very important for protein folding through its interaction with the side chains of Thr-12, Glu-27 and Arg-37. Alternation of this residue may alter the binding pocket geometry which may affect the binding as well as membrane penetration.[9] Based on these, we designed the mutant

M21L/V22W for both MRCKα/β-C1 domain. Different experimental and theoretical analyses showed that C1 domain/phorbol ester binding affinity is very sensitive to the alternation of the amino acid residues in the position 20-27.[9] Therefore, I25V/R26K mutant was prepared for our present study. Molecular docking analyses of mutants M21L/V22W and I25V/R26K of MRCKα/β-C1 domain docked with PMA revealed that the phorbol ester also interacts with the backbone of Thr-9 and Thr-10 of MRCKα-C1 domain and Ser-9 of MRCKβ-C1 domain. Therefore, T9M/T10S and S9M mutants were prepared for MRCKα-C1 and MRCKβ-C1 respectively. A recent study showed that five crucial residues (Glu(9), Glu(10), Thr(11), Thr(24), and Tyr(26)) present along the rim of the binding cleft of atypical C1 domain of Vav have weakened the binding potency towards phorbol ester in a cumulative fashion.[18] Based on these idea, we prepared several triple, quadruple, quintuple and sextuple mutants of MRCKα/β-C1 domain.

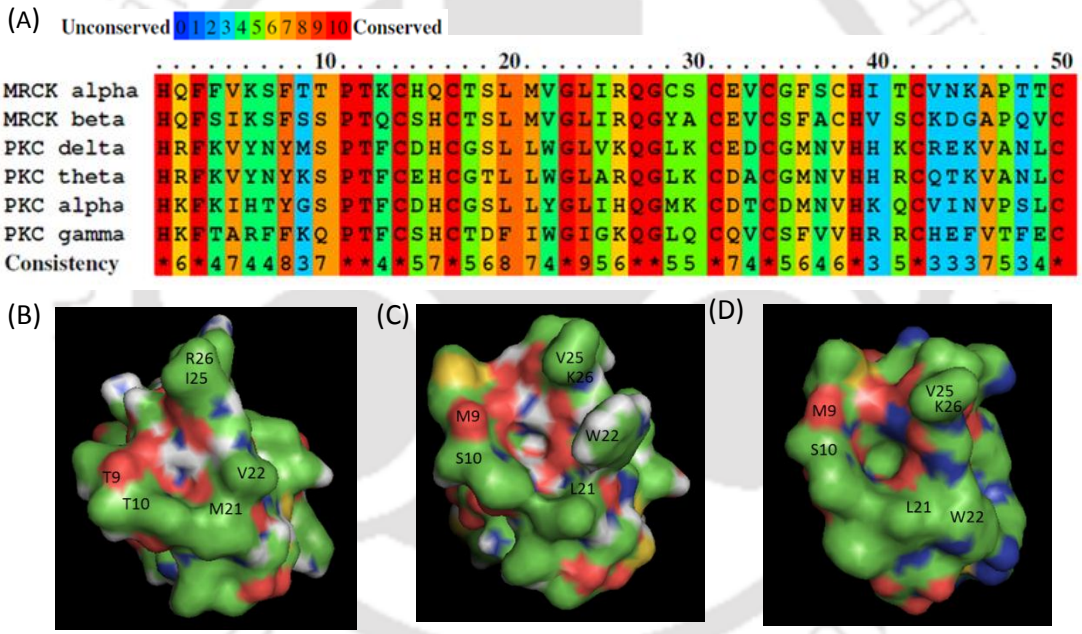


**Figure 5.1.** Amino acid sequence alignment of MRCKα-, MRCKβ-, PKCδ-, PKCθ-, PKCα- and PKCγ-C1 domains are shown using Praline (A). Model structures of of MRCKα-C1 (B), MRCKα-C1-T9M/T10S/M21L/V22W/I25V/R26K (C) and PKCδ-C1b (C) showing the proposed residues that may be crucial for binding with PMA.

For this purpose we selected following mutations for our current study-

| Protein | Selected mutations |
|---|---|
| MRCKα-C1 domain | T9M/T10S, M21L/V22W, I25V/R26K, T9M/T10S/M21L/V22W, T9M/T10S/I25V/R26K and T9M/T10S/M21L/V22W/I25V/R26K |
| MRCKβ-C1 domain | S9M, M21L/V22W, I25V/R26K, S9M/M21L/V22W, S9M/I25V/R26K and S9M/M21L/V22W/I25V/R26K |

**Binding studies of MRCK-C1 domain with Phorbol ester/DAG**

Phorbol ester and DAG have been identified as the activator of MRCK isoforms by [3H]PDBu assay.[5, 8] It is demonstrated that phorbol ester binding to the C1 domain leads to the activation of MRCK protein through the disruption of the binding interaction between kinase domain and negative autoregulatory of CC2/3 domain.[5] It is recently described that the C1 domain of both MRCKα and MRCKβ have 60–90-fold weaker binding affinity for phorbol ester in comparison with the PKCδ-C1b subdomain and its binding affinity is dependent on the presence of phosphatidylserine.[8] Structure-activity analyses showed that the C1 domains of MRCKα and MRCKβ show ligand selectivity similar to the C1b subdomain of PKCα. It is also reported that both the C1 domains of MRCKα and β have 400–1000-fold weaker binding affinity for DAG than PKCδ-C1b subdomain.[8] However a mechanistic investigation of the phorbol ester/DAG binding properties of C1 domain of MRCK have not been carried out so far. In this regard, we quantitatively determined the binding properties of both wild type (WT) and mutated C1 domains of MRCK protein to liposome containing 12-N-methylanthraniloylphorbol 13-acetate (SAPD) and dipalmitoylglycerol ($DAG_{16}$) by fluorescence polarization assay and surface plasmon resonance (SPR) analyses, respectively.

**Fluorescence polarization based binding assay—** When a fluorescent molecule is excited by a polarized light, it emits light with different degree of polarization that is inversely proportional to the rate of molecular rotation. If the fluorophore binds to high molecular weight species, the rotations get restricted and the degree of polarization increases. Based on this concept, fluorescence polarization assay for protein-ligand binding measurements were forwarded.[19] The fluorescent phorbol ester, 12-N-methylanthraniloylphorbol 13-acetate [sapintoxin D (SAPD)] was used as both the probe and the ligand for the determination of binding properties of the C1 domain of MRCK protein. The binding properties of SAPD with PKCα-C1 domain has already been studied extensively by Stubbs and coworkers.[20] According to their report, the emission spectra of SAPD shows two components in the lipid vesicles-one component, centered at approximately 435 nm, is due to buffer-associated SAPD and the other, at approximately 395 nm, is due to membrane lipid-bilayer-associated SAPD. Concentration of the latter one increase in the presence of PKC enzyme and this behavior is correlated with its activation process. In our study, we determined the binding affinity ($K_{D1}$) values from the change in fluorescence polarization values of the SAPD upon titration by C1 domain of MRCKα/β under liposomal environment (Figure 5.2A and figure 5.3A). The polarization values of SAPD at the shorter wavelength component of the emission spectra i.e. 395 nm was considered for analysis when excited at 355 nm.

**Surface Plasmon Resonance Analysis —** The binding parameters of MRCK-C1 domains and their mutants with the $DAG_{16}$ under liposomal environment (PC/PE/PS/$DAG_{16}$ (50/20/20/10)) were quantitatively determined by using equilibrium SPR analysis. The protein was passed over the liposome coated L1 sensor chip with a flow rate of 30 μL/min and real time measurement of association phase was monitored for longer time (500 sec). Figure 5.2B and 5.3B represents binding isotherms of equilibrium-SPR analysis for the binding of MRCKα- and MRCKβ-C1 domain to the PC/PE/PS/$DAG_{16}$ (50/20/20/10) liposome, respectively.

**Characterization of the Phorbol Ester/DAG Sensitivity of MRCKα-C1 containing PKCδ-C1b like mutations**

**Introduction of six PKCδ-C1b-like mutations into the sequence of MRCKα-C1 resulted in an almost complete recovery of Phorbol Ester/DAG Sensitivity-** Through homology sequence alignment we identified six unique residues at the tip of the binding pocket of MRCKα-C1 domain, which can play a significant role in its binding to the phorbol ester or DAG molecules. In this regard mutation of those residues with respect to PKCδ-C1b subdomain was performed. The binding parameters of these mutants were measured by fluorescence polarization study and SPR analysis (Table 5.1). The measured binding parameters showed that MRCKα-C1-WT have 10-fold weaker binding affinity for SAPD (under PC/PE/PS(60/20/20) liposome) and PC/PE/PS/$DAG_{16}$ liposome in comparison with PKCδ-C1b subdomain under similar experimental conditions. It is also important to mention that SPR and fluorescence based binding measurements also showed that the binding affinity of MRCKα-C1-T9M/T10S/M21L/V22W/I25V/R26K mutant have 16- and 10-fold higher binding affinity for SAPD (under PC/PE/PS(60/20/20) liposome) and PC/PE/PS/$DAG_{16}$ liposome, respectively in comparison with MRCKα-C1-WT. This sextuple mutant showed 1.7-fold higher and similar affinity to SAPD (under PC/PE/PS (60/20/20) liposome) and PC/PE/PS/$DAG_{16}$ (50/20/20/10) liposome, respectively in comparison with PKCδ-C1b. Thus introduction of six PKCδ-C1b like mutations to MRCKα-C1 domain completely recovered its binding affinity.

**Introduction of double and quadruple C1b-like mutations into the sequence of MRCKα-C1 further dissects the role of the individual residues in the ligand affinity of MRCKα-C1-**

In order to explore the role of individual residues in the binding affinity, we generated double and quadruple mutant of MRCKα-C1. From the polarization study, we observed that MRCKα-C1 mutants T9M/T10S, M21L/V22W and I25V/R26K exhibit almost 4-, 3.3- and 3-fold higher binding affinity for SAPD, respectively than its WT-C1 domain. These results suggest that all these mutations have significant contribution towards SAPD binding of MRCKα-C1-sextuple mutant, but

these mutations alone are not sufficient for the complete recovery of the binding affinity. For further understanding of the role of these mutants, we generated two quadruple mutants T9M/T10S/M21L/V22W and T9M/T10S/I25V/R26K. The binding parameters revealed that T9M/T10S/M21L/V22W and T9M/T10S/I25V/R26K exhibit almost 12- and 1.2-fold higher binding affinity for SAPD in comparison with the MRCKα-C1-WT domain. This indicates that the mutations at 9, 10, 21 and 22 position, in combination are sufficient for the complete recovery of the binding affinity of MRCKα-C1 domain towards phorbol ester. At the same time, the lower binding affinity of T9M/T10S/I25V/R26K suggests that the mutations at the positions 21 and 22 of MRCKα-C1 domain are very crucial for phorbol ester binding. The T9M/T10S mutant alone or in combination with M21L/V22W increased the binding affinity significantly, indicating its significant contribution in phorbol ester binding. The comparatively lower binding affinity of I25V/R26K alone or in combination with T9M/T10S ruled out the importance of this mutation for phorbol ester binding.

**Table 5.1.** Membrane binding parameters of MRCKα-C1 domain and its mutants by fluorescence polarization assay[a] and SPR analysis[b] respectively.

| Protein | Fluorescence polarization data | | SPR data | |
|---|---|---|---|---|
| | $K_{D1}$ (μM) | Fold changes | $K_{D2}$ (nM) | Fold changes |
| PKCδ C1b | 0.267 ± 0.037 | 9.9 | 328 ± 97 | 9.43 |
| C1-WT | 2.643 ± 0.244 | 1 | 3095 ± 368 | 1 |
| C1-T9M/T10S | 0.656 ± 0.158 | 4 | - | - |
| C1-M21L/V22W | 0.785 ± 0.217 | 3.4 | 475 ± 151 | 6.5 |
| C1-I25V/R26K | 0.851 ± 0.061 | 3.1 | - | - |
| C1-T9M/T10S/M21L/V22W | 0.208 ± 0.063 | 12.7 | 1053 ± 416 | 2.9 |
| C1-T9M/T10S/I25V/R26K | 2.160 ± 0.776 | 1.2 | - | - |
| C1-T9M/T10S/M21L/ V22W/I25V/R26K | 0.156 ± 0.021 | 16.9 | 307 ± 98 | 10 |

[a] SAPD loaded vesicles (100 μM) containing PC/PE/PS (60/20/20) and varying concentration of proteins were incubated in a buffer solution (20 mM Tris, 150 mM NaCl, 50 μM $ZnSO_4$, pH 7.4) at room temperature.
[b] PC/PE/PS/$DAG_{16}$ (50/20/20/10) liposome coated sensor chip was incubated with varying concentration of protein in a buffer solution (20 mM Tris, 150 mM NaCl, 50 μM $ZnSO_4$, pH 7.4) at room temperature.

But, the higher binding affinity of T9M/T10S/M21L/V22W/I25V/R26K than T9M/T10S/M21L/V22W might be due to the involvement of the I25V/R26K mutation in the interaction with acidic phospholipid, because of its charged character and all these binding measurements were done in presence of liposomal environment. Similarly, SPR analysis also showed that with the introduction of the mutation M21L/V22W, the binding affinity of the MRCKα-C1 domain to PC/PE/PS/$DAG_{16}$ liposome is enhanced by 6.5 fold compared to the MRCKα-C1-WT domain. However no significant change in the binding affinity to PC/PE/PS/$DAG_{16}$ (50/20/20/10)

/PS/liposome is observed for the MRCKα-C1 quadruple mutant T9M/T10S/M21L/V22W, which suggests different orientation of SAPD and DAG in the binding pocket of MRCKα-C1 domain.

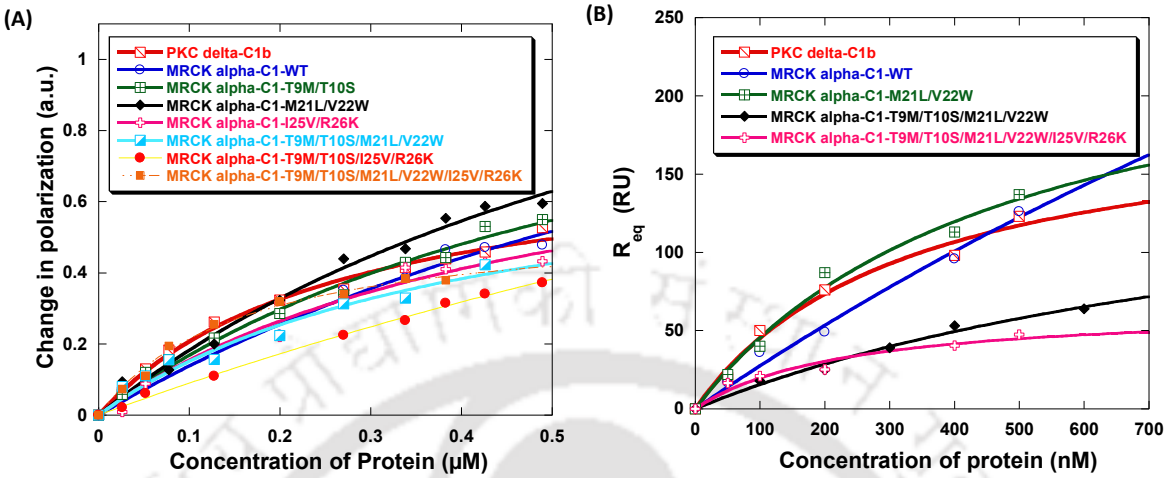


**Figure 5.2.** Binding isotherms generated from the fluorescence polarization assay for the interaction of MRCKα-C1 domain and mutants with SAPD loaded PC/PE/PS (60/20/20) liposome (A). Binding isotherms from SPR analysis for the interactions of MRCKα-C1 domain and mutants with PC/PE/PS/$DAG_{16}$ (50/20/20/10) liposome (B). The $R_{eq}$ values were collected after 500 sec of the sample injections.

## Characterization of the Phorbol Ester/DAG Sensitivity of MRCKβ-C1 containing PKCδ like mutations

**Introduction of five PKCδ-C1b-like mutations into the sequence of MRCKβ-C1 resulted in an almost complete recovery of phorbol ester/DAG sensitivity-** Similarly, for MRCKβ-C1 domain a quintuple mutant S9M/M21L/V22W/I25V/R26K was generated based on the amino acid homology sequence alignment of MRCKβ-C1 with PKCδ-C1b domain. Binding parameters obtained from the fluorescence polarization assay showed that MRCKβ-C1-WT domain responds to SAPD with 7.3-fold lower affinity than PKCδ-C1b domain under the liposomal environment (Table 5.2). The quintuple mutant showed 4- and 28-fold stronger binding affinity for SAPD than the PKCδ-C1b subdomain and MRCKβ-C1-WT domain, respectively. Similarly, SPR analysis also demonstrated that MRCKβ-C1-WT domain exhibit 4.7-fold weaker affinities towards PC/PE$DAG_{16}$ liposome compared to PKCδ-C1b domain. Introduction of five PKCδ-C1b like mutations significantly altered its binding affinity showing the enhancement of almost 9.3-fold compared to the MRCKβ-C1-WT domain. Therefore, both studies clarify that all these mutation together led to the recovery of the binding affinity completely even responding to the phorbol ester with better affinity than PKCδ-C1b domain under the experimental conditions.

**Table 5.2.** Membrane binding parameters of MRCKβ-C1 domain and its mutants by fluorescence polarization assay[a] and with by SPR analysis[b], respectively.

| Protein | Fluorescence polarization data | | SPR data | |
|---|---|---|---|---|
| | $K_{D1}$ ($\mu M$) | Fold changes | $K_{D2}$ ($nM$) | Fold changes |
| PKCδ-C1b | 0.267 ± 0.037 | 7.11 | 328 ± 97 | 4.7 |
| C1-WT | 1.9 ± 0.443 | 1 | 1565 ± 647 | 1 |
| C1-S9M | 1.038 ± 0.458 | 1.8 | - | - |
| C1-M21L/V22W | 0.472 ± 0.118 | 4.02 | - | - |
| C1-I25V/R26K | 0.382 ± 0.181 | 4.97 | 141 ± 13 | 11 |
| C1-S9M/M21L/V22W | 0.216 ± 0.018 | 8.79 | - | - |
| C1-S9M/I25V/R26K | 0.142 ± 0.023 | 13.3 | 453 ± 126 | 3.5 |
| C1-S9M/M21L/V22W/ I25V/R26K | 0.067 ± 0.024 | 28.3 | - 169 ± 16 | - 9.3 |

[a)] SAPD loaded vesicles (100 μM) containing PC/PE/PS (60/20/20) and varying concentration of proteins were incubated in a buffer solution (20 mM Tris, 150 mM NaCl, 50 μM $ZnSO_4$, pH 7.4) at room temperature.
[b)] PC/PE/PS/$DAG_{16}$ (50/20/20/10) liposome coated sensor chip was incubated with varying concentration of protein in a buffer solution (20 mM Tris, 150 mM NaCl, 50 μM $ZnSO_4$, pH 7.4) at room temperature.

**Introduction of single, double and triple mutation**- To explore the role of individual residues in the binding affinity single mutant S9M, double mutants M21L/V22W, I25V/R26K; triple mutants S9M/M21L/V22W and S9M/I25V/R26K were also introduced to MRCKβ-C1 domain as in like MRCKα-C1 domain. The polarization based binding studies revealed that the single mutant S9M has very little contribution towards binding of SAPD, showing an enhancement of the binding affinity only by 2-fold. On the other hand, significant increase in the binding affinity for SAPD was observed for the double mutants i.e. 4 and 5-fold for M21L/V22W and I25V/R26K mutants respectively, in comparison with PKCδ-C1b domain. Interestingly, the triple mutants S9M/M21L/V22W and S9M/I25V/R26K demonstrated that any of these two combinations was sufficient for the complete recovery of the binding affinity for SAPD. But SPR analysis showed that the triple mutant S9M/I25V/R26K exhibit only 3.5-fold higher affinity than MRCKβ-C1-WT domain. These results suggest that S9M/I25V/R26K exhibit ligand selectivity towards DAG and phorbol ester. Overall the binding parameters showed that both M21L/V22W and I25V/R26K are very important mutants for MRCKβ-C1 domain in order to respond to the phorbol ester at a comparable affinity with PKCδ-C1b domain.

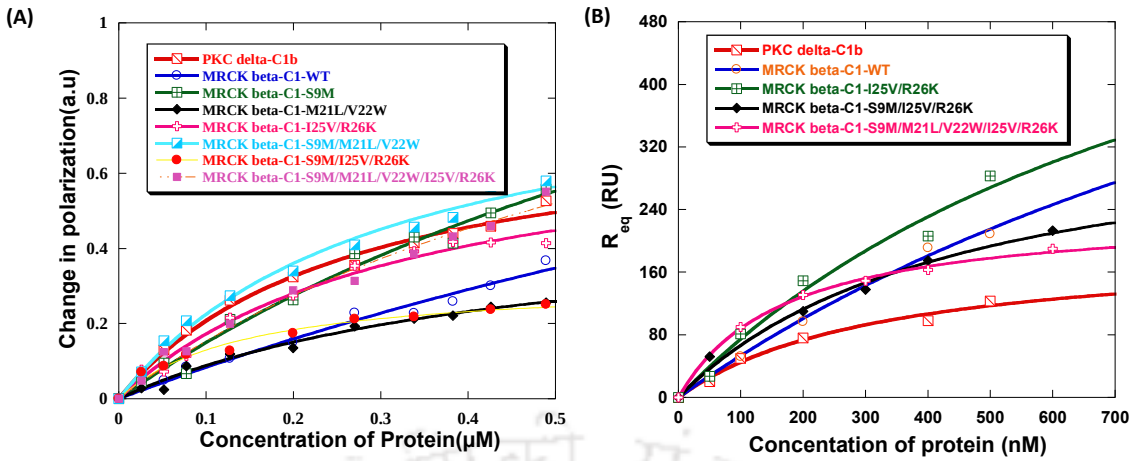


**Figure 5.3.** Binding isotherms generated from the fluorescence polarization assay for the interaction of MRCKβ-C1 domain and mutants with SAPD loaded PC/PE/PS (60/20/20) liposome (A). Binding isotherms from SPR analysis for the interactions of MRCKβ-C1 domain and mutants with PC/PE/PS/$DAG_{16}$ (50/20/20/10) liposome (B). The $R_{eq}$ values were collected after 500 sec of the sample injections.

## Rationalization of Binding Data from Molecular Docking Analysis

The model structure of WT and all mutants of MRCKα- and MRCKβ-C1 domain were prepared by EasyModeller 4.0.[12] The suitable templates, 1PTR, 1TBN were identified by searching the protein data bank of NCBI using PSI-blast.[21, 22] The prepared models were energy minimized through Swiss-Pdb viewer and stereo-chemical quality of each model was confirmed by PROCHECK and Ramchandran plot analyses.[23] The statistics of non-bonded interactions between different atom types were analyzed by ERRAT program which gives a measure of the structural error at each residue in the protein.[24] The compatibility of the atomic model (3D) with its own amino acid sequence was determined by Verify 3D software.[25, 26] Whenever required, energy minimization was again performed by Swiss PDB viewer till we get a good quality model with more than 95% of the residues in the allowed region of the Ramachandran plot. To have a better understanding on the interacting residues of C1 domains and the binding mode of phorbol esters we performed docking analyses with phorbol-13-O-acetate (PMA) to the modeled C1 domains of MRCKα and MRCKβ by Molegro Virtual Docker software, version 6.0 (Molegro ApS, Aarhus, Denmark).[13]

**Molecular Docking Analysis of MRCKα-C1 with PMA-** Docking analysis revealed that PMA is not properly fitting into the MRCKα-C1-WT pocket and its hydroxymethyl group is completely towards outside the pocket (Figure 5.4A). PMA probably interacts with the MRCKα-C1-WT domain through hydrogen bond formation with the backbone carbonyl and amine groups of 8F and 23G and side chain of 27Q residue. We also observed similar binding orientation of PMA with the mutants I25V/R26K (Figure 5.4C), T9M/T10S/M21L/V22W (Figure 5.4D) and T9M/T10S/I25V/R26K

(Figure 5.4E). However, PMA is well anchored to the binding pockets of mutants like M21L/V22W (Figure 5.4B) and T9M/T10S/M21L/V22W/I25V/R26K (Figure 5.4F) but in case of the former the ligand is oriented in somewhat different fashion than that of PKCδ-C1b domain.

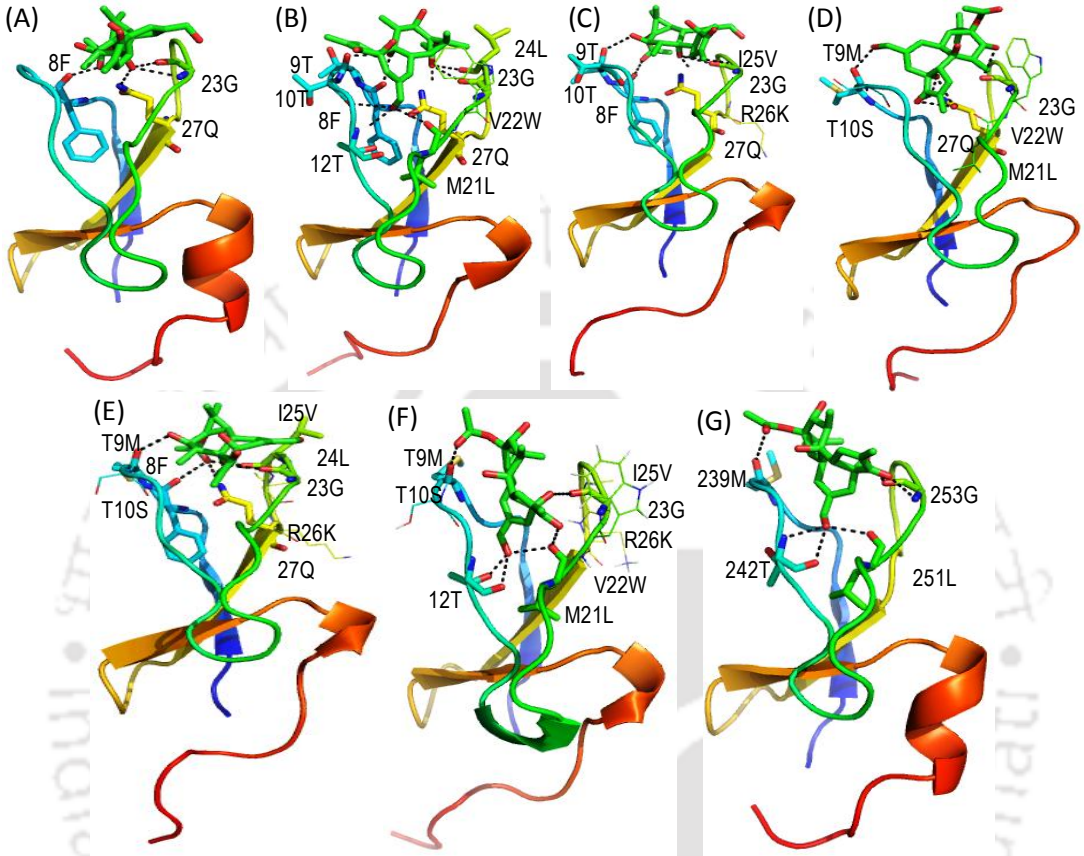


**Figure 5.4.** Mode of PMA interaction with the isolated MRCKα-C1 domain. Binding mode of PMA with model structures of MRCKα-C1-WT domain (A) and its mutants M21L/V22W (B), I25V/R26K (C), T9M/T10S/M21L/V22W (D), T9M/T10S/I25V/R26K (E) and T9M/T10S/M21L/V22W/I25V/R26K (F). Binding mode of PMA obtained from the crystal structure of PKCδ-C1b (1PTR) (G).

It is important to note that mutant T9M/T10S/M21L/V22W/I25V/R26K almost precisely mimics the PKCδ-C1b binding pocket and docking orientation of PMA matches with that of PKCδ-C1b subdomain obtained from the crystal structure (Figure 5.4G).[21] Hence, the molecular docking analyses suggests that all the proposed mutations of MRCKα-C1 domain in combination can play a major role in PMA-binding and membrane penetration rather than double or quadruple mutations. Overall, it can be presumed that mutations like T9M, M21L and V22W may be very important for PMA binding and membrane penetration. The other mutations like T10S, I25V and R26K can also play a major role in the conformational change of the C1 domain, thus indirectly affecting the binding affinity and membrane interaction.

**Molecular Docking Analysis of MRCKβ-C1 with PMA-** Molecular docking analysis of MRCKβ-C1-WT domain with PMA showed that the hydroxyl groups of PMA probably interacts through hydrogen bond formation with the backbone carbonyl and amine groups of 9S, 12T and 24L and side chain of 27Q residues but does not anchored within the pocket of the C1 domain (Figure 5.5A).

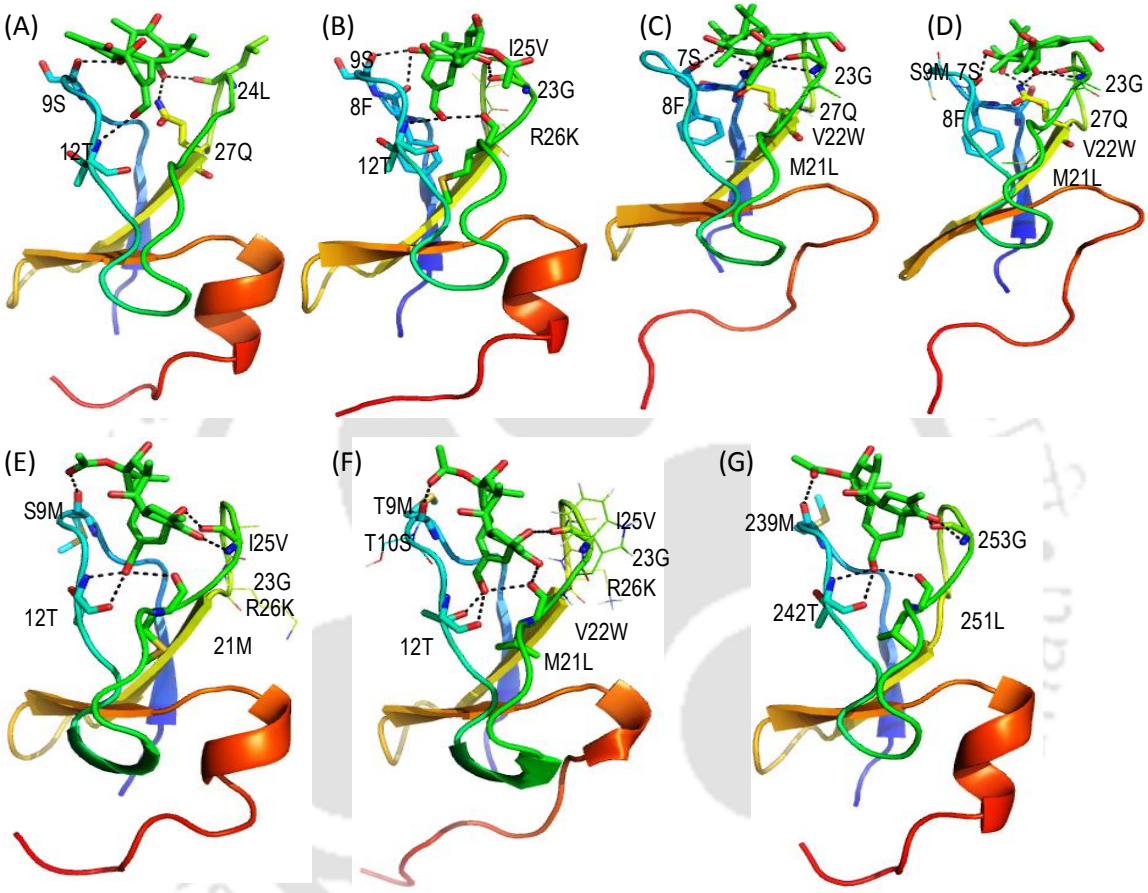


**Figure 5.5.** Mode of PMA interaction with the isolated MRCKβ-C1 domain**.** Binding mode of PMA with model structures of MRCKβ-C1-WT domain (A) and its mutants I25V/R26K (B), M21L/V22W (C), S9M/M21L/V22W (D), S9M/I25V/R26K (E) and S9M/M21L/V22W/I25V/R26K (F). Binding mode of PMA obtained from the crystal structure of PKCδ-C1b (1PTR) (G).

Our binding affinity values suggest that M21L/V22W and I25V/R26K mutants of MRCKβ-C1 domain have stronger interactions with PMA. However, our molecular docking analysis suggests that PMA does not well anchored to the binding pocket of I25V/R26K with the hydroxymethyl group orienting outside the pocket (Figure 5.5B). Similarly, PMA also does not fit properly within the pocket of M21L/V22W mutant, but still interacts through the formation of hydrogen bonds (Figure 5.5C). The triple mutant S9M/M21L/V22W does not have a suitable pocket to accommodate PMA

molecule (Figure 5.5D) while S9M/I25V/R26K mutant can accommodate it very well (Figure 5.5E). Only the quintuple mutant, S9M/M21L/V22W/I25V/R26K (Figure 5.5F) showed very similar docking pattern of PMA as that in with PKCδ-C1b (Figure 5.5G) domain orienting the hydroxymethyl group towards the binding pocket.

**Effect of the mutations on the membrane penetration of the MRCK-C1 domain**

Based on several studies, it is well documented that the phorbol ester/DAG binding facilitates the insertion of C1 domain into the membrane. The formation of C1 domain–ligand–membrane ternary-complex not only allows the C1 domains to specifically interact with the phorbol ester/DAG molecules through hydrogen bond formation but also allows them to penetrate into the membrane bilayer due to nonspecific hydrophobic and charged interaction with the phospholipid core and head groups, respectively.[10, 27] When phorbol ester or DAG molecule is docked into the binding pocket, the C1 domain undergoes considerable conformational change with the formation of hydrophobic surface surrounding the binding pocket, which drives the penetration of the domain into the bulk membrane. The basic residues surrounding the binding pocket of the C1 domain also have a significant contribution towards membrane interaction. The basic residues are involved in nonspecific electrostatic interaction with the anionic phospholipids at the membrane interface. In this respect, investigation of the membrane penetration properties of the WT-C1 domain and its mutants are necessary for better understanding of their membrane translocation activities.[11] Lipid monolayer at the air-water interface are widely used for studying membrane-protein interactions, because the surface packing density of the lipids can be readily and accurately varied in the system. Studies have shown that monolayer and bilayer have many common physical properties and that information about one state can be translated to other.[28, 29, 30] The lipid monolayer system is particularly useful for measuring membrane-penetrating activities of proteins in terms of change in surface pressure ($\Delta\pi$) at constant surface area or change in surface area at constant surface pressure. The measured $\Delta\pi$ is in general proportional to the initial surface pressure ($\pi_0$) of the lipid monolayer and an extrapolation of the $\Delta\pi$ versus $\pi_0$ plot yields critical surface pressure ($\pi_c$) which specifies the upper limit of $\pi_0$ that the protein can penetrate into. The surface pressure of the cell membranes has been estimated to be 31-35 dyne/cm. The recent studies on many lipid binding proteins have shown that those proteins whose physiological action involved penetration into particular cell membrane can penetrate the cell membrane mimicking monolayer with $\pi_c > 31$ dyne/cm.[31]

**Membrane penetration properties of MRCKα-C1 domain and its mutants-** We measured the membrane penetration ability of the WT and the mutants of MRCKα-C1 domain in terms of change

in surface pressure of the lipid monolayer by using a Langmuir Blodgett trough (Figure 5.6). We first measured the monolayer penetration properties of MRCKα-C1-WT and PKCδ-C1b subdomain using PC/PE/PS/$DAG_{16}$ (55/20/20/5) containing lipid monolayer. Monolayer penetration data showed that PKCδ-C1b subdomain had significant monolayer penetration ability with $\pi_c$ value 39-40 dyne/cm while MRCKα-C1-WT exhibited weak penetration ability with $\pi_c$ value 30-31 dyne/cm under similar experimental conditions. This signifies the requirement of additional structural elements in MRCKα-C1 domain in order to have membrane translocation ability with the same efficiency as of PKCδ-C1b domain. Monolayer penetration data of the sextuple mutant T9M/T10S/M21L/V22W/I25V/R26K demonstrated complete recovery of the membrane penetration efficiency with $\pi_c$ value around 38-39 dyne/cm. We also measured the $\pi_c$ values of double and quadruple mutants to identify their individual role in membrane penetration.

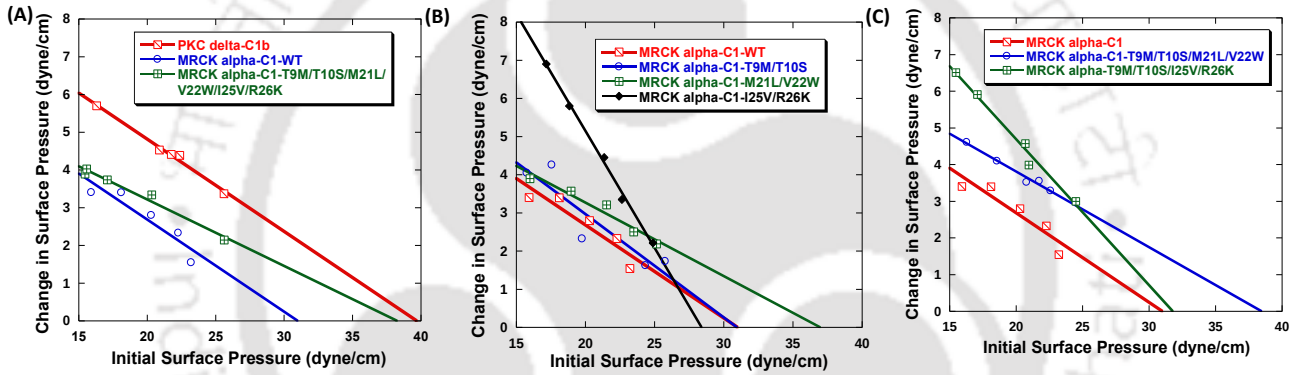


**Figure 5.6.** Interaction of MRCKα-C1-WT domain and mutants with lipid monolayer. Interaction of MRCKα-C1-WT, PKCδ-C1b subdomain and T9M/T10S/M21L/V22W/I25V/R26K mutant with PC/PE/PS/$DAG_{16}$ (55/20/20/5) lipid monolayer (A). Interaction of MRCKα-C1-WT domain and mutants, T9M/T10S, M21L/V22W and I25V/R26K with PC/PE/PS/$DAG_{16}$ (55/20/20/5) lipid monolayer (B). Interaction of MRCKα-C1-WT domain and mutants, T9M/T10S/M21L/V22W and T9M/T10S/I25V/R26K with PC/PE/PS/$DAG_{16}$ (55/20/20/5) lipid monolayer (C).

It was observed that double mutants T9M/T10S and I25V/R26K did not show any significant membrane penetration ability with $\pi_c$ values 30-31 and 28-29 respectively. Whereas, mutants M21L/V22W and T9M/T10S/M21L/V22W showed $\pi_c$ value of 36-37 dyne/cm and 38-39 dyne/cm respectively. T9M/T10S/I25V/R26K exhibited very weak penetration ability like WT-C1 domain. These results demonstrate that M21L/V22W is very crucial mutations for membrane penetration of MRCKα-C1 domain.

**Membrane penetration properties of MRCKβ-C1 domain and its mutants-** Monolayer penetration data of WT-MRCKβ-C1 domain showed that it does not penetrate ($\pi_c$ value 26-27

dyne/cm) the lipid monolayer (Figure 5.7). Alternation of five different residues (with the PKCδ-C1b subdomain like residues) almost completely recovered its membrane penetration efficiency. The S9M/M21L/V22W/I25V/R26K mutant of MRCKβ-C1 domain has a $\pi_c$ value around 38-39 dyne/cm which is very similar with that of PKCδ-C1b subdomain under similar experimental conditions. The $\pi_c$ values of the single mutant S9M was found to be 32-33 dyne/cm showing moderate contribution of this mutation in membrane penetration. The double mutants, M21L/V22W and I25V/R26K showed pronounced effect with $\pi_c$ value 36-37 dyne/cm and 34-35 dyne/cm, respectively.

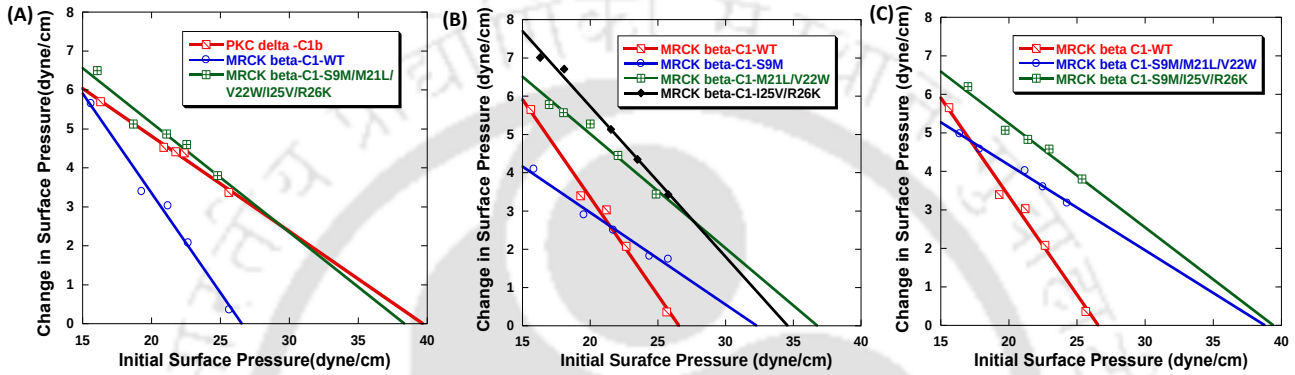


**Figure 5.7.** Interaction of MRCKβ-C1 domain and mutants with lipid monolayer. Interaction of MRCKβ-C1-WT, PKCδ-C1b subdomain and S9M/M21L/V22W/I25V/R26K mutant with PC/PE/PS/$DAG_{16}$ (55/20/20/5) lipid monolayer (A). Interaction of MRCKβ-C1-WT domain and mutants, S9M, M21L/V22W and I25V/R26K with PC/PE/PS/$DAG_{16}$ (55/20/20/5) lipid monolayer (B). Interaction of MRCKβ-C1-WT domain and mutants, S9M/M21L/V22W and S9M/I25V/R26K with PC/PE/PS/$DAG_{16}$ (55/20/20/5) lipid monolayer (C).

Almost complete regaining of membrane penetration ability was observed for S9M/M21L/V22W and S9M/I25V/R26K mutants showing $\pi_c$ value 38-39 and 39-40 dyne/cm respectively. Therefore, these results suggest that both these mutants are able to penetrate the membrane with comparable efficiency as PKCδ-C1b domain. This also indicated that M21L/V22W and I25V/R26K have similar effect on membrane penetration properties of MRCKβ-C1 domain.

**Structural Change measurement**

We performed the circular dichroism (CD) spectral analysis to determine whether the mutations had altered the structural integrity of the C1 domain or not. The CD spectra of the MRCKα-C1-WT MRCKα-C1-T9M/T10S/M21L/V22W/I25V/R26K and PKCδ-C1b are shown in figure 5.8. The contents of secondary structural units of the protein can be measured from the negative ellipticity in the range 225-200 nm and positive ellipticity around 195 nm which respectively stands for α-helix and β-sheets (Table 5.3). CD spectral analysis demonstrates that the secondary structure of MRCKα-

C1 domain has significant difference with that of PKCδ-C1b. The CD spectra of PKCδ-C1b matched with the previous report.[32] The similar CD spectra of MRCKα-C1-WT and MRCKα-C1-T9M/T10S/M21L/V22W/I25V/R26K signify that the mutations did not alter the secondary structure.

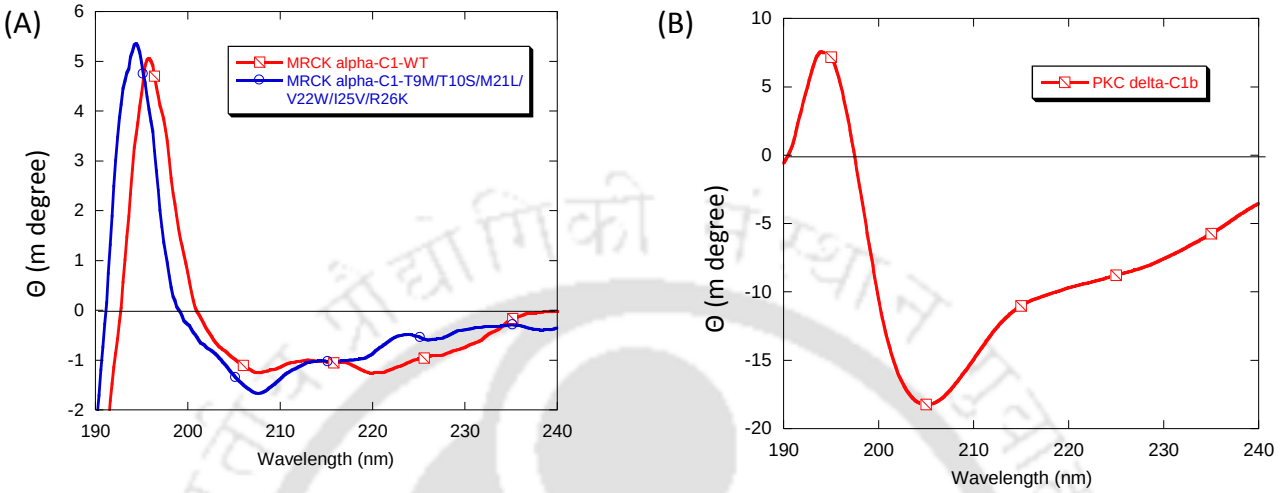


**Figure 5.8.** Effect of mutations on the secondary structure of MRCKα-C1 domain. Far UV CD Spectra of MRCKα-C1-WT domain and MRCKα-C1-T9M/T10S/M21L/V22W/I25V/R26K in 10 mM phosphate containing 10 mM NaCl buffer (pH 7.2) (A). Far UV CD Spectra of PKCδ-C1b domain (B).

**Table 5.3.** CD spectroscopy results

| Proteins | Helix (%) | Beta (%) | Turn (%) | Random (%) |
|---|---|---|---|---|
| PKCδ-C1b | 10.1 | 50.2 | 6 | 33.6 |
| MRCKα-C1-WT | 11.3 | 76.1 | 5.6 | 7 |
| MRCKα-C1-T9M/T10S/M21L/V22W/I25V/R26K | 19.5 | 69.3 | 0 | 11.2 |

**Discussion**

It is well documented that MRCK is involved in the myosin light chain phosphorylation and actin-myosin dynamics which regulates cell shape, cell division, motility, invasion and others. The binding of phorbol ester with C1 domain of MRCK results in kinase activation and membrane translocation.[5, 8] The C1 domain of MRCKα and MRCKβ has been shown to bind phorbol ester with nanomolar affinity.[8] Also it has been demonstrated that 50-100 fold higher concentration of phorbol ester is required for the membrane translocation of MRCKα/β-C1 domain compared to PKCδ-C1b subdomain. The reported binding affinities of MRCK-C1 domain with ligands including, PDBu, DAG-lactone and SAPD confirmed that MRCK-C1 domain exhibit similar ligand selectivity

with PKCα-C1b domain. However the mechanism of DAG/phorbol ester-dependent membrane binding properties of MRCK-C1 domain is still unexplained. In this regard, the present study determines the key structural elements in the C1 domain of MRCKα and MRCKβ responsible for its weaker affinity towards DAG/phorbol ester in comparison with the PKCδ-C1b domain. This study also provides membrane penetration behavior of the MRCK-C1 domain in respond to DAG, which helps to understand its DAG-dependent membrane binding properties.

Model structures and homology alignment identified T9, T10, M21, V22, I25 and R26 residues for MRCKα-C1 and S9, M21, V22, I25 and R26 residues for MRCKβ-C1 that may hinder the binding to DAG/phorbol ester. Our fluorescence polarization assay and SPR analyses clearly showed that the isolated MRCKα- and MRCKβ-C1 responds to phorbol ester/DAG with much weaker affinity than PKCδ-C1b domain. These binding parameters of MRCK-C1 and PKCδ-C1b are in good agreement with the reported one.[8] Similarly, SPR analysis also showed that MRCKα-C1-T9M/T10S/M21L/V22W/I25V/R26K and MRCKβ-C1-S9M/M21L/V22W/I25V/R26K mutants exhibit 10- and 9.3-fold higher affinities for DAG containing liposome , respectively than their respective WT-C1 domains. Molecular docking analyses also revealed that MRCK α/β-C1-WT domains are not able to properly accommodate the phorbol ester into the binding pocket. On the other hand introduction of PKCδ-C1b like mutations to MRCK-C1 completely changed the binding scenario. The binding affinity of MRCKα-C1-T9M/T10S/M21L/V22W/I25V/R26K and MRCKβ-C1-S9M/M21L/V22W/I25V/R26K mutants with SAPD is enhanced by 16.9- and 28.3-fold, respectively in comparison with its WT-C1 domains. Molecular docking analyses showed that phorbol ester is well anchored in the binding pocket of both the mutants and its orientation is very similar with that of PKCδ-C1b subdomain. Further binding studies were performed to understand the role of these residues in binding with phorbol ester and DAG. The binding parameters determined for double mutants T9M/T10S, M21L/V22W and I25V/R26K of MRCKα-C1 with SAPD showed that, these mutants also have significant contribution towards binding but neither of these alone is sufficient for regaining the binding affinity completely. Similar phenomenon was observed for S9M, M21L/V22W and I25V/R26K mutants of MRCKβ-C1 domain. The significantly stronger binding affinity of MRCKα-C1-T9M/T10S/M21L/V22W and weaker binding affinity of MRCKα-C1-T9M/T10S/I25V/R26K towards phorbol ester clearly demonstrates that M21L/V22W is a very crucial mutation for MRCKα-C1. On the other hand, the higher binding affinity of MRCKβ-C1-S9M/I25V/R26K mutant compared to MRCKβ-C1-S9M/M21L/V22W mutants signifies that I25V/R26K is very crucial mutation for MRCKβ-C1 domain. In addition, fluorescence polarization assay and SPR analyses showed that MRCKα-C1-M21L/V22W, MRCKα-C1-T9M/T10S/M21L/V22W and MRCKβ-C1-S9M/I25V/R26K exhibit ligand selectivity towards DAG

and phorbol ester. M21L/V22W mutant of MRCKα-C1 has stronger binding affinity for DAG containing membrane compared to phorbol ester while the opposite phenomenon is observed for mutants MRCKα-C1-T9M/T10S/M21L/V22W and MRCKβ-C1-S9M/I25V/R26K. This phenomenon may be attributed to the flexible nature of the side chain of Trp-22, Ile-25 and Arg-26 residues as reported earlier.[10] Molecular docking analyses also revealed that phorbol ester is well anchored to the binding pockets of mutants MRCKα-C1-M21L/V22W, MRCKα-C1-T9M/T10S/M21L/V22W, MRCKβ-C1-I25V/R26K and MRCKβ-C1-S9M/I25V/R26K mutants. However, no significant change in the docking pattern was observed for MRCKα-C1-T9M/T10S, MRCKα-C1-I25V/R26K, MRCKα-C1-T9M/T10S/I25V/R26K, MRCKβ-C1-S9M, MRCKβ-C1-M21L/V22W and MRCKβ-C1-S9M/M21L/V22W mutants in comparison with their WT-C1 domains. Overall, both experimental and molecular docking analyses confirmed that alternation of six residues of MRCKα-C1 and five residues of MRCKβ-C1 allow them to regain their binding affinity almost completely towards DAG and phorbol ester.

Several studies have confirmed that activation of PKC and some other C1 domain containing protein initiates through the localization of the protein to plasma membrane. C1 domain has been considered as a membrane targeting domain which first weakly interacts with the phospholipid headgroups and then specifically interacts with PMA/$DAG_{16}$ to penetrate into the membrane. Several studies have shown that the membrane penetration efficiency of the C1 domain depends upon the presence of hydrophobic and charged residues in the tip of the binding pocket. It has been shown that 50-100 fold higher concentration of PMA is required for translocation MRCKα/β-C1 domains to the plasma membrane of LNCaP cells compared to PKCδ-C1b domain.[8] However, it is still remain unclear which residues are primarily responsible for the lowering of membrane affinity of MRCKα/β-C1 domains compared to PKCδ-C1b subdomain. Our monolayer penetration measurements showed weak penetration of MRCKα/β-C1 domains to the PC/PE/PS/$DAG_{16}$ (55/20/20/5) lipid monolayer. Monolayer penetration efficiency of the MRCK-C1 domain was substantially increased by the introduction of PKCδ-C1b like residues. Monolayer penetration data showed that M21L/V22W mutant alone could regain the membrane penetration efficiency completely for both MRCKα/β-C1 domains. This could be primarily due to the V22W mutation, because Trp-22 has been identified as the crucial residue for membrane penetrations of PKCδ-C1b domain by several studies.[10, 16, 30] In addition to M21L/V22W mutant I25V/R26K mutant of MRCKβ-C1 domain is also capable of penetrating the membrane with similar efficiency like PKCδ-C1b domain. Previous studies showed that Ile25, which is exposed at the membrane binding surface of the C1 domain, contributes to the formation of hydrophobic cap to facilitate the insertion of the protein to the membrane. Also molecular dynamics studies of PKC-C1 domain showed that the

mutation of Leu-20 to glycine residue significantly affect the backbone conformation of Val-25 and Leu-26, which suggests that these residues contribute towards the proper folding of C1 domain through its backbone-backbone interaction.[10] Taken together, it can be assumed that mutations at 25 and 26 position may significantly alter the hydrophobic property as well as conformation of the C1 domain which enhances its DAG/phorbol ester dependent membrane affinity of MRCKβ-C1 domain.

MRCKs preferentially phosphorylate nonmuscle myosin light chain at serine 19, which is known to be crucial for activating actin-myosin contractility and thus regulates numerous cellular activities such as motility, adhesion, cytokinesis and changes in morphology.[2, 4] It has been demonstrated that the interaction of PMA with MRCK releases the kinase domain for phosphorylation and activates the enzyme.[5] Therefore, identification of the crucial residues in the DAG/phorbol ester binding pocket of MRCK-C1 domain can be useful in rational designing of activators/inhibitors for this protein. In this regard, mechanistic investigation of the phorbol ester/DAG binding properties of MRCK isoforms was carried out in our present study. Fluorescence polarization based binding assay, SPR analyses and molecular docking analyses identified the crucial residues in MRCK α/β-C1 domain that may be responsible for its lack of binding affinity towards DAG/phorbol ester. However some discrepancies have been observed between our in vitro binding affinity data and the reported data. Previous studies using radioactive labeled PDBu showed that MRCK-C1 domain has 50-100 fold weaker affinity for phorbol ester compared to PKCδ-C1b.[8] But in our present study (using fluorescence and SPR based techniques ), MRCK-C1 domain showed only 7-10 fold weaker affinity for phorbol ester compared to PKCδ-C1b. Generally, this kind of discrepancy occurs due to the different experimental design (e.g. fluoremetric, lipid dot blot, vesicle pelleting, SPR and others) and conditions. Our monolayer penetration measurements of the WT-C1 domain and mutants also showed that the hydrophobic residues present at the circumferences of the DAG/phorbol ester binding pocket play critical role in membrane penetration. This finding suggests that these mutations might significantly affect the localization of the isolated C1 domain and also the full length MRCK α/β protein to the cell membrane. In addition, cellular localization study of the wild type (WT) and mutants would provide more details about the mechanism of MRCK activation; however it is beyond the scope of our present study.

**Conclusion**

Overall, our experimental results and molecular docking analyses confirmed that M21L/V22W plays a pivotal role both in DAG/phorbol ester binding and membrane penetration of MRCKα-C1 domain. However, both M21L/V22W and I25V/R26K have been considered to be important for

DAG/phorbol ester binding and membrane penetration of MRCKβ-C1 domain. Only MRCKα-C1-T9M/T10S/M21L/V22W/I25V/R26K and MRCKβ-C1-S9M/M21L/V22W/I25V/R26K have shown complete regaining of the binding affinity both for phorbol ester and DAG. Both these mutations are also able to penetrate the membrane with similar efficiency like PKCδ-C1b domain. Molecular docking analyses revealed that only MRCKα-C1-T9M/T10S/M21L/V22W and MRCKβ-C1 S9M/M21L/V22W/I25V/R26K precisely mimic the docking pattern of PKCδ-C1b domain. These findings suggest that all these mutations together are able to enhance the binding affinity of MRCKα-C1 and MRCKβ-C1 rather than single mutations.

### 5.3. Experimental section

**Materials and methods-** 1-palmitoyl-2-oleoyl-sn-glycero-3-phosphocholine (PC), 1-palmitoyl-2-oleoyl-sn-glycero-3-phosphoethanolamine (PE) and 1-palmitoyl-2-oleoyl-sn-glycero-3-phosphoserine (PS) were purchased from Avanti Polar Lipids. The fluorescent phorbol ester 12-N-methylanthraniloylphorbol 13-acetate [sapintoxin D (SAPD)] was purchased from Sigma. All the required enzymes and buffers for cloning were purchased from NEB.

**Vector construction and mutagenesis-** The C1 domain of MRCKα and MRCKβ are generous gifts from Professor Peter M. Blumberg (National Cancer Institute, USA). The mutants were prepared by overlap extension PCR based on these templates (Figure 5.9). Then the cDNA of the C1 domain of MRCKα/β were subcloned between EcoR-I and XhO-I sites of $_{P}$GEX-4T1 vector for bacterial expression and between EcoR-I and BamH-I of $_{P}$EGFP-N1 vector for mammalian expression. All constructs were transformed into $DH_5\alpha$ cells for plasmid isolation. All plasmid DNA sequences were verified by sequence analysis.

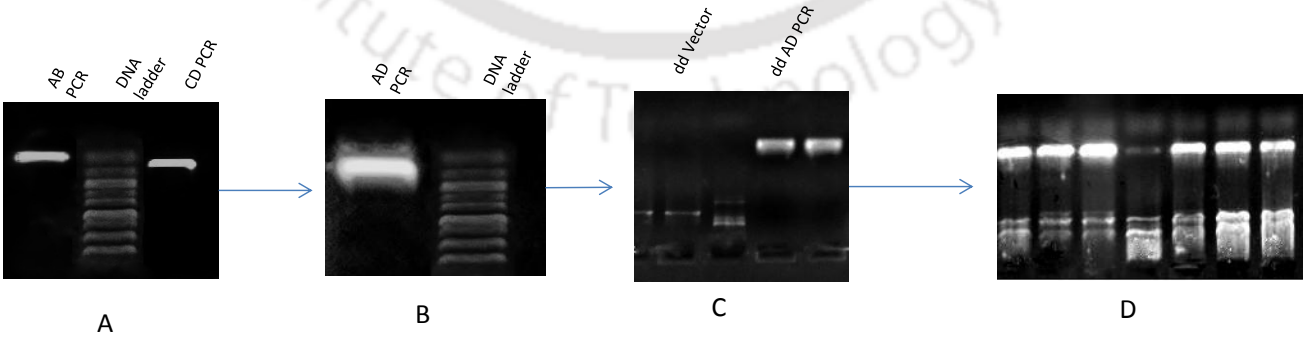


**Figure 5.9.** Representative agarose gel image of different steps of vector construction and mutagenesis of MRCKα-C1-21/22. AB and CD fragments prepared by PCR were verified with DNA ladder (A) and allowed to anneal to give AD fragments which contains the required mutations (B). Both the AD fragment and the vector are double digested with restriction enzymes (C). Cross checking PCR (D) confirmed that the vector contains the required insert.

**Protein expression and purification-** The GST fused WT and mutated C1 domain constructs of MRCKα and MRCKβ were transformed into BL21 (DE3) bacterial cells and plated on an ampicillin plate for protein expression. Then a single colony was resuspended in a 6 ml Luria Broth media using 100µg/ml ampicillin to produce a starter culture which was grown overnight at 37 °C and 180 rpm. Then the starter culture was inoculated to a 1 litre Luria broth containing 100µg/ml ampicillin at a 1:100 dilution and cells were grown at 37 °C and 120 rpm till it reached approximately 0.8 O.D. at 600 nm wavelengths. Then the cells were kept on ice for 10 minutes to stop its growth and 500µM Isopropyl β-D-1-thiogalactopyranoside (IPTG) was added along with 72 nM $ZnSO_4$. It was then kept at 18 °C with shaking at 120 rpm for 12 h for protein expression. Then the cells were pelleted by centrifugation at 5000×g and suspended in 20 mL lysis buffer containing 20 M Tris, 160 mM NaCl, PH-8 and stored at -80 °C till purification. The protein was purified by affinity chromatography. Briefly the pellets were sonicated by adding 50 µM phenylmethylsulphonyl fluoride (PMSF) , 2 mM dithiothreitol (DTT) and 0.1% Triton X-100 and centrifuged for 30 min at 4 °C, 48000×g. The resultant supernatant was incubated with 300 µl of glutathion S-transferase Tag$^{TM}$ (Genscript) resin for 45 min at 80 rpm. Then the solution was passed through a pre-rinsed column, washed with 20 mM Tris containing 160 mM KCl, pH-8 and then the protein was eluted with 20 mM reduced glutathione prepared in the wash buffer. The protein was stored at 4 °C. Purity of the protein was checked by SDS-PAGE gel electrophoresis (Figure 5.10).

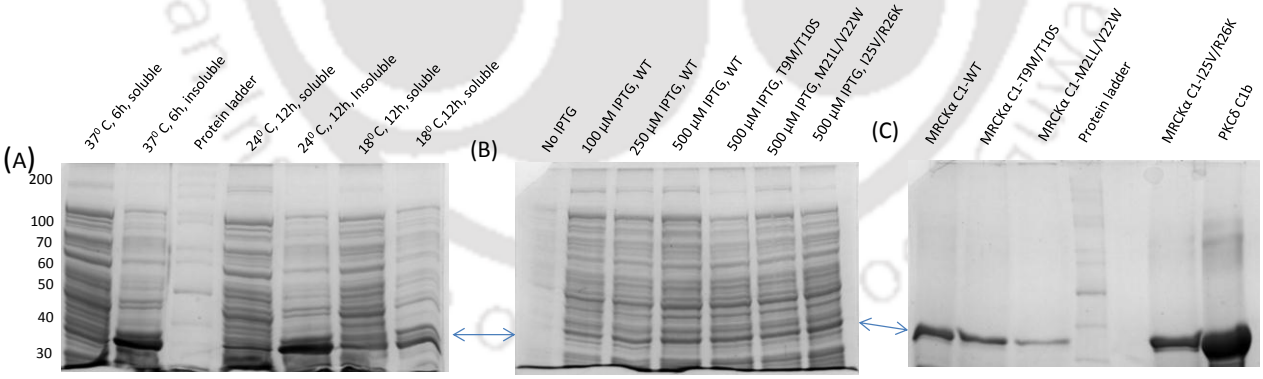


**Figure 5.10.** Representative SDS-PAGE gel images of MRCKα-C1 domain and mutants. Protein was expressed in different temperature (A) and different IPTG concentration (B) in order to find out the optimum condition. Purity of the protein is also checked after purification (C).

**Phospholipid Vesicles-** Large unilamellar vesicles (LUV) were prepared as previously described.[31] Briefly, aliquots of the required amounts of lipid in chloroform were placed in a test tube and the solvents removed under a stream of nitrogen. Then 50 mM Tris-HCl (pH 7.4) was added, and the contents were vortexed before being passed through 0.1 µM polycarbonate filters

using an Avanti Mini-Extruder (Avanti Polar Lipids, Albaster, AL). For fluorescence polarization assay LUV consisted of dipalmitylphosphatidylcholine (DPPC), dipalmitoylphosphatidethanolamine (DPPE) and dipalmitoyl phosphatidylserine (DPPS) in the molar ratio 60:20:20 to yield a final concentration of 100 μM. SAPD (1 μM) in dimethyl sulfoxide (DMSO) was added to preformed vesicles as required. For SPR studies the liposome used are PC/PE/PS/$DAG_{16}$ (50/20/20/10) and PC/PE/PS (60/20/20) as control.

**Fluorescence polarization based binding assay-** Fluorescence polarization based binding assay was carried out using Fluoromax-4 spectrofluorometer at room temperature. The qualitative binding affinity and specificities of the purified MRCKα/β-C1 domains and their mutants were determined in presence of liposome PC/PE/PS (60/20/20). Steady-state fluorescence polarization was measured, using 355 nm as the excitation wavelength and 395 nm as the emission wavelength. The SAPD loaded liposomes (100 μM) and varying concentration of proteins were incubated in a buffer solution (20 mM Tris, 150 mM NaCl, 50 μM $ZnSO_4$, pH 7.4) at room temperature. Steady-state fluorescence polarization P was calculated according to equation 1:

$$P = \frac{F_{II} - F_{\perp}}{F_{II} + F_{\perp}} \qquad (1)$$

Where $F_{II}$ and $F_{\perp}$ are the fluorescence intensity parallel and perpendicular to the excitation plane respectively.

**Surface Plasmon Resonance-** All surface plasmon resonance(SPR) measurements were performed (at 25 °C, in 20 mM Tris, 150 mM NaCl, 50 μM $ZnSO_4$, pH 7.4, flow rate of 30 mM/min) using a lipid-coated L1 sensorchip in the Biacore-X100 (GE Healthcare) system as described earlier. [27, 28] Vesicles for SPR analysis were prepared at a concentration of 0.5 mg/ml in 20 mM Tris, 150 mM NaCl, 50 μM $ZnSO_4$, pH 7.4 and were vortexed vigorously and passed through a 100 nm polycarbonate filter using an Avanti Mini Extruder (Avanti Polar Lipids, Albaster, AL) according to manufacturer's protocol. After washing the sensor chip surface with the running buffer (20 mM Tris, 150 mM NaCl, 50 μM $ZnSO_4$, pH 7.4) , PC/PE/PS/$DAG_{16}$ (50/20/20/10) and PC/PE/PS (60/20/20) vesicles were injected at 5 μL/min to the active surface and the control surface, respectively, to achieve similar response unit (RU) values. To minimize non-specific adsorption, the control surface was also coated with 40 μl BSA (.1 mg/ml in the running buffer) at a flow rate of 5μl/min, and equilibrated for 20 min before the injection of the protein.

**Monolayer measurement-** The monolayer penetration of MRCKα- and MRCKβ-C1 domains and their mutants were measured by Langmuir-Blodget trough (10 mL circular Teflon trough) using a

Wilhelmy plate (KSV NIMA).[17, 32] The lipid solution consisted of desired lipid composition (prepared in hexane/ethanol (9:1,v/v)) was spreaded on to a subphase of the buffer (containing 10 mM Tris, 160 mM KCl and 50 µM $ZnSO_4$, pH=7.4). The lipid composition used here is PC/PE/PS/$DAG_{16}$ (55/20/20/5). When a stable monolayer is formed after spreading the lipid solution, the surface pressure value is recorded which is the initial surface pressure ($\pi_0$). Then 100 µg protein was injected through a small hole on the trough to the subphase. The change in surface pressure ($\Delta\pi$) at a constant surface area was monitored for 60 min (with stirring the subphase at 60 rpm). $\Delta\pi$ was plotted versus $\pi_0$ and extra plotted to x -axis, yielding the critical surface pressure ($\pi_c$).

**References**

1. J. M. Arencibia, D. Pastor-Flores, A. F. Bauer, J. O. Schulze and R. M. Biondi, *Biochim. Biophys. Acta*, 2013, **1834**, 1302–1321.

2. T. Leung, X.-Q. Chen, I. Tan, E. Manser and L. Lim, *Mol. Cell Biol.*, 1998, **18**, 130–140.

3. I. Tan, C. H. Ng, L. Lim and T. Leung, *J. Biol. Chem.*, 2001, **276**, 21209–21216.

4. M. Unbekandt and M. F. Olson, *J. Mol. Med.*, 2014, **92**, 217–225.

5. I. Tan, K. T. Seow, L. Lim, and T. Leung, *Mol. Cell Biol.*, 2001, **21**, 2767–2778.

6. P. A. Gagliardi, L. d. Blasio, A. Puliafito, G. Seano, R. Sessa, F. Chianale, T. Leung, F. Bussolino and L. Primo, *J. Cell Biol.*, 2013, **206**, 415–433.

7. S. Wilkinson, H. F. Paterson and C. J. Marshall, *Nature Cell Biol.*, 2005, **7**, 255-261.

8. S. H. Choi, G. Czifra, N. Kedei, N. E. Lewin, J. Lazar, Y. Pu, V. E. Marquez and P. M. Blumberg, *J. Biol. Chem.*, 2008, **283**, 10543-10549.

9. M. G. Kazanietz, S. Wang, G. W. A. Milne, N. E. Lewin, H. L. Liu, and P. M. Blumberg, *J. Biol. Chem.*, 1995, **37**, 21852–21859.

10. Q. J. Wang, T.-W. Fang, K. Nacro, V. E. Marquez, S. Wang, and P. M. Blumberg, *J. Biol. Chem.*, 2001, **276**, 19580–19587.

11. J. S. Kelsey, T. Geczy, N. E. Lewin, N. Kedei, C. S. Hill, J. S. Selezneva, C. J. Valle, W. Woo, I. Gorshkova and P. M. Blumberg, *Chembiochem*, 2014, **15**, 1131–1144.

12. B. K. Kuntal, P. Aparoy and P. Reddanna, *BMC Research Notes*, 2010, **3**, 226-231.

13. R. Thomsen and M. H. Christensen, *J. Med. Chem.*, 2006, **49**, 3315-3321.

14. M. G. Kazanietz, X. R. Bustelo, M. Barbacid, W. Kolch, H. Mischak, G. Wong, G. R. Pettit, J. D. Bruns and P. M. Blumberg, *J. Biol. Chem.*, 1994, **269**, 11590–11594.

15. S. Wang, M. G. Kazanietz, P. M. Blumberg, V. E. Marquez, and G. W. A. Milne, *J. Med. Chem.*, 1996, **39**, 2541–2553.

16. S. Wang, N. E. Lewin, A. P. Kozikowski, G. W. A. Milne and P. M. Blumberg, *J. Med. Chem.*, 1999, **42**, 3436–3446.

17. M. Medkova and W. Cho, *J. Biol. Chem.*, 1999, **274**, 19852–19861.

18. T. Geczy, M. L. Peach, S. El. Kazzouli, D. M. Sigano, J. H. Kang, C. J. Valle, J. Selezneva, W. Woo, N. Kedei, N. E. Lewin, S. H. Garfield, L. Lim, P. Mannan, V. E. Marquez and P. M. Blumberg *J. Biol. Chem.*, 2012, **287**, 13137-13158.

19. W. A. Lea and A. Simeonov, *Expert Opin. Drug Discov.*, 2011, **6**, 17–32.

20. C. HO, S. J. Slater, B. A. Stagliano and C. D. Stubbs, *Biochem. J.*, 1999, **344**, 451-460.

21. G. Zhang, M. G. Kazanietz, P. M. Blumberg and J. H. Hurley, *Cell*, 1995, **81**, 917-924.

22. R. X. Xu, T. Pawelczyk, T. H. Xia and S. C. Brown, *Biochemistry*, 1997, **36**, 10709-10717.

23. R. A. Laskowski, M. W. MacArthur, D. S. Moss and J. M. Thornton, *J. Appl. Cryst.*, 1993, **26**, 283-291.

24. M. W. MacArthur, R. A. Laskwoski and J. M. Thornton, *Curr. Opin. Struct. Biol.*, 1994, **4**, 731-737

25. J. U. Bowie, R. Lüthy and D. Eisenberg, *Science*, 1991, **253**, 164-170.

26. R. Lüthy, J. U. Bowie and D. Eisenberg, *Nature*, 1992, **356**, 83-85.

27. J. S. Kelsey, T. Geczy, N. E. Lewin, N. Kedei, C. S. Hill, J. S.Selezneva, C. J. Valle, W. Woo, I. Gorshkova, and P. M. Blumberg, *Chembiochem*., 2014, **15**, 1131–1144.

28. R. C. Macdonald and S. A. Simon, *Proc. Nat. Acad. Sci. USA*, 1987, **84**, 4089-4093.

29. H. Brockman, *Curr. Opin. Struct. Biol*., 1999, **9**, 438-443.

30. S. Feng, *Langmuir*, 1999, **15**, 998-1010.

31. M. J. Hope, M. B. Bally, G. Webb and P.R. Cullis, *Biochim. Biophys. Acta*, 1985, **812**, 55-65.

32. Joydip Das, Xiaojuan Zhou and Keith W. Miller, *Protein Science*, 2006, **15**, 2107–2119.

33. D. Manna, A. Albanese, W. S. Park and W. Cho, *J. Biol. Chem*., 2007, **282**, 32093-32105.

# Conclusion and future scope of the work

C1 domain plays a major role in cancer and several other diseases. The diacylglycerol (DAG)/phorbol ester binding site of C1 domain is considered as a crucial target for the development of activators and inhibitors of the host proteins, including protein kinase C (PKC). Based on the structural knowledge of the natural C1 domain ligands, a number of small molecules have been synthesized targeting this binding pocket. Also, studies have been carried out to understand the mechanism of DAG/phorbol ester binding properties of different C1 domain. This thesis focused on developing small molecules targeting the DAG/phorbol ester binding pocket of C1 domain, understanding the effect of sterols like cholesterol and oxysterols on membrane binding properties as well as C1 domain mediated PKC activation properties and understanding mechanism of DAG/phorbol ester binding of the C1 domain of myotonic dystrophy kinase-related Cdc42-binding kinases-α and β (MRCKα/β) protein. Several biophysical techniques including, fluorescence spectroscopy, surface plasmone resonance spectroscopy (SPR), Langmuir Blodgett monolayer and circular dichroism (CD) and others were used in this thesis work.

We have successfully developed kojic acid esters and γ-hydroxymethyl-γ-butyrolactone substituents which showed very high affinity towards C1b subdomain of PKCδ/θ in **Chapter 2** and **Chapter 3** respectively. In **Chapter 2**, fluorescence quenching and fluorescence resonance energy transfer (FRET)-based competitive binding assay showed that kojic acid ester with unsaturated oleic acid side chain has the higher affinity than the other compounds. Also, determination of phase transition temperature as well as membrane permeability measurements using 1-Naphthol as a fluorescent probe showed that the kojic acid esters decrease phase transition temperature and increases membrane permeability. This signifies loose headgroup packing of the membrane in the presence of these compounds that allow PKC C1 domain to penetrate into the lipid bilayer. In **Chapter 3**, similar binding studies for γ-hydroxymethyl-γ-butyrolactone derivatives showed that the hydroxymethyl and acyl-groups of the γ-hydroxymethyl-γ-butyrolactone substituents are important for PKC-C1 domain binding. Fluorescence anisotropy measurements with DPH showed that the γ-hydroxymethyl-γ-butyrolactone substituents increase the membrane fluidity which again signifies loose headgroup packing that enhances PKC-C1 domain-membrane interaction. In addition, non-radioactive fluorescence-based PKC activity assay showed that γ-hydroxymethyl-γ-butyrolactone substituents could activate PKC enzyme with similar or higher efficiency than DAG molecules. Furthermore, sodium dithionite-based NBD-PE

quenching study showed that both kojic acid esters and γ-hydroxymethyl-γ-butyrolactone substituents are localized at the bilayer-water interface and easily accessible for the C1 domain binding. Consequently, these findings suggest that these kojic acid esters and γ-hydroxymethyl γ-butyrolactone substituents are potential regulator of PKC isoforms and can be further used for PKC-based drug development process.

Cell membrane consists of different lipid molecules that may interfere in DAG-dependent membrane binding of C1 domain and activation of its host proteins. In this regard, in **Chapter 4**, we investigated the role of cholesterol and two oxysterols (cholestane-3β,5α,6β-triol (triol) and cholestane-6-oxo-3β,5α-diol (6-keto)) on membrane properties as well as DAG-induced PKC activation properties. From fluorescence anisotropy measurements (with DPH) and detergent resistance membrane studies, we observed that both cholesterol and DAG have a synergistic effect on the membrane for the formation of liquid ordered phase that dehydrates the membrane. As a result, the DAG-dependent membrane binding of PKC C1 domain increases by two-fold which also increases the PKC activation. On the other hand, in the presence of oxysterols like triol- and 6-keto, the DAG-dependent membrane binding properties of PKC C1 domain decreases by two-fold which also decreases PKC activation efficiency. Differential scanning calorimetric (DSC) studies showed that 6-keto compound decreases the headgroup separation in membrane which inhibits the membrane penetration of the C1 domain. The exact mechanism of the reduction in binding affinity in the presence of triol- is not clear from our present study, but it can be assumed that this compound may increase the width of the bilayer hydrophilic head group regions, which restricts the insertion of the hydrophobic residues of the C1 domain into the core of the lipid bilayer. However, further studies are needed to understand this mechanism.

In **chapter 5**, DAG and phorbol ester dependent membrane binding mechanism of MRCK-C1 domains were studied. MRCK-C1 domain has also been identified as the binding module of DAG/phorbol ester by previous studies. Comparative studies showed that it has 50 to 100-fold lower affinities towards phorbol ester compared to PKCδ-C1b subdomain. Though these studies suggest the requirement of additional structural elements in MRCK-C1 domain for DAG/phorbol ester binding, till now no report is available on the mechanism of DAG/phorbol ester binding of MRCK-C1 domain. In this chapter thorough amino acid-based sequence homology modeling and molecular docking studies were used to predict the probable residues of C1 domain of MRCKα (T9, T10, M21, V22, I25 and R26) and MRCKβ (S9, M21, V22, I25 and R26) that may inhibit its interaction with DAG/phorbol ester. Fluorescence polarization-based binding assay and SPR analyses showed that the lowering of

binding affinity of MRCKα/β-C1 domain towards DAG/phorbol ester is the cumulative effect of all the predicted residues, not because of single residues. Molecular docking analyses also support these binding properties of MRCKα/β-C1 domain. Monolayer penetration measurements showed that M21L/V22W mutant plays a major role in the membrane penetration of MRCKα/β-C1 domain while I25V/R26K of MRCKβ-C1 domain also showed similar results. Therefore, we have successfully identified the residues of MRCKα/β-C1 that are primarily responsible in lowering its binding affinity towards DAG/phorbol ester molecules and membrane penetration. We hypothesize that these mechanistic studies would be helpful in designing activators or inhibitors of MRCK protein.

Therefore, this thesis demonstrated development of PKC-C1 domain targeted lipophilic molecules, which can be used in PKC-based drug development process. However, to understand the PKC activation/inhibition properties of the lipophilic molecules some other activation studies (e.g. [3H]PDBu assay) should be performed. Also, the effect of these compounds on the kinase activity of PKC should be performed in various cell lines. The effect of cholesterol and oxysterols on membrane properties and DAG-induced PKC activation properties demonstrated the role of different membrane constituents in C1 domain mediated PKC activation processes. For the first time, the mechanism of DAG/phorbol ester binding properties of MRCKα/β-C1 domain is reported. This MRCKα/β-C1 domain-DAG/phorbol ester binding study is not only important for further understanding their cellular activity but also helpful for designing activator/inhibitor for these kinase proteins. Overall, our findings in this thesis may immensely help in designing more selective and specific molecules for C1 domain and understanding its membrane interaction properties.

# List of publications

1. S. Gorai, S. Paul, G. Sankaran, R. Borah, M. K. Santra and D. Manna, *Med. Chem. Commun.*, 2015, **6**, 1798-1808.

2. S. Gorai, P. Ray Bagdi, R. Borah, D. Paul, M. K. Santra, A. T. Khan and D. Manna, *Biochem. Biophys. Rep.*, 2015, **2**, 75-86.

3. R. Borah, N. Mamidi, S. Panda, S. Gorai, S. K. Pathak and D. Manna, *Mol. Biosyst.*, 2015, **11**, 1389-1399

4. N. Mamidi, S. Panda, R. Borah and D. Manna, *Mol. Biosyst.*, 2014, **10**, 3002-3013.

5. D. Talukdar, S. Panda, R. Borah, D. Manna, *J. Phys. Chem. B*, 2014, **118**, 7541-7553.

6. R. Borah, D. Talukdar, S. Gorai, D. Bain and D. Manna, *RSC Adv.*, 2014, **4**, 25520-25531.

7. N. Mamidi, R. Borah, N. Sinha, C. Jana and D. Manna, *J. Phys. Chem. B*, 2012, **116**, 10684-10692.